# COLLECTIVE EFFECTS IN THREE-PULSE CYCLOTRON ECHOES

Thesis by

Richard Ross Smith

In Partial Fulfillment of the Requirements

for the Degree of

Doctor of Philosophy

California Institute of Technology

Pasadena, California

1972

(Submitted December 13, 1971)

ACKNOWLEDGMENT

The author is grateful for the assistance he has received in preparing this thesis. Professor Robert S. Harp suggested the essential starting point, a suitable problem for investigation. Special thanks are due Dr. Reiner Stenzel, Charles Moeller, and the other students who have helped with the experimental and theoretical aspects of the work. The typing of the manuscript was very competently done by Ruth Stratton and also by Aldre' Khoury. Working with the people of Steele Laboratory has been both enjoyable and rewarding. The author thanks the National Science Foundation for its financial support throughout his graduate education.

## Abstract

Three-pulse cyclotron echoes, 3PE, in rare gas afterglow plasmas are investigated. The experiments are performed with the magnetic field parallel to the discharge tube, which passes perpendicularly through an S-band waveguide. The echo properties are experimentally shown to be incompatible with previous models.

Experiments on 3PE are performed, which show that the electron density is the most important parameter, especially for the growth and decay of the echo following the first two pulses. The density is shown to have a qualitative as well as quantitative effect on the echo. Periodic modulation of both the emission and absorption of the plasma is observed following the first two pulses, and these additional methods of investigating echo processes will be helpful in formulating a satisfactory theory.

A model containing the experimentally important parameters is developed, and it is based upon the relatively simple case of the generation of plasma waves following an impulsive excitation for times so small that the original transient response has lost negligible energy. Better agreement than with previous theories is obtained, especially in the qualitative dependence of the echo on the electron density. Electron velocity space instabilities are briefly examined and discarded as influences in echo experiments.

The detection and qualitative theoretical explanation of slow wave pulses created inside the plasma by the applied microwave pulses supports the mode conversion echo model.

Table of Contents

## List of Illustrations

# I. INTRODUCTION

## 1.1 The Discovery of Cyclotron Echoes

Echoes are macroscopically observable signals that are produced by a system at times and/or locations in space which are different from the exciting signals. For example, one can produce plasma wave echoes which appear in space at a third location following excitation at two discrete planes spaced along the magnetic field [1,3]. This thesis deals with cyclotron echoes which are characterized by the incident signal's wave vector and electric field and the static magnetic field being mutually perpendicular. The phenomenon occurs when the incident signal frequency is close to the electron gyrofrequency in a magnetic field $eB/m$.

The discovery of cyclotron echoes in plasmas was by Hill and Kaplan in 1965 [2]. They used an RF afterglow discharge in which a 21 MHz high power pulse repetitively ionized the working gas, which was either argon, neon, or nitrogen. During the intervals when the ionizing source was turned off they applied bursts of microwave energy in the X-band (8.2 - 12.4 GHz). Following two pulses separated by $\tau$ seconds there was a string of echo pulses at multiples of $\tau$ following the second pulse. After applying a third pulse at some variable time following the first two pulses, another string of pulses would appear at intervals of $\tau$ following the third pulse. They noted that the effect only occurred when the incident signals propagated perpendicular to the magnetic field in what is known as the extraordinary mode of propagation. If this mode propagates in an infinite plasma and the wave frequency approaches the upper hybrid resonance frequency [4], then the electric field becomes parallel to the direction of propagation and the

incident signal can couple to the longitudinal or electrostatic plasma waves [5].

Subsequent cyclotron echo work has been similar to Hill and Kaplan's, although the complexity of the phenomena prevents simple all-inclusive explanation. One important difference between Hill and Kaplan's first experiments and the work of other investigators is the small rectangular plasma bottle which Hill and Kaplan used instead of a long cylindrical plasma tube. The latter has much better uniformity in one dimension and is preferred since the electron density gradient perpendicular to the magnetic field has been identified as the source of the spread of oscillator frequencies.

## 1.2 Other Echo Systems

Echoes were originally discovered in 1950 in paramagnetic samples in which the system response is a rotation of the net magnetization vector [6]. Echoes have also been reported in electron spin resonance [7]; optical transitions in atoms [8]; ferrimagnetic resonance [9]; type II superconductors [10]; and certain silver alloys [11]. These diverse types of echoes suggest that any resonance phenomenon involving a large group of oscillators may produce echoes.

## 1.3 Gould Diagrams and Nonlinearity

A crucial concept in understanding echo processes is phase mixing. This is the process by which microscopic signals caused by some group of sources become sufficiently scrambled in phase so that the macroscopic sum of these signals becomes undetectable. The situation is analogous to the problem of incoherent vs. coherent radiation from a

group of $N$ sources. The power of an incoherent signal is proportional to $N$ but the coherent power is proportional to $N^2$. The important point is that the energy in the individual oscillators or signal sources has not been lost by collisions or any other mechanism and is still present in the system.

In the case of two-pulse cyclotron echoes, R. W. Gould has illustrated the basic processes of echo formation [12]. Consider a group of independent electrons in a slightly inhomogeneous magnetic field, so that there is a range of cyclotron resonant frequencies. Initially these electrons are at rest so that in a two-dimensional phase space diagram they would all be at the origin where $V_x = V_y = 0$. If an impulse is applied to the system, then all the electrons will be given the same initial velocity and the situation will be as in Figure 1.1a. Because of their different resonant frequencies they will soon spread out in phase space and produce situation (b) in which there is no net displacement with respect to the origin. This spreading in phase space will occur in $2\pi/\Delta\omega$ seconds, where $\Delta\omega$ is the spread of oscillator resonant frequencies, and this time can be used to define the maximum length of a signal burst that can be approximated by an impulse. The Fourier spectrum of the applied signal must be wider than the bandwidth of the resonant system.

After the phases of the oscillators have scrambled as in (b), a second impulse is applied at time $\tau$ after the first one. The response to this impulse soon phase mixes to zero and produces the situation in (d). At times $2\tau$ and $3\tau$ following the first impulse

# GOULD'S ECHO DIAGRAMS

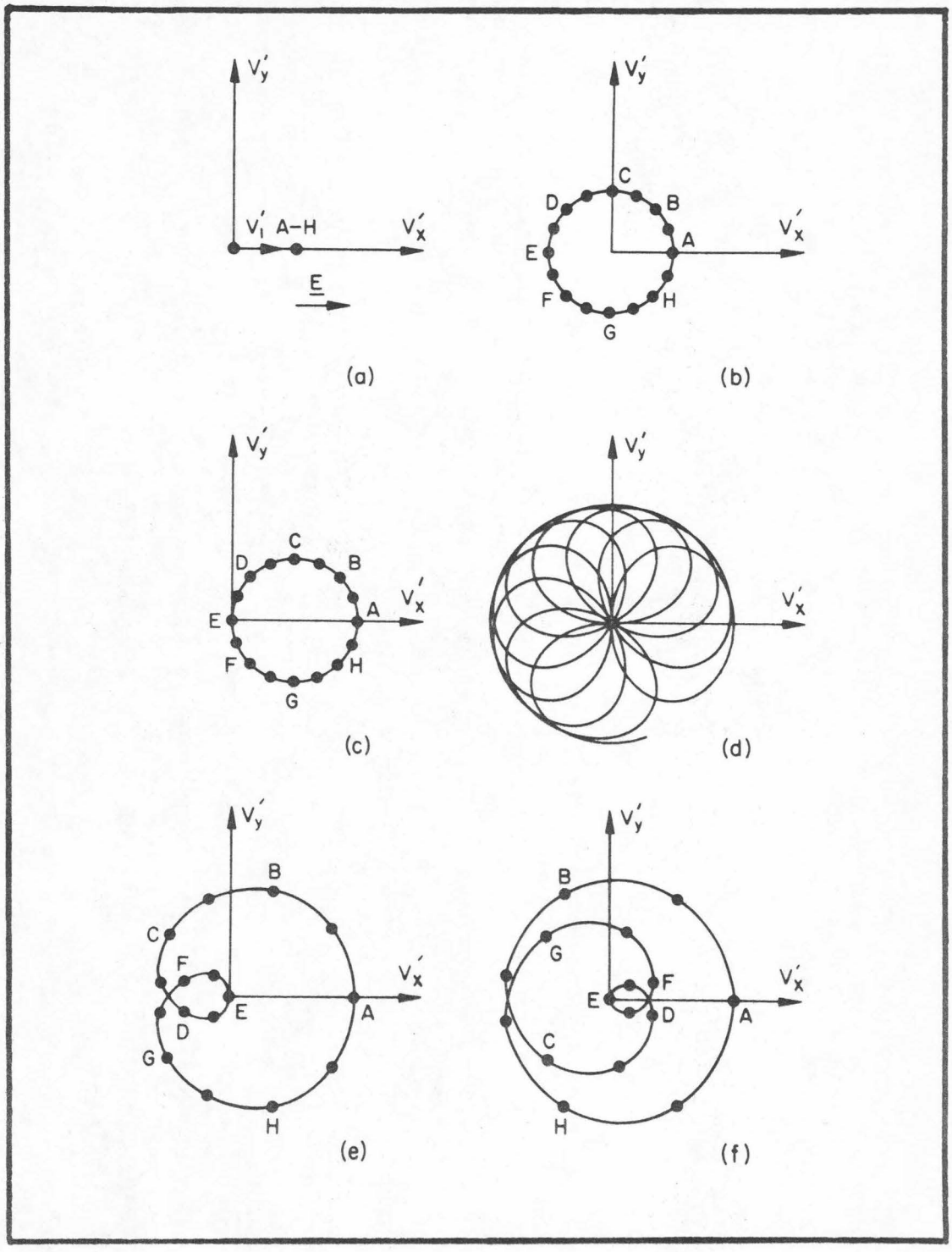


Fig. 1.1

the phase space pictures are (e) and (f) respectively. There is considerable symmetry in the configuration, but the total displacement weighted by distance from the origin and number at that distance is zero. However, if the high speed particles are preferentially removed from the plasma by more frequent collisions, then there will be a net displacement or echo which is out of phase at (e) and in phase at (f) with the applied pulses. We see that this collisional echo alternates in phase.

In general, any nonlinear process will spoil the phase mixing at times $n\tau$ and produce an echo. A linear system obeys the principle of superposition and the response to a group of stimuli is the sum of the responses caused by each stimulus acting alone.

To summarize, echoes require a spread of oscillator frequencies which phase mix to zero macroscopic response after a single pulse, but which do not dissipate their microscopic energy for a sufficiently long time, and echoes also require a nonlinear process to modify the phase mixing.

Several nonlinear mechanisms have been proposed for cyclotron echoes, including electron-neutral collisions in gases with a Ramsauer minimum and a strongly nonlinear collision frequency vs. electron speed curve; relativistic mass shifts; nonlinear oscillations due to sheath fields; and nonlinear oscillations due to electrostatic oscillations in a density gradient. In this work another possible source of nonlinearity is proposed: temperature dependent decay of ringing response by mode conversion into plasma waves.

## 1.4 Previous Cyclotron Echo Work

L. O. Bauer and F. Blum have worked on a $^{2PE}$ model in which the echoes are produced by nonlinear electrostatic oscillations of charge sheets in a one-dimensional model of the magnetized plasma [13]. The plasma is assumed to have a density gradient perpendicular to the plates of the exciting capacitor. As in other echo work, the dimensions of the plasma are small compared to a free space wavelength, so there is no phase change of the exciting wave as it crosses the plasma. As a charge sheet moves in response to an applied electric field, the ions which are left behind by the rapidly moving electrons create a restoring force which is not proportional to displacement because of the gradient in electron density. When the responses from all the independent charge sheets are summed, the small nonlinear frequency shift can accumulate during the several hundred cycles of oscillation between the second pulse and the echo time. In this theory, electrons are not removed, but the higher energy oscillators rotate from the positions on Gould's diagrams which they would have in linear oscillation. Thus one might expect a strong echo.

The experiments of Bauer and Blum clearly identified the spread of resonant frequencies caused by the density gradient, which is present in all laboratory plasmas, as an important source of echoes. This had been obscured in earlier x-band experiments because the range of upper hybrid frequencies was narrower relative to the cyclotron or signal frequency than it was in the S-band experiment of Bauer and Blum.

Although the echo was found to be largest when the center frequency of the applied pulses was near the maximum upper hybrid frequency

this did not prove anything about the nature of the nonlinearity because the echo will always peak where the density of oscillators in frequency space is largest. When they measured the power law of their echoes they obtained about 4 for the power laws of the first and second 2PE, whereas their theory predicted 3 and 5 respectively [14].

But by far the most serious objection to their echo theory is that the predicted echoes are much smaller than the measured echoes. The opposite situation could be explained in terms of loss mechanisms not included in the theory, such as e-n or Coulomb collisions, drifts parallel to the tube axis, etc. From Blum and Gould's paper [15], we see that the voltage amplitude of the first echo pulse is proportional to $\sqrt{J_1^2(z) + J_2^2(z)}$, where $z$ is approximately $\Delta\omega_H \tau/8 \cdot V_o^2/\omega_c^2 a^2$, $\tau$ is the spacing of the first two pulses, $V_o$ is the velocity acquired by an electron as a result of either of the first two pulses, $a$ is the density profile scale length, and $\Delta\omega_H = \{\omega_{po}^2 + \omega_c^2\}^{1/2} - \omega_c$. $\omega_{po}$ is the maximum plasma frequency $\omega_{po} = 5.64 \times 10^4 \{\text{MAX Ne}\}^{1/2}$. If $\tau = 10^{-7}$ sec, $a = 1$ cm, $V_o = 6 \times 10^7$ cm sec$^{-1}$ (1 eV), $\Delta\omega_H = 2\pi \times 10^8$, and $\omega_c = 2\pi \times 2.5 \times 10^9$ sec$^{-1}$, then the parameter $z$ is $1.15 \times 10^{-4}$. Using the small argument expansion $J_n(z) \approx \frac{1}{n!}(\frac{z}{2})^n$, we find that the first echo power is about 85 dB below the transient response. Since the echo is typically 20 dB down, the discrepancy is serious and indicates that the oscillating charge sheet model may not include the major source of nonlinearity.

Two-pulse echoes have been studied with considerable success by Henderson [16] who used the strongly varying electron-neutral collision

curve in argon to supply the nonlinearity, following the work of Crawford, Harp, and Bruce [20,21]. In his experiment Henderson was able to show agreement between theoretical and experimental echo phases. He operated at gas pressures of 20-200 microns, which were considerably higher than 1-20 microns considered by most other cyclotron echo experiments, including the one presented in this thesis. Thus e-n collisions were much more frequent in his case and seem to have been the dominant nonlinearity. However, when he tried to operate at lower pressures the experimental echo phases no longer agreed with theory [17]. Thus there is still room for work in the regime where collective effects seem to dominate single particle collisional effects.

None of the three previous investigators studied 3PE. The nonlinear oscillation model is ruled out because collisions would surely destroy electron phase memory over the time scale of microseconds on which 3PE exist. A thorough study of the e-n collisional nonlinearity has been made by R. L. Bruce [18,19], who had worked on echoes with Harp and Crawford [20,21]. His computed 2PE are quite strong, but his 2PE vs. input power curves have sharp phase reverses which are not experimentally observed. He assumed that his plasma density was low enough so that collective effects were negligible but the experiments described below show that this is not the case. Density effects were not included explicitly in his calculations, i.e., the electron density only specified the number of electrons participating and did not qualitatively affect the response.

Three models were considered for 3PE: (a) the highly excited particles lose phase more rapidly; (b) the fast particles diffuse down the discharge tube at a different rate; (c) the fast particles diffuse

more rapidly in a plane perpendicular to the static field and cause perturbations in the density. These models are named the collisional, parallel diffusion, and perpendicular diffusion models, respectively. The parallel diffusion model resulted in extremely small echo strengths and was discarded.

The perpendicular diffusion model involves accumulations and rarefactions of electrons in the plane perpendicular to the static magnetic field, thereby causing a perturbation in the number of oscillators experiencing a given local density and having a given upper hybrid resonance frequency. This would produce an echo linear with respect to the third pulse and would not require electron phase memory. This model was also discarded because it requires much higher input powers to make the theoretically predicted echoes as strong as the measured ones, i.e., the diffusion rate is too low. A further objection was the strong space charge which would be created if the necessary large fraction of electrons tried to move rapidly away from their neutralizing ion background.

It was decided on the basis of echo strength vs. input power curves that the collisional model was the one which agreed best with theory. However, the collisional model is nonlinear with respect to the third pulse amplitude. In reality 3PE are linear in the third pulse strength, as shown in this thesis and by the recall of stored pulses [18,21]. To exhibit explicitly this nonlinearity, we will repeat Bruce's derivation but with an independent third pulse amplitude.

Let the speeds which would be acquired by an electron if the first two impulses or the third impulse acted alone be denoted by $V_o$ and $V_p$, respectively. The impulse response of an electron is gyration at some local resonant frequency, so that in complex notation the velocity would be

$$V = V_x + jV_y = V_o\, e^{j\omega t} \tag{1.1}$$

The response to an arbitrary electric field is found by a convolution of the electric field and the impulse response

$$V = \frac{q}{m} \int_{-\infty}^{t} E(u)\, \exp[j\omega(t - u)]\, du$$

$$= \frac{q}{m}\, e^{j\omega t} \int_{-\infty}^{t} E(u)\, \exp(-j\omega u)\, du \tag{1.2}$$

Since the electric field is assumed to exist only for times between zero and the observation times, the range of integration can be extended to make

$$V(\omega) = \frac{q}{m}\, E(\omega) \tag{1.3}$$

where we have defined $V(\omega) = V(t)\, \exp(-j\omega t)$ .

If we use the current density

$$J = nq\, V(\omega)\, \exp(j\omega t) = J(t) \tag{1.4}$$

and the Green's function for the excitation of the dominant mode in a rectangular waveguide [22], and change to an integration over frequency space, we obtain Bruce's equation (2.9b)

$$E_p = -\frac{V_g \mu_o q}{ab} \int n(\omega)\, V(\omega)\, \exp(j\omega t)\, d\omega \qquad (1.5)$$

The imaginary part of $J$ has been manipulated, since it does not excite the dominant mode of the waveguide. $V_g$ is the waveguide phase velocity, $\mu_o$ is the permeability of free space, $q$ is the electron charge, and $a$ and $b$ are the waveguide width and height, respectively.

At the time of the third pulse, the electron velocity vector is assumed to have been spread into a spherical shell by electron-neutral collisions. The number of electrons at a given angle $\theta$ with respect to the $V_x$ axis is proportional to $\sin\theta$ and the normalized fraction of electrons is $\frac{1}{2}\sin\theta$ when integrating only over the $\theta$ coordinate in velocity space. The echo strength is evaluated from the $V_x$ component of the velocity just before application of the third impulse plus the third pulse speed $V_p$. At that time

$$V_x(\omega) = V_p + V' \cos\theta \qquad (1.6)$$

where

$$V' = 2V_o \left|\cos(\Omega\tau/2)\right| \qquad (1.7)$$

and due to the assumed wide bandwidth of the applied pulses it is only necessary to consider the difference $\Omega \equiv \omega - \omega_o$. $\omega_o$ is the mean upper hybrid frequency.

The speed at which the collision frequency after the third pulse must be evaluated is

$$V_3 = \{V_x^2 + V_y^2\}^{1/2} = \{(V_p + V'\cos\theta)^2 + (V'\sin\theta)^2\}^{1/2} \qquad (1.8)$$

Including an exponential collision factor for the particles which have lost their phase memory, the echo strength is

$$E = \frac{-V_g \mu_o q}{ab} \int_0^{\pi} \frac{\sin\theta\, d\theta}{2} \int d\omega\, n(\omega)\, e^{j\omega t}(V_p + V'\cos\theta) e^{-\nu\{V_3\}t} \qquad (1.9)$$

Now we normalize the echo to the transient response, which is

$$E_t = \frac{-V_g \mu_o q}{ab} \int d\omega\, n(\omega)\, V_p\, e^{j\omega t}\, d\omega = \frac{-2\pi V_g \mu_o V_p N(0)}{ab} \qquad (1.10)$$

where we have used

$$n(\omega) \equiv \int N(t')\, e^{-j\omega t'}\, dt' \qquad (1.11)$$

$$N(t) \equiv \frac{1}{2\pi} \int n(\omega)\, e^{j\omega t}\, d\omega \qquad (1.12)$$

Thus the normalized echo amplitude is

$$A = \frac{1}{2\pi N(0)} \int_0^{\pi} \frac{\sin\theta\, d\theta}{2} \int d\omega\, n(\omega)\, e^{j\omega t}\, e^{-\nu\{V_3\}t}\left(1 + \frac{V'}{V_p}\cos\theta\right) \qquad (1.13)$$

Now using the facts

$$\int d\omega\, e^{j\omega(t-t')} = 2\pi\, \delta(t - t') \qquad (1.14)$$

and

$$\frac{1}{2\pi} \int d\omega\, f(\omega)\, g(\omega)\, e^{j\omega t} = \int dt' f(t')\, g(t - t') \equiv f * g \qquad (1.15)$$

we obtain

$$A = \frac{N(t) * G(t)}{N(0)} \qquad (1.16)$$

where

$$G(\omega) = \int_0^{\pi} \frac{\sin\theta\, d\theta}{2} \left(1 + \frac{V'}{V_p}\cos\theta\right) e^{-t\nu\{V_3\}} \tag{1.17}$$

Now we must find $G(t)$ from

$$G(t) = \int e^{j\omega t}\, d\omega\, \frac{1}{2\pi} \int_0^{\infty} \frac{\sin\theta\, d\theta}{2} \left(1 + \frac{V'\cos\theta}{V_p}\right) e^{-t\nu\{V_3\}} \tag{1.18}$$

The integrand, except for the factor $e^{j\omega t}$, is periodic with period $2\pi/\tau$, so the integral can be reduced to a sum of sub-integrals. Recall that $\Omega \equiv \omega - \omega_o$

$$G(t) = \sum_{n=-\infty}^{\infty} \frac{1}{4\pi} \int_{-\pi/\tau + \frac{2\pi n}{\tau}}^{+\pi/\tau + \frac{2\pi n}{\tau}} d\Omega \tag{1.19}$$

In each sub-integral, replace $\Omega$ by $\Omega + 2\pi n/\tau$.

$$G(t) = \frac{1}{4\pi} \sum_{n=-\infty}^{\infty} \int_{-\pi/\tau}^{\pi/\tau} d\Omega\, e^{j\omega_o t}\, e^{j\Omega t}\, e^{j2\pi n t/\tau} \int_0^{\pi} \sin\theta\, d\theta$$

$$\times \left[1 + \frac{2V_o}{V_p}\cos\theta \left|\cos\frac{\Omega\tau}{2}\right|\right] \exp\left[-t\nu\left\{\sqrt{V_p^2 + V'^2 + 2V_p V'\cos\theta}\right\}\right]$$

$$= \frac{1}{4\pi}\left[\sum_{n=-\infty}^{\infty} e^{j2\pi n t/\tau}\right] \int_{-\pi/\tau}^{\pi/\tau} d\Omega\, e^{j\omega_o t}\, e^{j\Omega t} \int_0^{\pi} \sin\theta\, d\theta$$

$$\times \left[1 + \frac{2V_o}{V_p}\cos\theta\cos\frac{\Omega\tau}{2}\right] \exp[-t\nu\{V_3\}] \tag{1.20}$$

By applying a convergence factor to the geometric series, one can show

$$\sum_{n=-\infty}^{\infty} e^{j2\pi n t/\tau} = \sum_{n=-\infty}^{\infty} \delta\left(\frac{t}{\tau} - n\right) \equiv \text{ш}(t/\tau) \tag{1.21}$$

Let $\Omega\tau = \phi$ , $d\Omega \rightarrow d\phi/\tau$

$$G(t) = \frac{1}{4\pi} \frac{\text{Ш}(t/\tau)}{\tau} e^{j\omega_o t} \int_{-\pi}^{\pi} d\phi \; e^{j\frac{\phi t}{\tau}} \int_{0}^{\pi} \sin\theta \, d\theta \left[1 + \frac{2V_o}{V_p}\right.$$

$$\left. \times \cos\theta \cos\frac{\phi}{2}\right] \exp\left[-t\nu\left\{\sqrt{V_p^2 + 4V_o^2 \cos^2\frac{\phi}{2} + 4V_p V_o \cos\theta \cos\frac{\phi}{2}}\,\right\}\right] \tag{1.22}$$

Because $\cos\phi$ is an even function, the $\phi$ integration can be rewritten to give

$$G(t) = \frac{1}{2\pi} \frac{\text{Ш}(t/\tau)}{\tau} e^{j\omega_o t} \int_{0}^{\pi} d\phi \int_{0}^{\pi} \sin\theta \, d\theta \cos\frac{\phi t}{\tau} \left[1 + \frac{2V_o}{V_p}\right.$$

$$\left. \times \cos\theta \cos\frac{\phi}{2}\right] \exp\left[-t\nu\left\{\sqrt{V_p^2 + 4V_o^2 \cos^2\frac{\phi}{2} + 4V_p V_o \cos\theta \cos\frac{\phi}{2}}\,\right\}\right] \tag{1.23}$$

Because of $\text{Ш}(t/\tau)$, $\cos\phi t/\tau$ is equivalent to $\cos n\phi$ . If $\nu_o$ denotes the collision frequency at an electron speed of $V_o$, and if we use a square law collision frequency curve, we obtain

$$G(t) = \frac{1}{2\pi} \frac{\text{Ш}(t/\tau)}{\tau} e^{j\omega_o t} \int_{0}^{\pi} d\phi \int_{0}^{\pi} \sin\theta \, d\theta \cos n\phi \left[1 + \frac{2V_o}{V_p}\right.$$

$$\left. \times \cos\theta \cos\frac{\phi}{2}\right] \exp\left[-t\nu_o\left(\frac{V_p^2}{V_o^2} + 4\cos^2\frac{\phi}{2} + 4\frac{V_p}{V_o}\cos\theta\cos\frac{\phi}{2}\right)\right] \tag{1.24}$$

Thus the final answer for the echo amplitude is

$$A = \frac{N(t)}{N(0)} * \left\{\frac{\text{Ш}(t/\tau) e^{j\omega_o t}}{\tau} C_n(t)\right\} \tag{1.25}$$

where

$$C_n(t) = \frac{1}{2\pi}\int_0^{\pi} d\phi \int_0^{\pi} \sin\theta \cos n\phi \, d\theta [1 + \frac{2V_o}{V_p}\cos\theta \cos\frac{\phi}{2}]$$

$$\times \exp[-t\nu_o(\frac{V_p^2}{V_o^2} + 4\cos^2\frac{\phi}{2} + 4\frac{V_p}{V_o}\cos\theta\cos\frac{\phi}{2})] \qquad (1.26)$$

When $V_p = V_o$, this is equal to Bruce's result [23]. It is quite obvious that the result is nonlinear with respect to the third pulse amplitude $V_p$, and thus the collisional 3PE model is in qualitative disagreement with experiment.

From this brief introduction we see that the quantitative and qualitative properties of cyclotron echoes are still unclear six years after their discovery. We will now discuss experimental results which make clearer the physical processes responsible for three-pulse echoes.

## 1.5 References for Chapter I


1. T. M. O'Neil and R. W. Gould, Phys. Fluids 11, 134 (1968).
2. R. M. Hill and D. E. Kaplan, Phys. Rev. Lett. 14, 1062 (1965).
3. J. H. Malmberg, C. B. Wharton, R. W. Gould and T. M. O'Neil, Phys. Fluids 11, 1147 (1968).
4. M. A. Heald and C. B. Wharton, Plasma Diagnostics with Microwaves, John Wiley & Sons, New York, 1965, p. 34.
5. T. H. Stix, Phys. Rev. Lett. 15, 878 (1965).
6. E. L. Hahn, Phys. Rev. 80, 580 (1950).
7. J. P. Gordon and K. D. Bowers, Phys. Rev. Lett. 1, 368 (1958).
8. N. A. Kurnit, I. D. Abella, and S. R. Hartmann, Phys. Rev. Lett. 13, 567 (1964).
9. D. E. Kaplan, Phys. Rev. Lett. 14, 254 (1965).
10. I. B. Goldberg, E. Ehrenfreund, and M. Weger, Phys. Rev. Lett. 20, 539 (1968).
11. R. J. Snodgrass, Phys. Rev. Lett. 24, 864 (1970).
12. R. W. Gould, Am. Jour. Phys. 37, 585 (1969).
13. L. O. Bauer, F. A. Blum, and R. W. Gould, Phys. Rev. Lett. 20, 435 (1968); L. O. Bauer and F. A. Blum, Phys. Fluids 13, 2162 (1970).
14. L. O. Bauer, Ph.D Thesis, California Institute of Technology, May 1968, p. 114.
15. R. W. Gould and F. A. Blum, Proc. 8th Int. Conf. on Phenomena in Ionized Gases, Vienna, Austria, August 1967, Springer Verlag, Vienna, 1967, p. 405.
16. D. M. Henderson, Ph.D Thesis, Yale University, 1970; D. M. Henderson and J. L. Hirshfield, Bull. Am. Phys. Soc. 14, 1008 (1969).
17. D. M. Henderson, private communication.

18. R. L. Bruce, Ph.D Thesis, Stanford University, 1969.

19. R. L. Bruce, Jour. Plasma Phys. 5, Part 3, 385 (1971).

20. F. W. Crawford and R. S. Harp, Phys. Lett. 1, 292 (1966); F. W. Crawford and R. S. Harp, Jour. Appl. Phys. 37, 4405 (1966).

21. R. S. Harp, R. L. Bruce, and F. W. Crawford, Jour. Appl. Phys. 38, 3385 (1967).

22. R. E. Collin, Field Theory of Guided Waves, McGraw-Hill, New York, 1960, pp. 198-200.

23. Reference 18, p.96.

# II. EXPERIMENTAL ECHO WORK

## 2.1 Experimental Setup and Diagnostic Techniques

Most of the experiments used argon, although helium and neon were occasionally used. Electrons have only elastic collisions in these gases under our experimental conditions. The gas was admitted to the discharge region by differential pumping. The end of the tube opposite the leak and gate valves was sealed. A simple finger style $LN_2$ cold trap was installed between the experimental region and the vacuum pump. The gas pressure was measured by a Hastings thermocouple gauge about 25 cm from the gas inlet point, and the pressure readings were corrected for the different gases using the charts supplied with the gauge.

The experimental geometry is typical of echo experiments (Fig. 2.1). An S-band waveguide passed between two Helmholtz coils in a plane perpendicular to the static magnetic field which was uniform to at least .1% . The discharge tube was about one meter long and 2.6 cm in inside diameter. It passed through the short sides of the waveguide and was parallel to the magnetic field. A hybrid or magic tee was connected between the plasma arm of the waveguide system and a dummy arm which had an identical hole and a length of open glass tube to balance the plasma tube. Waveguide terminations closed the ends of the bridge arms for the echo experiments. The magic tee was adjusted by means of slide screw tuners to form a balanced bridge in which the reflection from the holes, glass tubes, and irregularities was 50 dB below the pulse amplitude caused by shorting one arm of the bridge.

The imbalance signal caused by the plasma went from the fourth arm of the bridge through a precision attenuator and a traveling wave tube amplifier. A filter with a bandpass of 100 MHz centered on 2.5 GHz was used between the traveling wave tube and the crystal detector to reduce noise. The detected signals were displayed with either a Tektronix type 585 oscilloscope, a sampling plug-in unit, or a boxcar integrator.

The master timer of the experiment was a Tektronix type 162 pulse generator operated at about 50 Hz (Fig. 2.2). This triggered a Tektronix type 161 square wave generator which gated on the oscillator tube of an RF transmitter, and this produced the discharge by an electric field between two copper bands wrapped around the discharge tube. The negative-going trailing edge of the square wave pulse marked the beginning of the afterglow and triggered time base B of the type 585 oscilloscope, which operated in the "A delayed by B" mode. The delayed output triggered the two or three HP type 214A pulse generators which turned on a Litton 10W traveling wave tube. The tube was normally biased out of conduction and received a continuous S-band input signal from a Hewlett Packard type 616A generator. The pulsed microwave signals went through an isolator to the first arm of the microwave bridge.

For some of the echo experiments a 1 KW Hughes traveling wave tube was used to produce the third pulse. This tube required a 1 watt continuous drive signal. The grid was biased too negatively to be driven by a transformer, so a blocking oscillator was used. The output of the two pulsed traveling wave tubes was combined in a coaxial

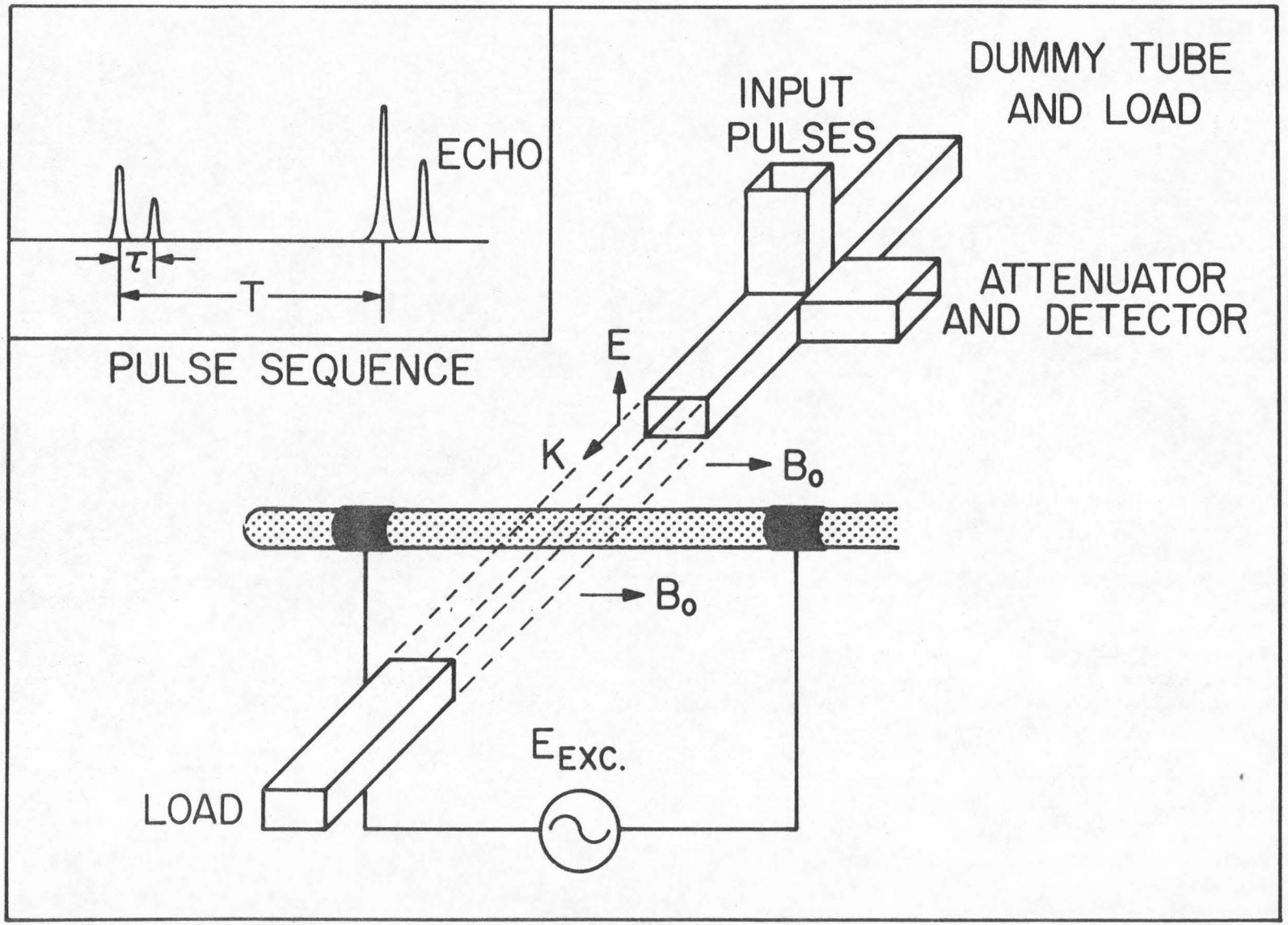


Fig. 2.1 Waveguide Orientation and Pulse Sequence

hybrid.

The average electron density was measured by a reflection technique developed by Bruce and Harp [1]. This method has the advantage that the same bridge setup is used for both the echo experiment and the density measurement. The plasma column is modeled as a uniform dielectric cylinder with the cold plasma dielectric constant

$$\frac{\varepsilon_p}{\varepsilon_o} = 1 - \frac{\omega_p^2}{\omega^2 - \omega_c^2}$$

This method is valid when the signal frequency is far enough above the maximum upper hybrid frequency so that the reflection coefficient is small. The scattering from such a column in a waveguide was calculated and a proportionality was found between the measured reflection coefficient $\Gamma$ and the susceptibility $(\varepsilon - 1)$ of the plasma. The proportionality constant is evaluated for the particular waveguide system by measuring the reflection from a glass tube of the same sort as the plasma tube which is filled with styrofoam of known dielectric constant. The dielectric constant of the styrofoam was determined by filling a resonant cavity with it and measuring the shift of the resonant frequency. The bridge was balanced for the density measuring frequency by a slide screw tuner which was only used for this purpose and could be conveniently removed for the echo experiments. The CW bridge balance was better than 60 dB, and the wide spectrum pulses could only be balanced to 50 dB. The frequency used for the density measurements was 2.95 GHz when the cyclotron frequency was 2.5 GHz. The density measurements used microwave pulses about 500 nsec long, so the method is capable of time-resolved density

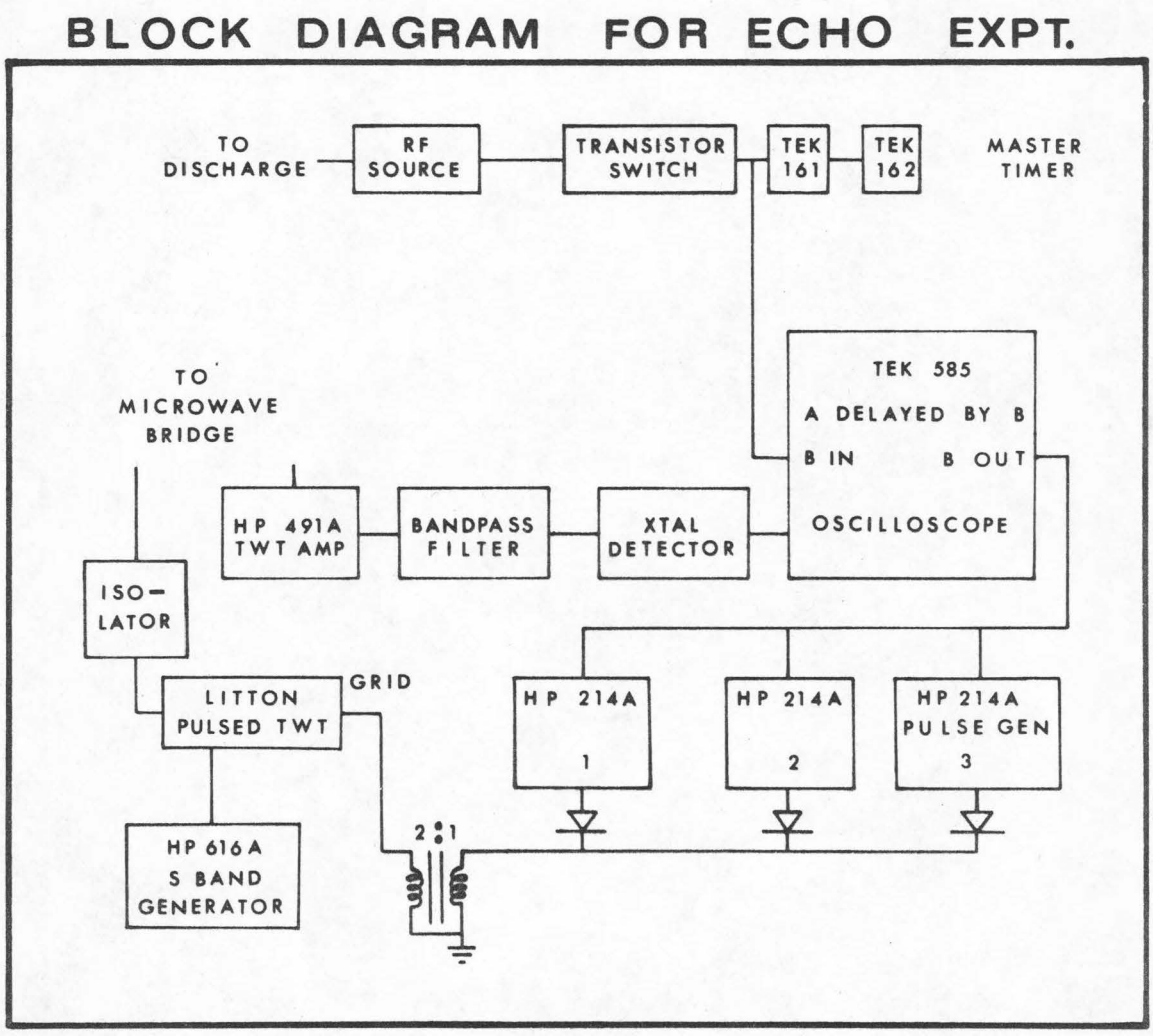
BLOCK DIAGRAM FOR ECHO EXPT.
TO DISCHARGE
RF SOURCE
TRANSISTOR SWITCH
TEK 161
TEK 162
MASTER TIMER
TO MICROWAVE BRIDGE
TEK 585
A DELAYED BY B
B IN
B OUT
OSCILLOSCOPE
HP 491A TWT AMP
BANDPASS FILTER
XTAL DETECTOR
ISO-LATOR
LITTON PULSED TWT
GRID
HP 214A 1
HP 214A 2
HP 214A PULSE GEN 3
HP 616A S BAND GENERATOR
2:1

Fig. 2.2

determination. The reflected signals were measured with the HP precision attenuator to avoid the nonlinear crystal response. The calibration curve for average densities is shown in Fig. 2.3.

It was also possible to measure the peak densities in a time-resolved manner by sweeping the frequency of a low amplitude test pulse in an absorption setup. One method replaced the hybrid tee with a 20 dB waveguide dual directional coupler. A short was placed beyond the plasma so that the signal returned by the plasma-containing section of waveguide would be equal in amplitude to the incident signal except for absorption by the plasma. Any leakage through the waveguide holes was ignored because the absolute magnitude of the absorption was of little significance. Also, cold plasma absorption experiments have been done in similar waveguide geometries with considerable success [2]. The test pulse did not perturb the plasma since it was 40 or 50 dB lower in power than the typical echo producing pulses. The first 100 nsec of the 500 nsec test pulse was created by a Hewlett Packard S-band sweep generator and an HP PIN diode modulator. As the test pulse frequency is swept from below the cyclotron frequency, the signal abruptly begins to decrease at the cyclotron frequency, reaches a minimum, then rises to its original value at the maximum upper hybrid frequency. This is shown on an inverted scale by Fig. 2.17.

There is a second method of obtaining peak densities at a given afterglow time which is simpler than the PIN diode modulated method. A CW signal of one microwatt or less is sent into the absorption microwave setup. The signal will be absorbed during the RF breakdown pulse, and the absorption will cease when there is no longer

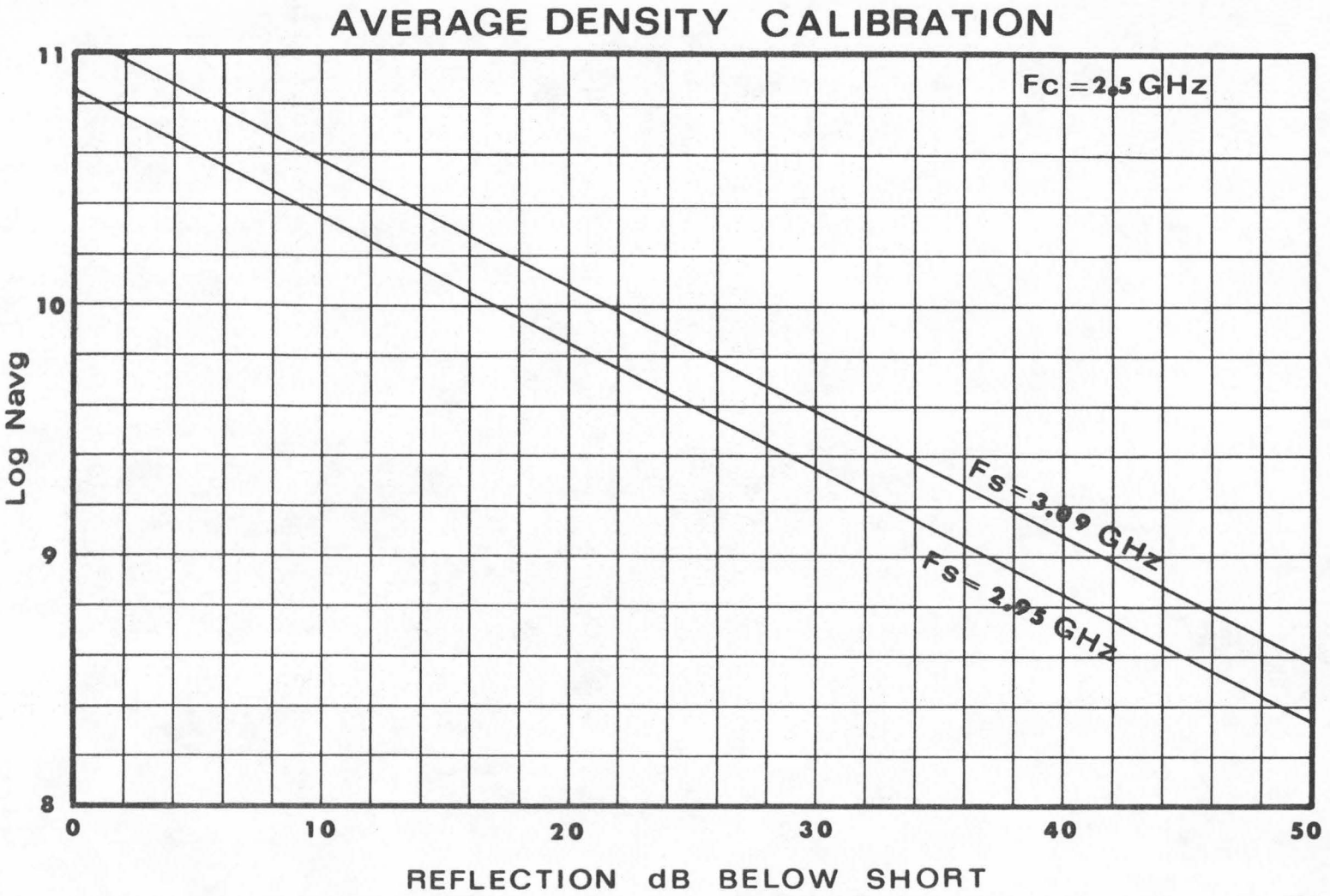


Fig. 2.3 Average Density vs. Reflection Coefficient

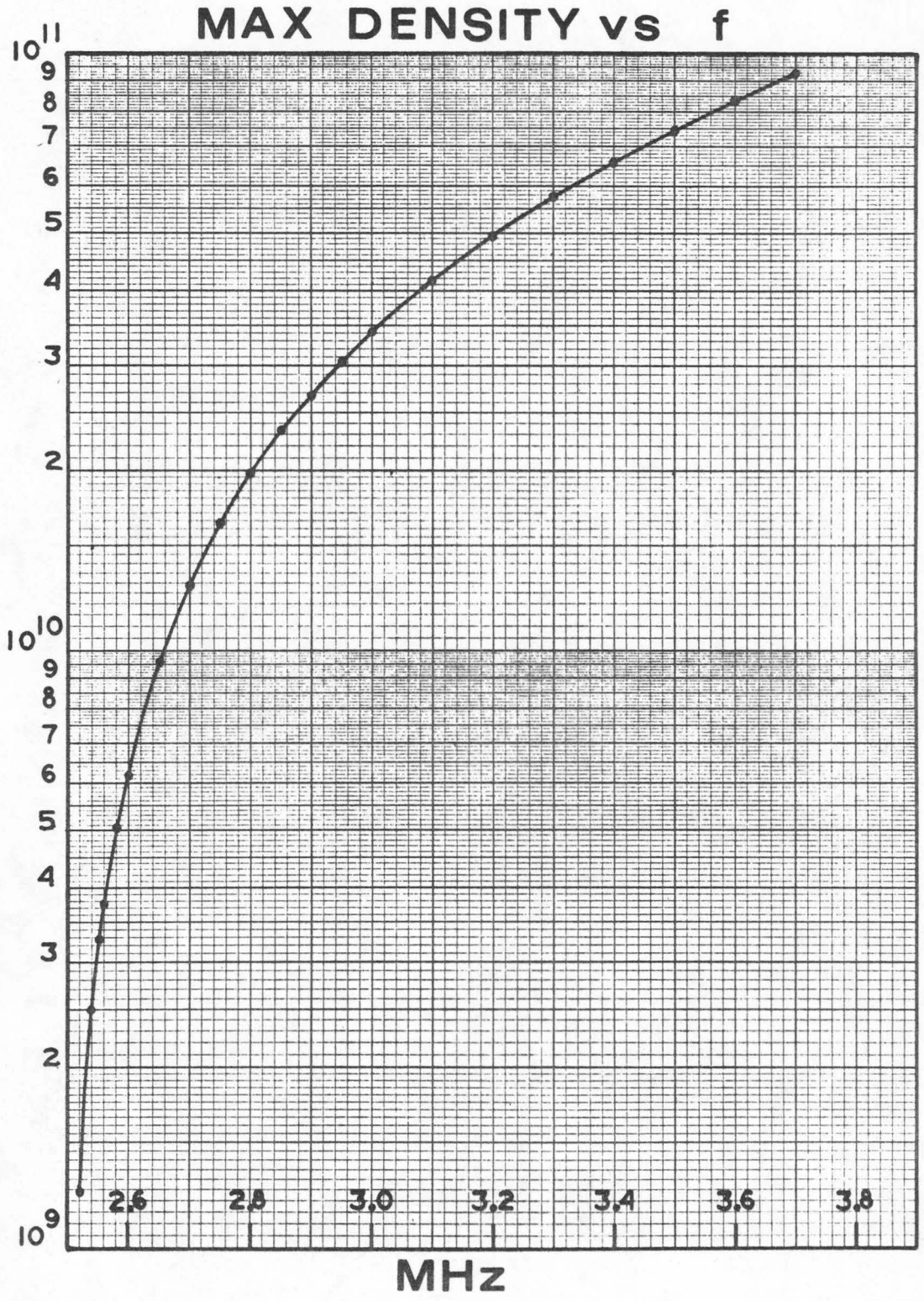


Fig. 2.4 Maximum Density vs. Frequency

an upper hybrid layer in the plasma for the signal frequency. For a fixed cyclotron frequency one can plot $Ne_{max}$ vs. the signal frequency for which the absorption ceases at the desired time [3]. Such a curve is shown in Fig. 2.4.

## 2.2 3PE Linearity

As noted above, one of the essential differences between 3PE and 2PE is that the former are linear wih respect to the third pulse and the latter are nonlinear with respect to the amplitudes of either of the first two pulses. This linearity was shown in an experiment using up to 1 KW peak power pulses for the third pulse [4]. The afterglow time was adjusted at several different argon gas pressures so that the average density was held constant. As shown in Fig. 2.5, the three-pulse echo was quite linear over a wide range of input power. The maximum echo decreased as the gas pressure increased, and this was attributed to the effects of e-n collisions in the 50 nsec between the third pulse and the echo.

For these experiments the spacing of the first two pulses was 50 nsec, and the spacing of the first and third pulses was 800 nsec. The shorted input of the first two pulses was at 46.6 on the scale of Fig. 2.5, so the echo is 3 dB larger than the input pulse. The 10W tube was attenuated by 20 dB and the average density was $3.4 \times 10^{9} cm^{-3}$. Figure 2.6 shows the results of another experiment as a superposition of three sampling scope traces: the first two pulses shorted with no plasma, the third input pulse shorted with no plasma and attenuated 15 dB, and the echo. Since the transient response is typically 15 dB

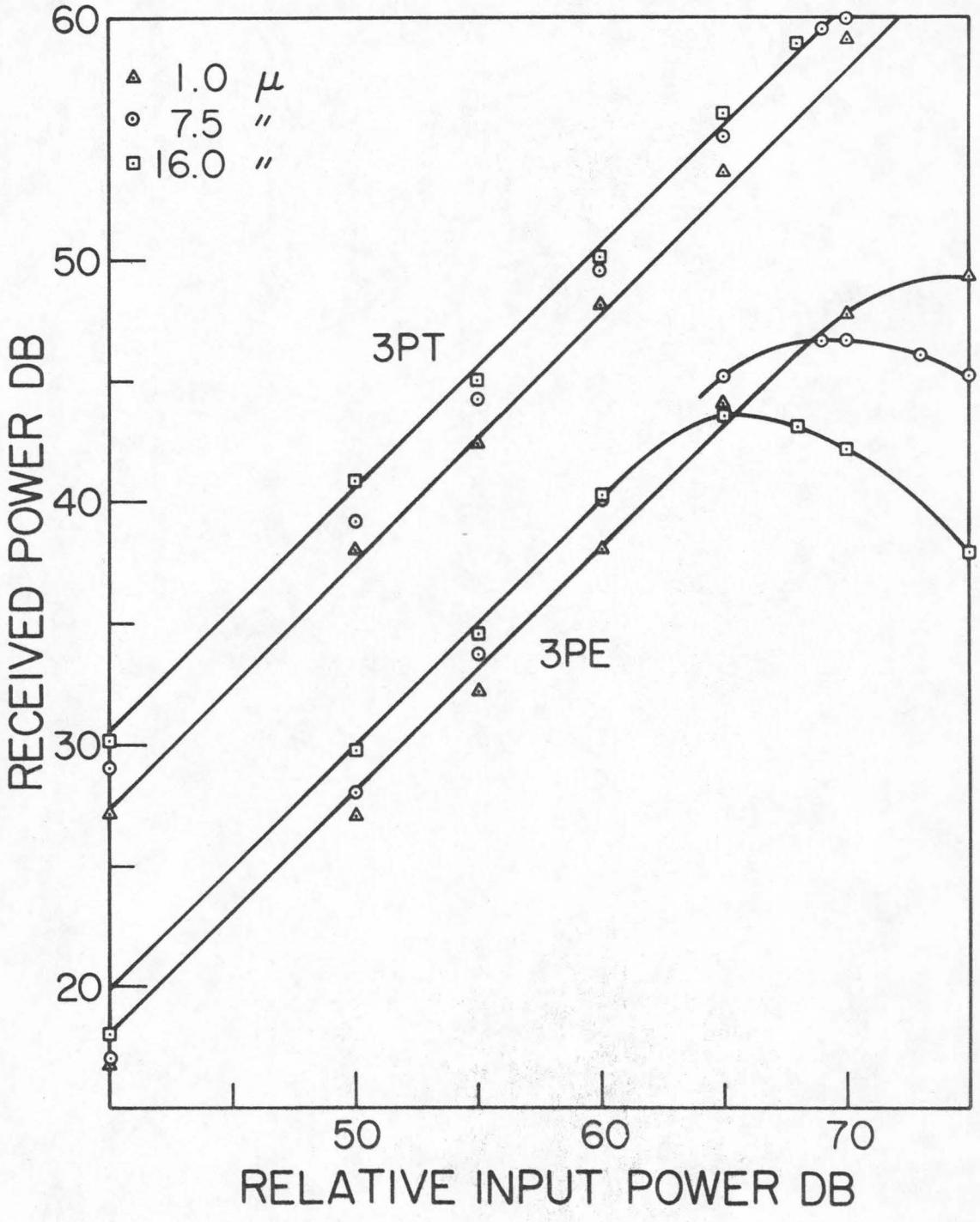


Fig. 2.5 3PE Linearity wrt Third Pulse

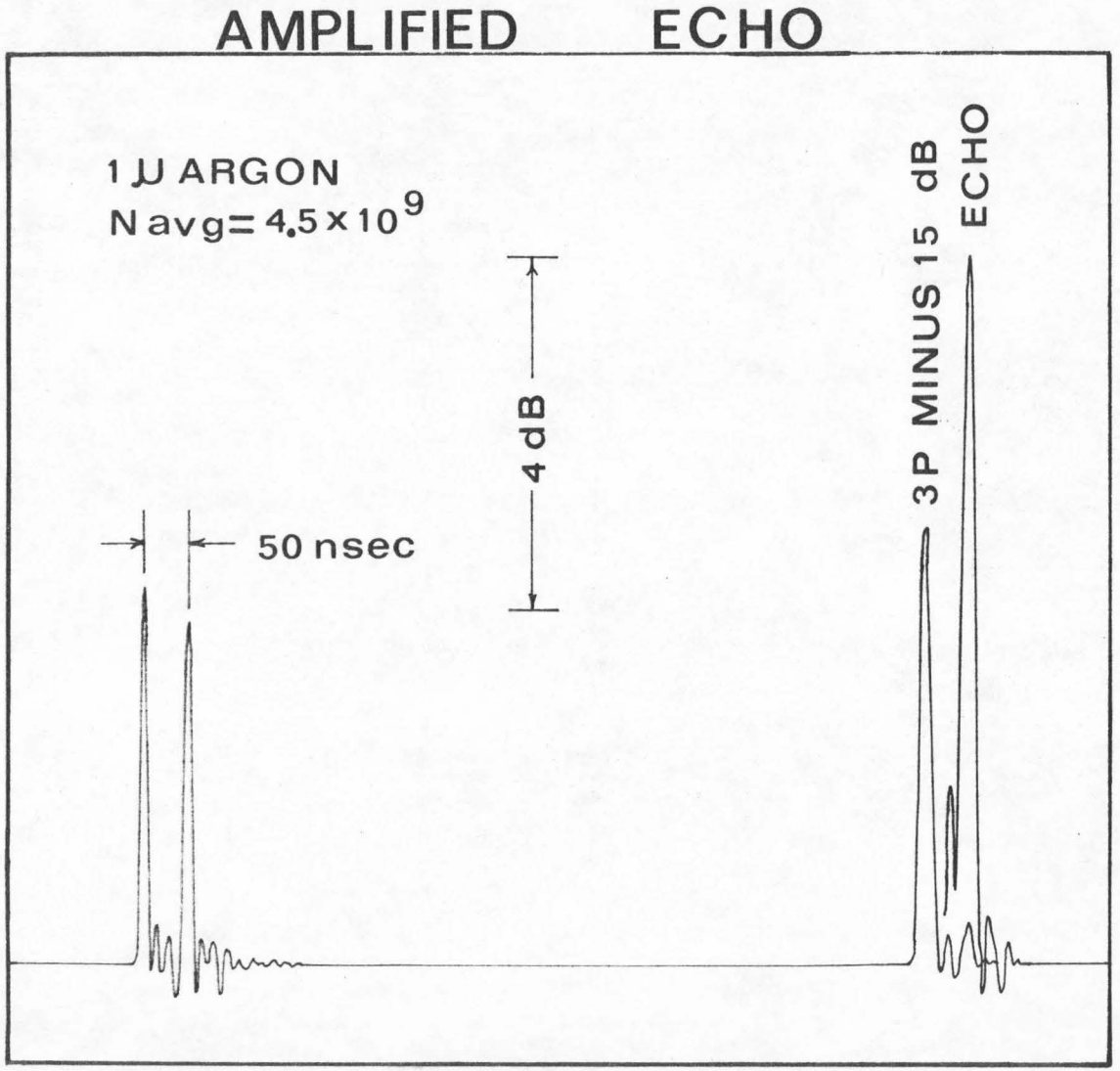
AMPLIFIED ECHO
1 J ARGON
N avg = 4.5 x 10^9
4 dB
50 nsec
3P MINUS 15 dB
ECHO

Fig. 2.6

below the input pulse amplitude, with better coupling to the plasma substantial amplification of these pulses should be possible.

## 2.3 3PE vs. Density Gradient

Although it is not known how to measure the profile of such small low density plasmas since they are too small for interferometry and too rarified to be probed, it was possible by the methods already mentioned to find the ratio of peak to average electron density and compare it with the 3PE. Such an experiment produced the results of Fig. 2.7, which shows that the echo strength continues to grow even though the density is decreasing. For this experiment $\tau$ = 100 nsec, the spacing of the second and third pulses was 500 nsec, and all pulse powers were equal. This echo is not normalized to the 3P transient. The results seem to show that a strong density gradient is important in the creation of echoes, and this was originally interpreted as support for the perpendicular diffusion model.

## 2.4 Experimental Dependence on Pulse Power and Neutral Gas Pressure

Because Bruce's 3PE model invokes e-n collisions as the nonlinearity, experiments in which the electron density was fixed and the background gas pressure was changed were performed to determine whether the model is valid. The third pulse position reflects the number of collisions which an electron has experienced since the first two pulses, and the number of collisions is directly proportional to the gas pressure. Figure 2.8 shows the results of an experiment in argon at an average electron density of $2 \times 10^{9} cm^{-3}$. There was no consistent variation with pressure. That is, the optimum third pulse spacing T

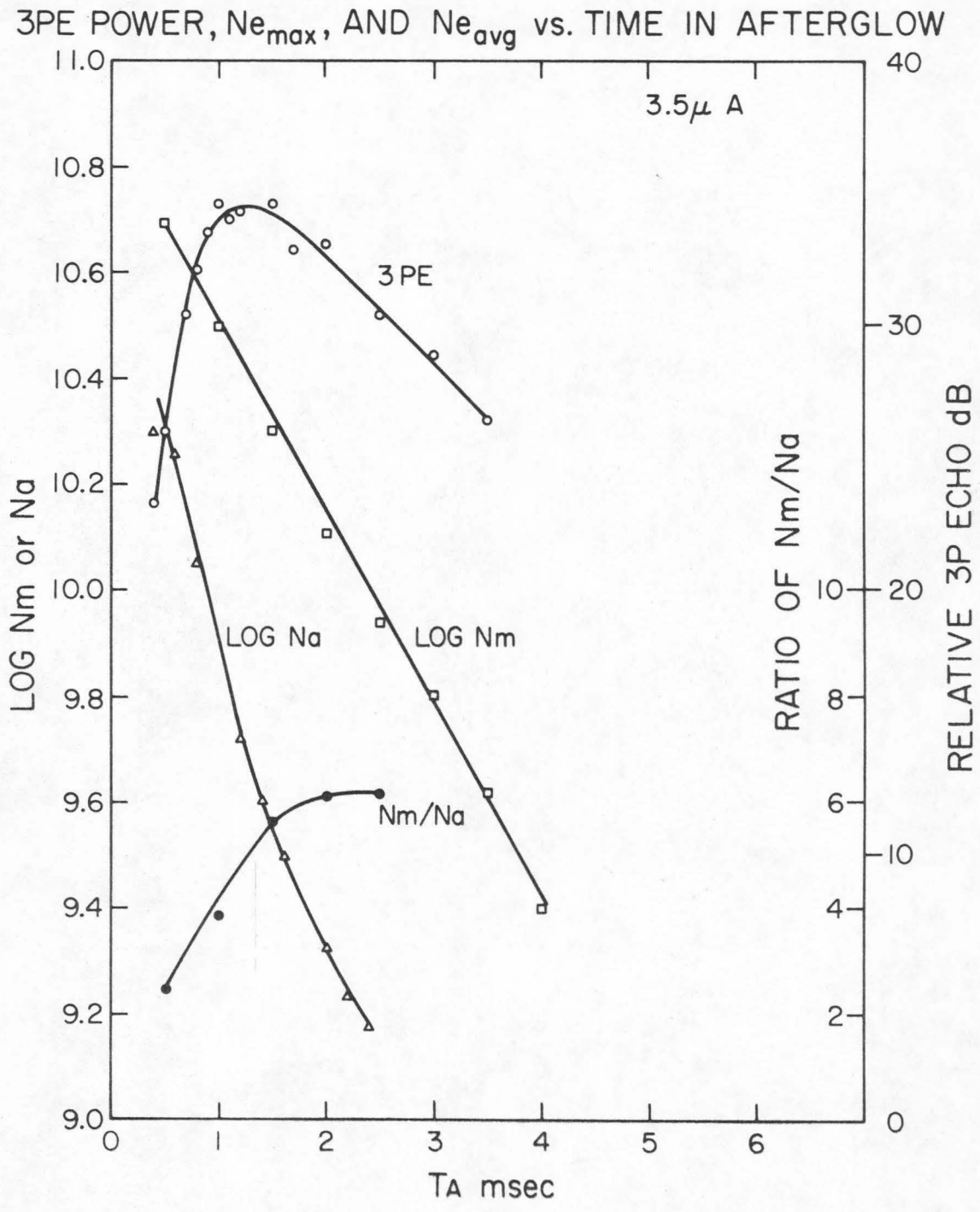
3PE POWER, Ne$_{max}$, AND Ne$_{avg}$ vs. TIME IN AFTERGLOW
3.5μ A
3PE
LOG Na
LOG Nm
Nm/Na
LOG Nm or Na
RATIO OF Nm/Na
RELATIVE 3P ECHO dB
TA msec
11.0
10.8
10.6
10.4
10.2
10.0
9.8
9.6
9.4
9.2
9.0
40
30
20
10
8
6
4
2
0
0
1
2
3
4
5
6

Fig. 2.7

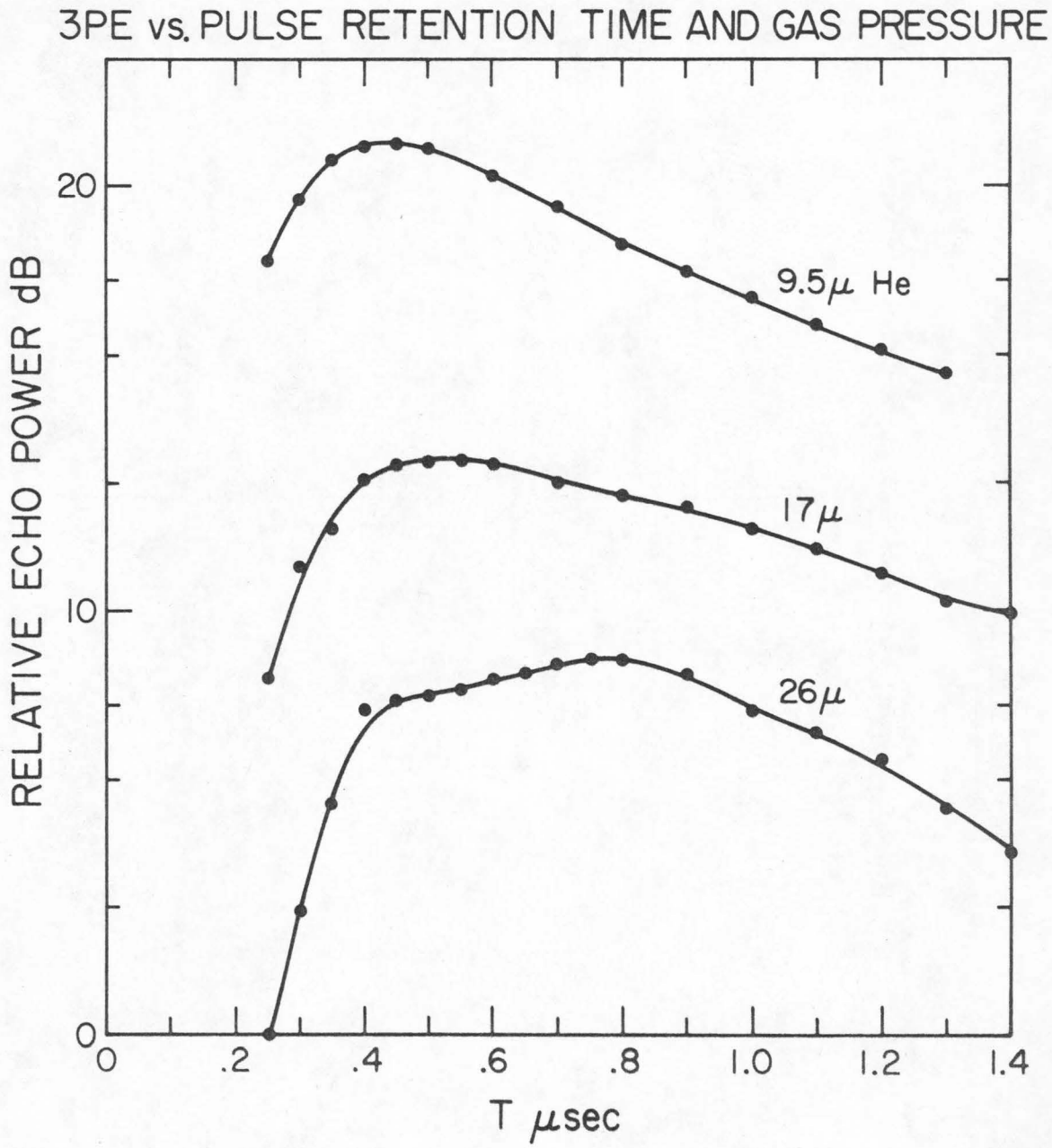
3PE vs. PULSE RETENTION TIME AND GAS PRESSURE
RELATIVE ECHO POWER dB
20
10
0
9.5μ He
17μ
26μ
0
.2
.4
.6
.8
1.0
1.2
1.4
T μsec

Fig. 2.8

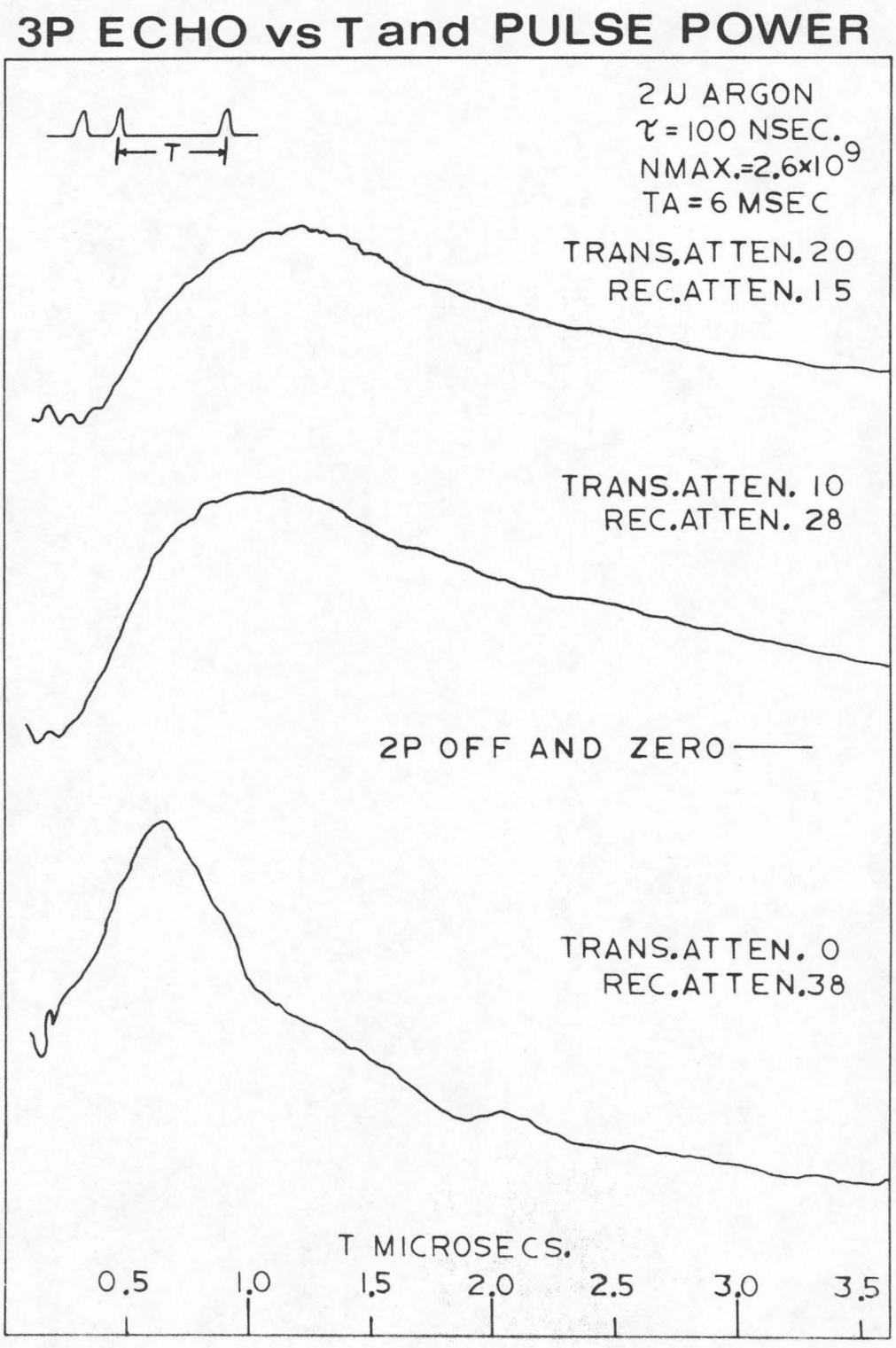
3P ECHO vs T and PULSE POWER
T
2 μ ARGON
τ = 100 NSEC.
NMAX.=2.6×10^9
TA = 6 MSEC
TRANS.ATTEN. 20
REC.ATTEN. 15
TRANS.ATTEN. 10
REC.ATTEN. 28
2P OFF AND ZERO
TRANS.ATTEN. 0
REC.ATTEN.38
T MICROSECS.
0.5
1.0
1.5
2.0
2.5
3.0
3.5

Fig. 2.9

was not inversely proportional to pressure, which one would expect if collisions created the conditions for three-pulse echoes.

Pulse power was also investigated as a parameter in 3PE vs. T experiments. Here there was a significant effect: at the higher input powers the echo peaked at lower $T_{max}$, but at low to moderate powers $T_{max}$ did not change. The dominant factor in the decay of the echo was later interpreted to be thermal free streaming and the loss of hot electrons. In Fig. 2.9 all three incident pulses are attenuated together, and the receiver attenuator is varied to keep the curve amplitudes similar. Because the echoes are linear with respect to the third pulse amplitude, $T_{max}$ depends upon the first two pulses. Although there is some dependence upon pulse power, it is clearly not the most important parameter in creating 3PE.

## 2.5 3PE Dependence upon Electron Density

The collisional model of 3PE is discredited by the insensitivity of the optimum third pulse position to the background gas pressure and thus to the e-n collision frequency. Because the third pulse acts as a linear readout of the echo-producing conditions, the most significant interval is that between the second and third pulses. Although e-n collisions do not seem to be important during that interval in creating echoes, the density of electrons has a simple and powerful influence on the growth and decay of three-pulse echoes. As the density decreases, it takes longer for the echo to peak after the first two pulses and the decay is also slower. The density is changed by experimenting at different times in the afterglow at fixed gas pressure. We know from

R. Stenzel's work in essentially identical systems that the plasma temperature initially decreases rapidly in the afterglow [2], then levels off, hence as TA is varied we believe that the temperature is relatively constant. Figures 2.10 and 2.11 show the effects of electron density on the growth and decay of 3PE in helium and argon, respectively. There is a slight difference in the meanings of T in the two curves: in Fig. 2.10 T is measured between the first and third pulses, while in Fig. 2.11 it is measured between the second and third pulses. In Fig. 2.10 a cold trap was used, and the lowest curve was taken with 6 dB higher sensitivity than the other two curves. In this case the echo amplitude increased from .4 to 1.0 milliseconds even though the density decreased. In Fig. 2.11 TA is the afterglow time in milliseconds, RA is the receiver attenuation in dB, Nm is the measured maximum electron density, and dB is the power ratio in dB between the transient response and the echo strength at T = 1 μsec. From these results it is clear that the electron density is the dominant parameter in the echo processes between the second and third pulses.

## 2.6 Similarities of 2PE and 3PE

The electron density is a dominant parameter in the creation of 2PE as well as 3PE. An experiment was performed to show this by measuring the amplitude of the 2PE as $\tau$ was varied. The results are in Fig. 2.12 in which the second pulse is centered on zero of the time scale and the first pulse is moved successively further from the second pulse. For each $\tau$ a boxcar integrator with a time window of 10 nsec scans the crystal detector output after the second pulse and records the first 2PE pulse. As $\tau$ is varied, the echoes form an envelope

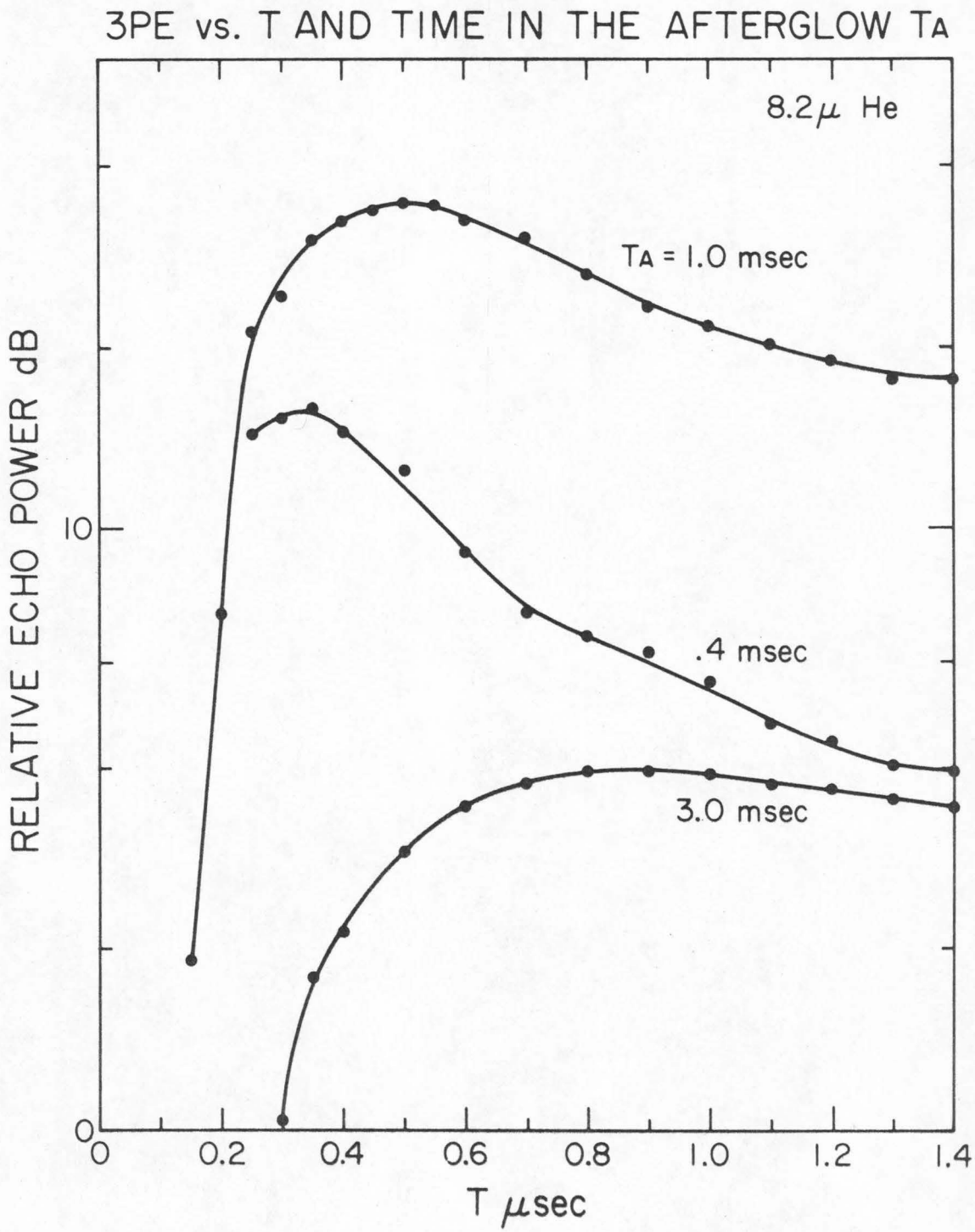
3PE vs. T AND TIME IN THE AFTERGLOW TA
8.2μ He
TA = 1.0 msec
.4 msec
3.0 msec
RELATIVE ECHO POWER dB
10
0
0
0.2
0.4
0.6
0.8
1.0
1.2
1.4
T μsec

Fig. 2.10

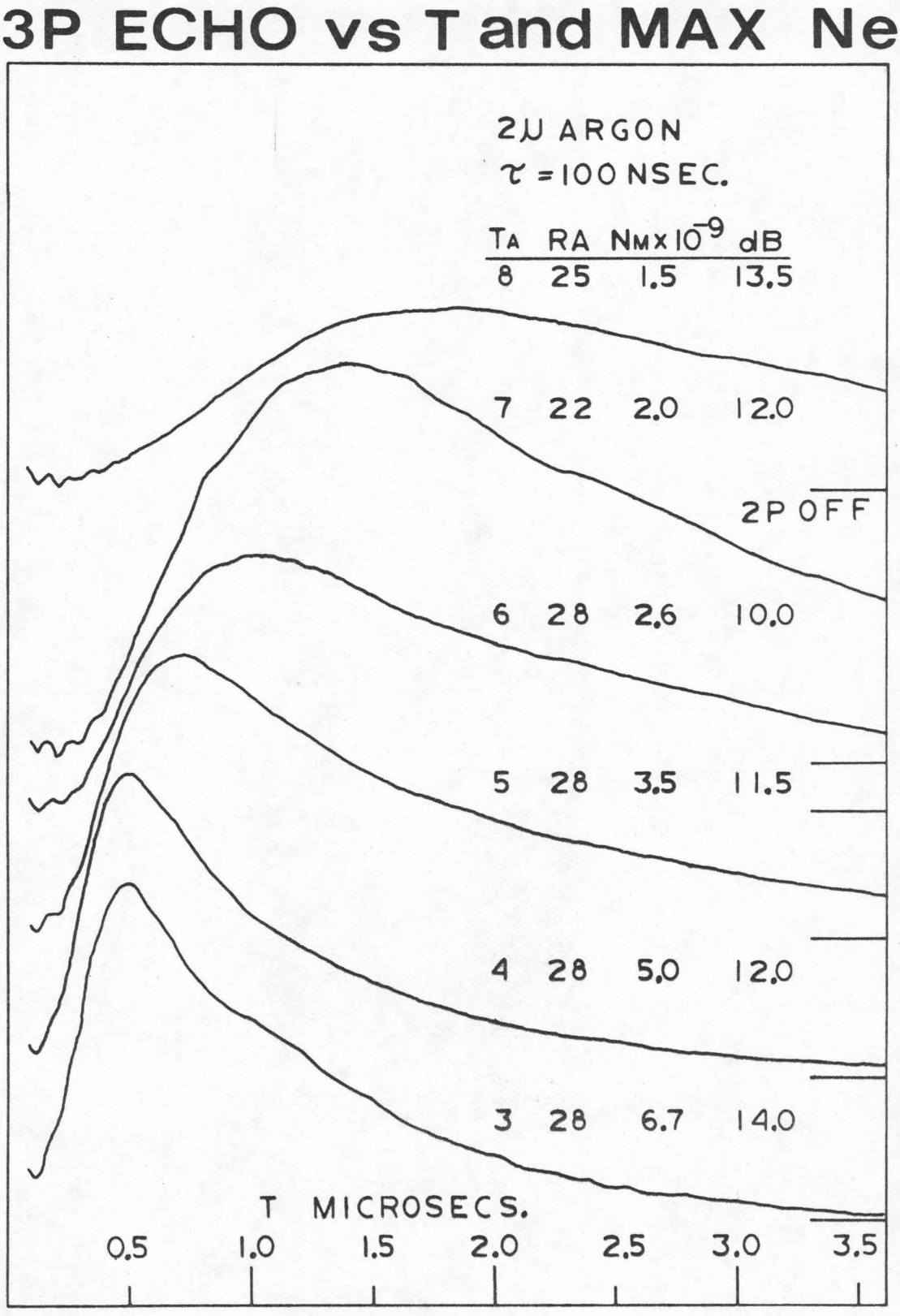
3P ECHO vs T and MAX Ne
2μ ARGON
τ = 100 NSEC.
TA RA NM x 10⁻⁹ dB
8 25 1.5 13.5
7 22 2.0 12.0
2P OFF
6 28 2.6 10.0
5 28 3.5 11.5
4 28 5.0 12.0
3 28 6.7 14.0
T MICROSECS.
0.5
1.0
1.5
2.0
2.5
3.0
3.5

Fig. 2.11

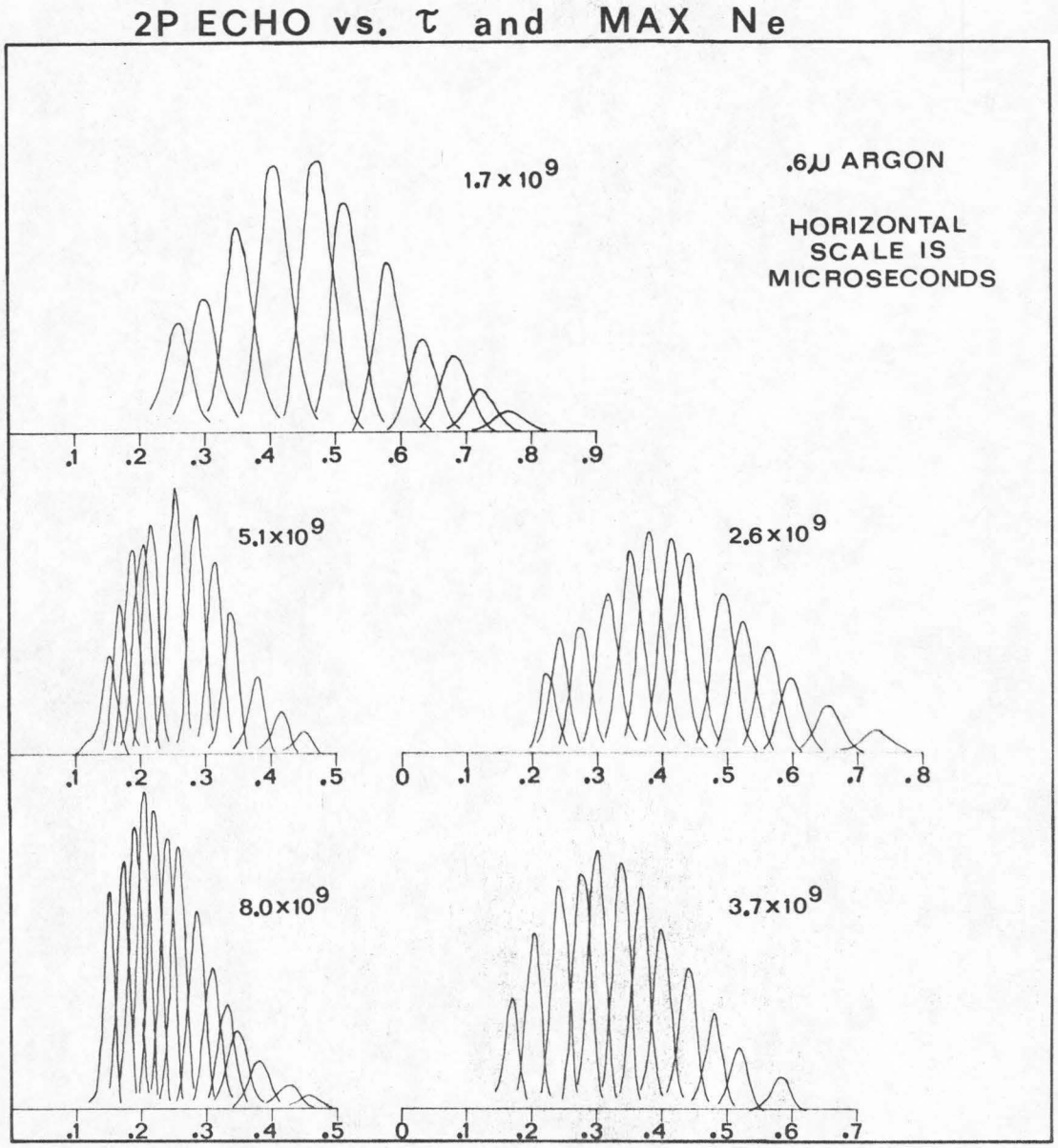
2P ECHO vs. τ and MAX Ne
.6μ ARGON
HORIZONTAL SCALE IS MICROSECONDS
1.7 x 10^9
.1 .2 .3 .4 .5 .6 .7 .8 .9
5.1x10^9
.1 .2 .3 .4 .5
2.6x10^9
0 .1 .2 .3 .4 .5 .6 .7 .8
8.0x10^9
.1 .2 .3 .4 .5
3.7x10^9
0 .1 .2 .3 .4 .5 .6 .7

Fig. 2.12

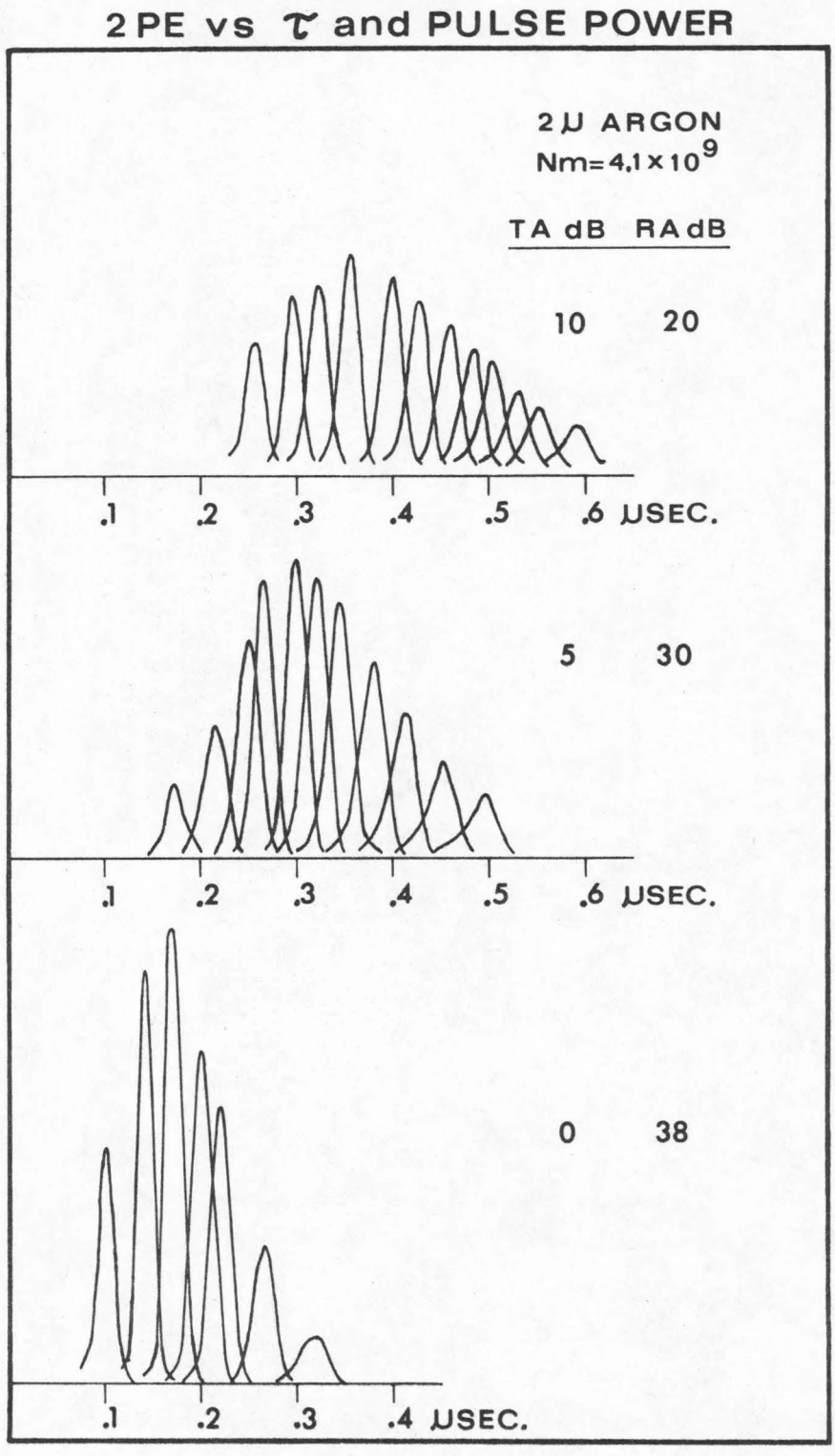
2PE vs τ and PULSE POWER
2μ ARGON
Nm=4.1×10^9
TA dB RA dB
10 20
.1 .2 .3 .4 .5 .6 μSEC.
5 30
.1 .2 .3 .4 .5 .6 μSEC.
0 38
.1 .2 .3 .4 μSEC.

Fig. 2.13

with an optimum $\tau$ which steadily increases as the density falls. Thus the nonlinear processes need more time to develop as the density decreases, which is not part of the collisional explanation for 2PE. These echoes were about 20 dB below the transient response. Similar results were obtained by Bauer [5].

This delay in echo formation with lower densities could not be due to electron-ion Coulomb collisions because if one varies the pulse power as a parameter in a 2PE vs. $\tau$ experiment one obtains the results of Fig. 2.13. The echo takes longer to develop as the input power is decreased. Because Coulomb collisions decrease for higher electron speeds, this experiment shows that e-i collisions cannot be the cause of 2PE.

## 2.7 Hot Layers of Electrons after the First Two Pulses

The first two pulses have a frequency spectrum which is periodic and they excite the plasma into hot bands. These were experimentally observed by modifying R. Stenzel's radiometer which he built for measuring afterglow plasma temperature decay so that shorter time scales could be observed and so that the high powered input pulses did not saturate the receiver. Both the instrumentation and the microwave setup were different from those of the echo experiments. The hybrid tee and dummy tube were replaced by a circulator which separated the heating pulses from the plasma signal. The signal frequency was changed to the center frequency of the circulator, 3.0 GHz, and a much longer stack of coils kept the magnetic field uniform over a length of about one meter. The radiometer was a heterodyne receiver described elsewhere [2]. A PIN diode was used before the front end and a balanced mixer was used as a

switch in the IF circuit to prevent overloading and excessive recovery time after the heating pulses.

Figure 2.14 shows a typical emission record. The two pulses were spaced by 35 nsecs so that the wide bandwidth of the receiver (5 MHz on either side of the carrier) would not average out the periodic effect we sought. The flat tops are due to saturation, and the double peaks are due to the double side band response. The vertical scale is proportional to emitted power, but the absolute magnitude is not indicated. The emission peaks are quite sharp compared to spectrum analyzer displays of the input spectrum, and the peak spacing in frequency space is what one would expect from an impulse spacing of 35 nsecs.

## 2.8 Modulated Absorption Spectrum after the First Two Pulses

As mentioned above, the perpendicular diffusion model produces a periodic perturbation in the number of electrons with a given upper hybrid frequency. In order to obtain direct information on $n(\omega)$, we have measured the absorption spectrum following the application of two pulses of about 15 nsec full width at half power. As described above, a short was placed behind the plasma so that all the incident power would be reflected except for the amount that the plasma absorbed. The electronic equipment is shown in Fig. 2.15.

Figure 2.16 shows absorption records with several locations of the observation window following the first two pulses. The time scale on which the absorption decayed was about the same as the decay time of 3PE, and when the absorption modulation did not extend uniformly

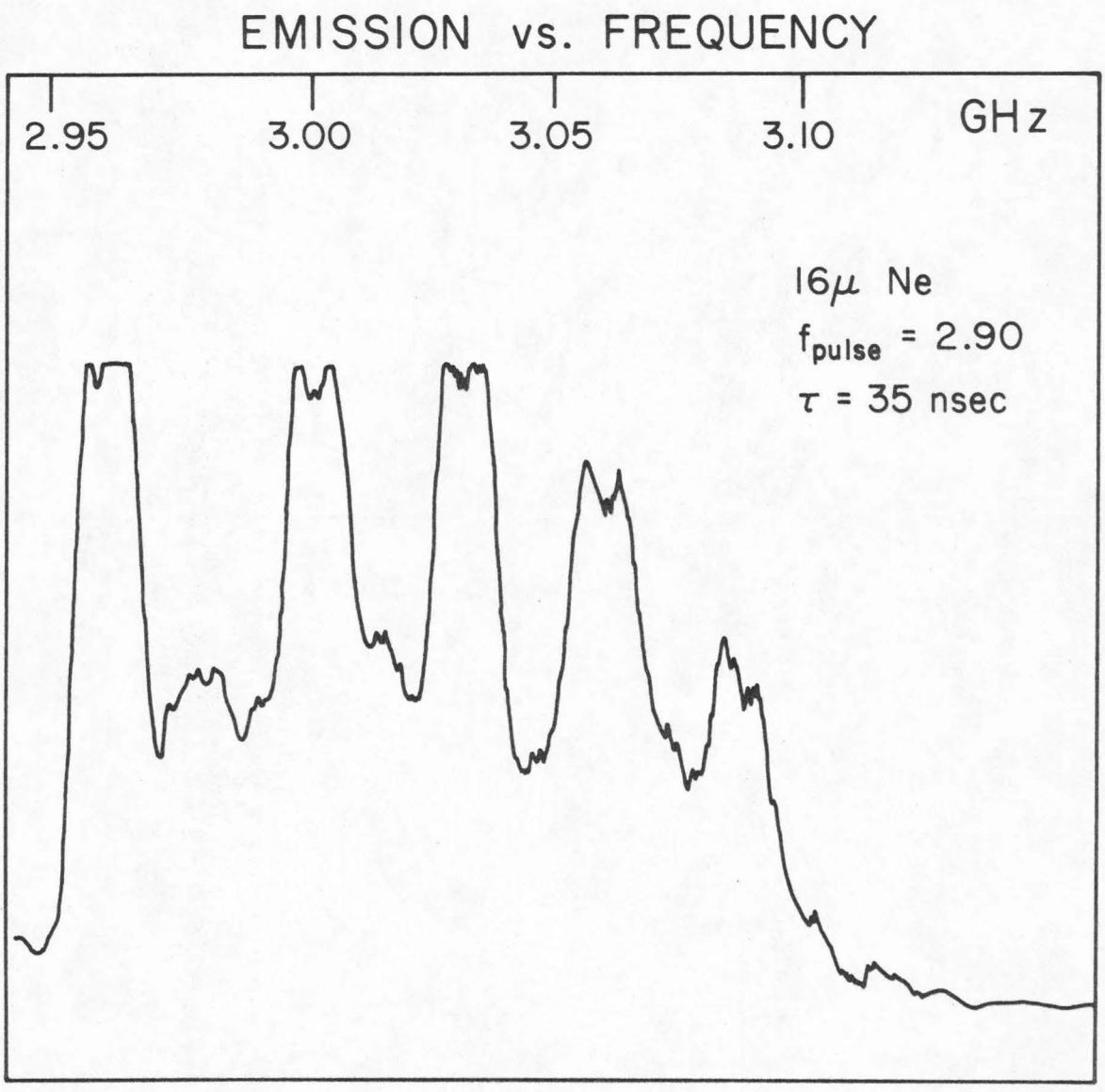
EMISSION vs. FREQUENCY
2.95
3.00
3.05
3.10
GHz
16μ Ne
$f_{pulse}$ = 2.90
τ = 35 nsec

Fig. 2.14

# BLOCK DIAGRAM FOR ABSORPTION EXPT.

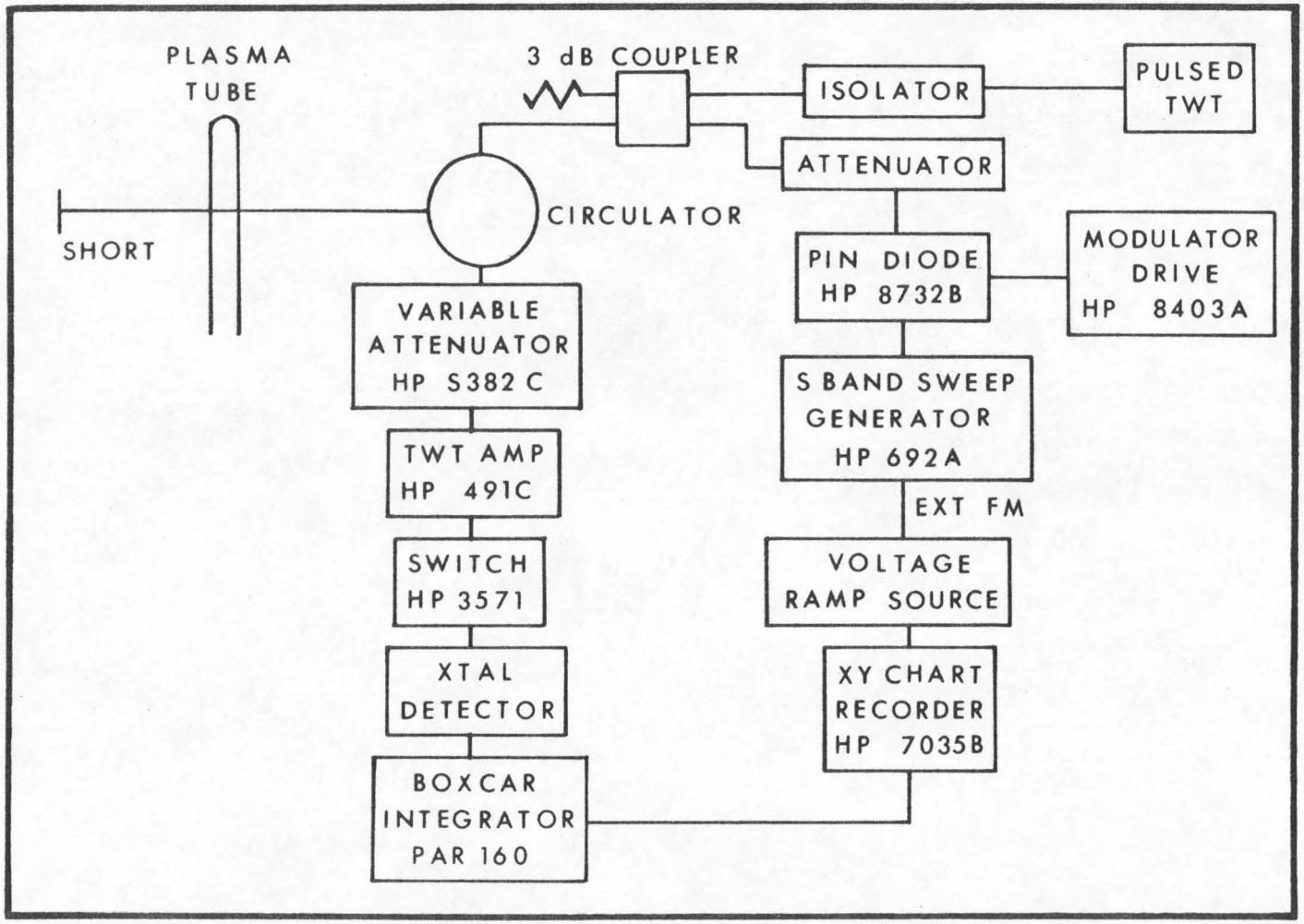


Fig. 2.15

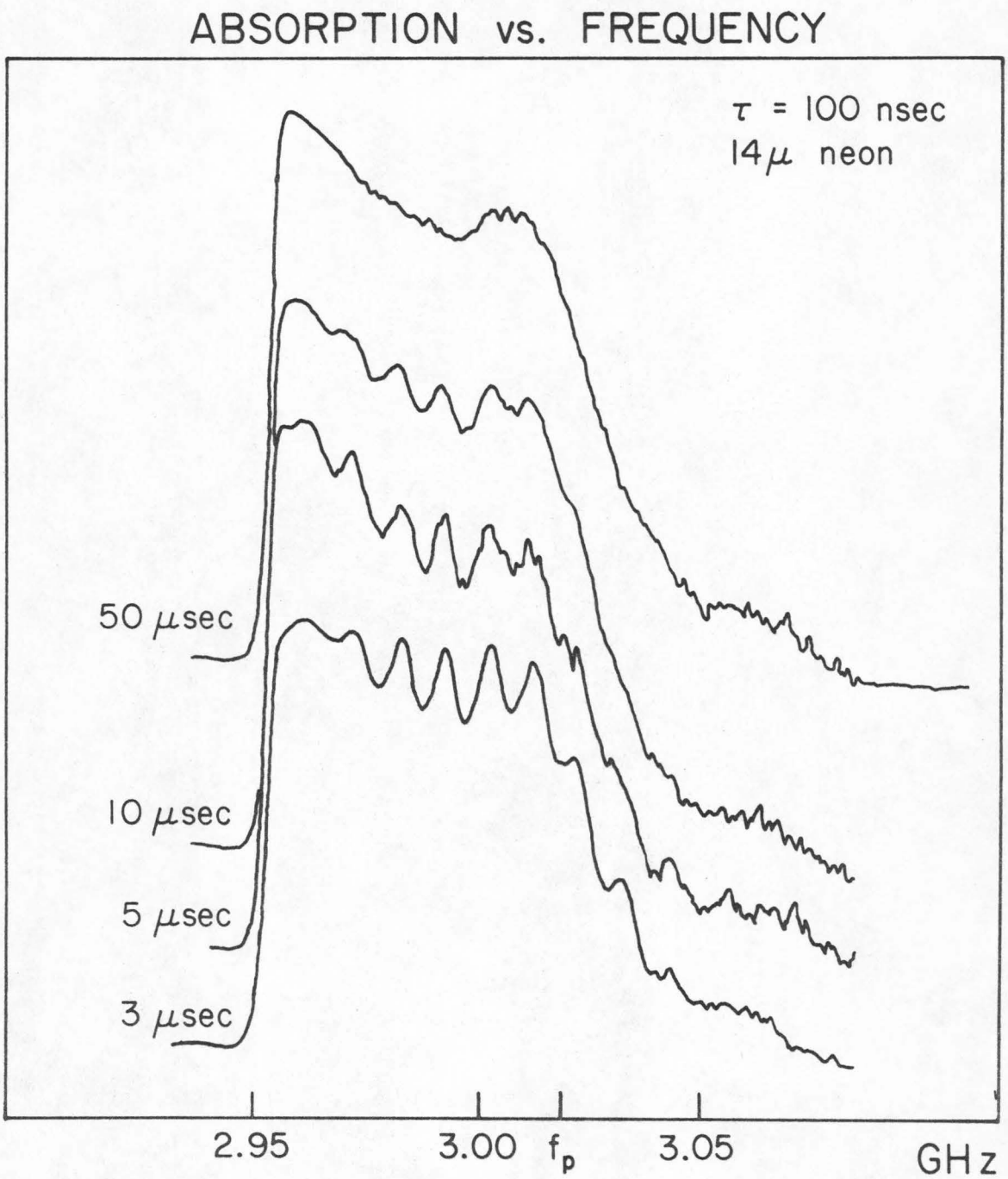
ABSORPTION vs. FREQUENCY
τ = 100 nsec
14μ neon
50 μsec
10 μsec
5 μsec
3 μsec
2.95
3.00
f_p
3.05
GHz

Fig. 2.16

across the plasma bandwidth, the 3PE was very distorted as in Fig. 2.17. In this figure the pressure is 15μ argon, and absorption is indicated by a lowering of the signal amplitude. This figure shows a definite connection between echoes and absorption experiments. Returning to the multiple-time Fig. 2.16, we see that the absorption 50μ sec after the heating pulses is unmodulated, and it is in fact indistinguishable from the absorption spectrum with no pulses. (An instrumental effect caused an apparent lowering of the 3μ sec curve height.) Specifically, the two curves are the same width, indicating that the peak densities are the same. This implies that the excited electrons did not migrate from the waveguide region, or else that outside electrons filled in the vacancies if they left.

To investigate the possibility of electron migration down the tube, we excited the plasma in one waveguide and looked for an effect in a second guide 16.9 cm from the first one. This was in a stack of magnet coils that kept the magnetic field uniform to one part in $10^4$. Under conditions causing strongly modulated emission and absorption in the first guide, no modulation was detected in the second guide. It is possible that an effect would have been noticed at a smaller waveguide spacing, but this wasn't possible with our coil setup. We conclude that echoes are not produced by the collisions of electrons with neutrals and the subsequent rapid flight of the electrons down the tube axis. If electrons were driven out of the waveguide region, one would expect electrostatic restoring forces to cause a density oscillation in time. Such oscillations did not appear in the 3PE vs. T experiments and seem unlikely in light of the two-waveguide

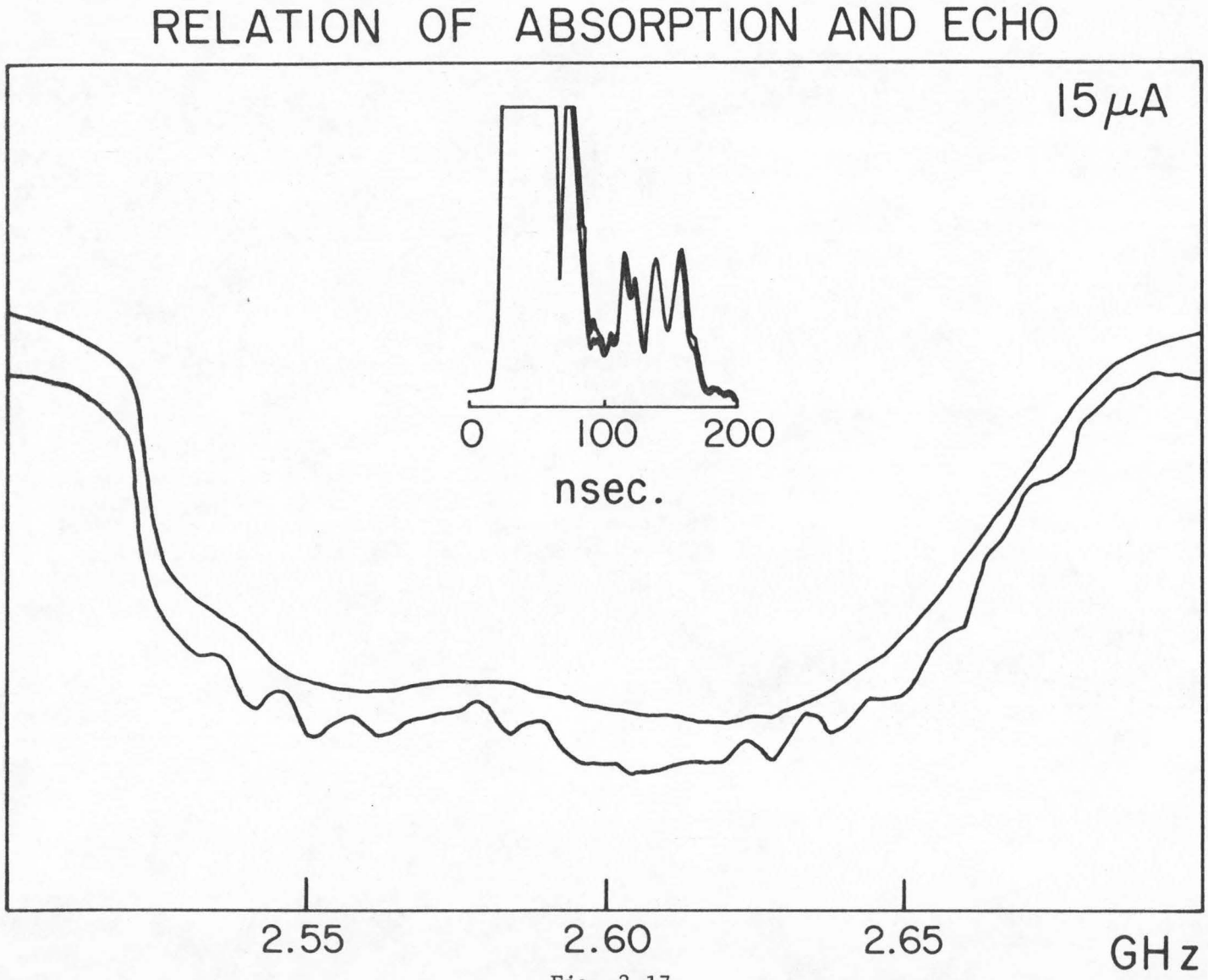
RELATION OF ABSORPTION AND ECHO
15μA
0
100
200
nsec.
2.55
2.60
2.65
GHz

Fig. 2.17

experiment.

## 2.9 Absence of Excited Layer Interactions

In his thesis, Bruce suggested that the hot layers might interact in some way. Specifically, if transverse diffusion occurs in echo time scales, then one would expect regions of charge imbalance to occur and to interact with each other. If such layers existed they might impede single particle diffusion, or their space charge fields might help create some mysterious plasma turbulence or enhanced diffusion by coupling different parts of the plasma. Such layers could not be detected with probes, but our absorption experiments could be used to test the interaction of the hot layers.

We used an absorption setup at 3 GHz with a circulator and a short behind the plasma. No directional coupler was used. A heating pulse having two main frequency components was applied to the plasma and the subsequent absorption spectrum was observed. The frequency components were then varied to test for interaction.

Two S-band generators fed through 3 dB pads and a coax hybrid into a traveling wave tube amplifier and thence into a Litton pulsed traveling wave tube. Its output was combined in a second coax hybrid with the absorption test pulse and they both went into the same arm of the circulator. The heating pulse was about 300 nsec wide at half power instead of the 10 or 15 nsec pulses used to create echoes. The amplitude of the long heating pulse was adjusted and compared with a typical short echo producing pulse on a spectrum analyzer. The spectrum amplitude over a 2 MHz bandwidth was comparable for the two pulses, so the dual frequency experiment is comparable in its effect on the plasma

with that of the echo experiments. The absorption test pulse was about 500 nsec long and we observed the last 200 nsec of it to avoid initial transient effects. It was created by an HP sweep generator slowly swept in the external FM mode and by a PIN diode modulator. The gas pressure was 2μ argon, the afterglow time was 1.2 msec, and the plasma bandwidth was about 100 MHz.

Figure 2.18 shows the absorption spectrum following a heating pulse. In order to fit as many curves onto one piece of paper as possible, only fragments of the curves have been retained and the absolute magnitude of the absorption is not indicated. There are five subcurves. No normalizing procedure was used and (a) contains a spurious small dip marked by $\Lambda$ , due to a distortion of the system's frequency response. This also appears in the other curves. In (a) both frequency generators marked by $\uparrow$ are on, and the observation time is 1.7 μsec after the heating pulse. In (b) 16 μsec have elapsed and the effects of the heating pulses have almost completely vanished. In (c) both heating frequencies are turned off for comparison with (b). Figures (d) and (e) show the effects of turning off and of moving the higher frequency component, respectively. There is clearly no interaction between the excited regions of the plasma.

## 2.10 Conclusions from the Experiments

It is obvious that 3PE are very complicated phenomena with many interacting parameters. The experiments described in this chapter greatly restrict the range of acceptable theories.

One of the most important properties of 3P echoes is their linearity with respect to the third pulse amplitude. This fact

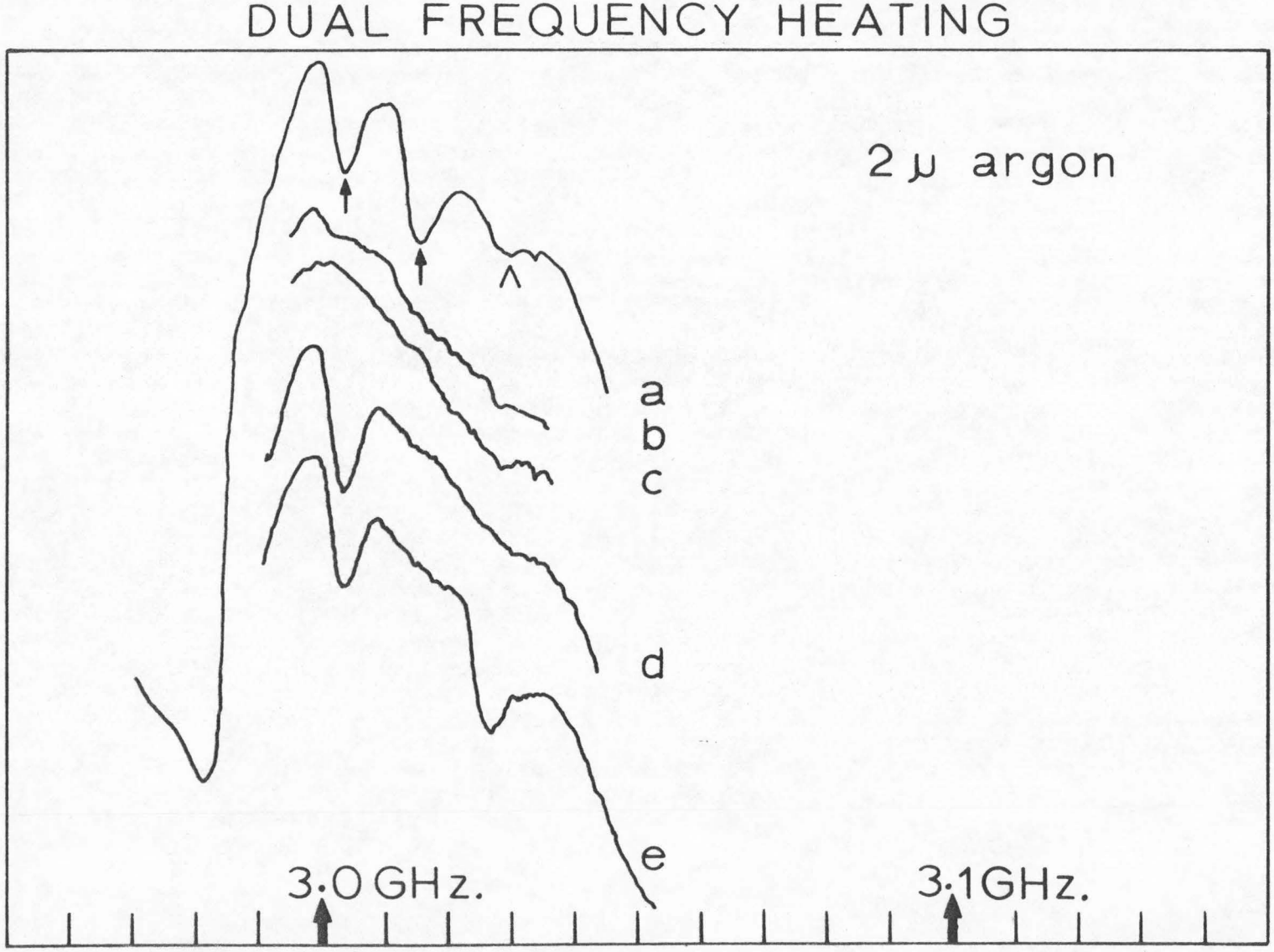


Fig. 2.18

excludes the collisional echo model, which is the three-pulse analog of the collisional phase scrambling process without diffusion. As a consequence of this linearity, the echo process must act between the second and third applied pulses.

In order to satisfy the linearity requirements, the diffusion models were developed. Unfortunately, perpendicular diffusion is too slow and parallel diffusion, in Bruce's formulation, produces too small an echo. We can crudely estimate the perpendicular diffusion rate. At 10 Ne with 1 eV electrons, the collision frequency is about $3\times10^{6}\text{sec}^{-1}$. The cyclotron radius at 2.5 GHz is $v/\omega_c = 6\times10^{7}/(2\pi\times2.5\times10^{9}) = 3.82\times10^{-3}$cm, so if the particle can move no faster than one gyroradius per collision, the maximum possible speed would be $1.15\times10^{4}\text{cm/sec}^{-1}$. An electron must move a distance on the order of 1 mm to experience a local resonant frequency differing by 1/10 the bandwidth from its unperturbed value. So one would expect $T_o$ to be about $10^{-5}$sec, which is an order of magnitude too long. The echo peaks at about 1 μsec even at 1μ pressure. Of course, this diffusion is a random walk process, and the time needed for an average particle to move a certain distance would be longer than if it had moved steadily at the rate of one gyroradius per collision. Furthermore, the resulting space charge could slow the process considerably. Bruce was dissatisfied with the perpendicular diffusion model because it needed a higher diffusion rate than he could justify in order to make experiment agree with theory [6].

Despite the slowness of perpendicular diffusion, the absorption experiments show a periodic effect after two pulses which could be interpreted as "hot" electrons piling up on either side of an excited

layer and leaving a hole in their previous location. However, if one tried to compute the absorption spectrum caused by a "bunched" column one would quickly become confused because there was no longer a unique relation between position and resonant frequency. The observed 3PE are quite strong, and a large change in local electron density, even if it were possible, would necessarily change the local resonant frequency. The other objection to this simple interpretation of the absorption experiments is that large electric fields would be created if the electrons tried to move away from their neutralizing ions. It would seem difficult to create such an imbalance. The two-frequency heating experiment implies that no layers of charge imbalance occur, because such layers would be expected to interact strongly.

Perhaps the absorption experiments can be interpreted another way. The cold plasma absorption, without collisions, is due to the storage of energy in a resonant layer. As the applied pulse continues in time, the number of oscillators which are resonant or which have not slipped out of phase decreases linearly with time. The ones still resonant have quadratically increasing energy, so the total energy absorbed increases linearly with time [7]. This is how a cold collisionless plasma can appear to have an absorption coefficient.

But the pulses used in echo work are quite strong, and they can easily excite electrons to 1 eV or more, as directly verified by Bruce's collision frequency measurements. So cold plasma theory may not be sufficient to explain the experiments. The conversion of electromagnetic waves into plasma waves in warm plasmas at an upper hybrid layer has recently received a great deal of attention [8,9,10,11]. We propose that the observed frequency periodic temperature after the first two

pulses may cause a frequency periodic wave coupling effect which could look like modulated absorption. The warm plasma has extra modes to absorb energy which a cold plasma does not. There would be no standing wave effects in the echo plasma because traveling plasma waves would be stopped by the unexcited cold regions of plasma; see the discussion in the caption of Fig. 2, Ref. [8].

Because of the experiments with 3PE vs. T at different pressures and at different 1P-2P powers, it seems that electron-neutral collisions cannot be the mechanism for 3PE. They could still have a destructive effect, as could electron-ion collisions. At the low pressures used, both 2PE and 3PE are dependent upon the electron density as the most significant parameter. This is not part of the previous 3PE models, and the collisional model does not provide an explanation for the observed periodic absorption modulation.

## 2.11 References for Chapter II


1. R. L. Bruce, F. W. Crawford, and R. S. Harp, J. Appl. Phys. 19, 3349 (1968).
2. R. L. Stenzel, Ph.D Thesis, California Institute of Technology, 1969; F. A. Blum, L. O. Bauer, R. W. Gould, and R. L. Stenzel, Phys. Fluids 12, 1018 (1969); R. H. Ault, Ph.D Thesis, California Institute of Technology, 1971.
3. Reiner Stenzel, private communication.
4. R. S. Harp and R. R. Smith, Phys. Lett. 29A, 317 (1969).
5. L. O. Bauer, Ph.D. Thesis, California Institute of Technology, May 1968, p. 133.
6. R. L. Bruce, Ph.D Thesis, Stanford University, 1969, p. 119.
7. D. M. Henderson, Ph.D Thesis, Yale University, 1970, p. 20.
8. S. Gruber, Phys. Fluids 11, 858 (1968).
9. S. Gruber and G. Bekefi, Phys. Fluids 11, 122 (1968).
10. H. H. Kuehl, B. B. O'Brien, and G. E. Stewart, Phys. Fluids 13, 1595 (1970).
11. Ting-Wei Tang, Phys. Fluids 13, 121 (1970).

# III. A DENSITY DEPENDENT 3PE MODEL

## 3.1 Motivation for a Warm Plasma Approach

The plan of this work was to form as complete an experimental picture as possible of 3PE and then to find a model to explain the facts. The experiments show that previous 3PE theories are inadequate because they do not predict the qualitative behavior of echo strengths on the experimental parameters. The most significant parameter is seen to be the electron density, which does not affect the echo process in a collisional theory, where the echo is proportional to $Ne$.

While looking for a model to explain the experiments, we came across a section in a thesis by Henderson [1] which contained the relevant parameters. He discussed the response of an unmagnetized plasma to an impulsive electric field, and he showed that the time behavior was first governed by cold plasma theory. After a short while it was necessary to include temperature effects, and the response was perturbed by the growth of thermal modes which were driven by the residual cold plasma type ringing response.

This hypothetical thermal mode growth is a possible mechanism for producing echoes. The effect increases with the density and the density gradient, and the effect can be independent of electron-neutral collisions. Thus it includes the correct dependence on the experimental parameters. The thermal modes predicted by the model seem to grow sufficiently rapidly to damp out the plasma ringing energy and if the plasma temperature is periodic from the effects of the first and second pulse, then the ringing response to the third pulse will have a

frequency periodic decay and will result in echoes.

To clarify this last point we are considering the plasma response to be an integral over frequency of the number of electrons oscillating with a given frequency times the single particle response at that frequency, similar to equation (1.5).

$$I(t) \propto \int d\omega\, n(\omega)\, R(\omega)\, e^{i\omega t} \qquad (3.1)$$

Now in the diffusion echo model $n(\omega) = n_o(\omega) + \varepsilon \cos \omega\tau$, where $n_o$ is the unperturbed density distribution, $\cos \omega\tau$ represents the periodicity of the plasma heating by the first two pulses and $\varepsilon$ represents the degree of perturbation caused by diffusion of the hot electrons. $R(\omega)$ is simply $v$, the speed imparted to all the electrons by the applied impulse. An echo will be produced at $t = \tau$ by the interaction of the $\cos \omega\tau$ and $e^{i\omega t}$ factors. The present work considers the case where $n(\omega)$ is not frequency periodic but $R(\omega)$ contains a frequency periodic damping caused by the production of thermal modes.

We were not able to extend the small perturbation analysis of thermal mode growth into the times for which the thermal modes have consumed a large fraction of the ringing response to the initial transient. However, after extending Henderson's work to the case with a static magnetic field we could develop a crude model for the damping of the ringing response into thermal modes and for the creation of 3PE. This is a model, not a theoretically correct derivation from first principles, but it is intended to show the possibility that 3PE are due to thermal mode damping and that the qualitative dependence of 3PE on the experimental parameters can be explained.

## 3.2 Pearson's Equation for a One-Dimensional Plasma Slab

In this section we will derive an equation for the electric field in a one-dimensional inhomogeneous plasma slab. The ambipolar electric field caused by the inhomogeneity will be included in the treatment. We will follow Pearson's derivation [2] closely.

All quantities are assumed to be independent of $y$ and $z$ and the static magnetic field is given by $B_o\hat{z}$. We assume that the scale length of the plasma in the x direction $L$ is much greater than the cyclotron radius $r_c$ and the Debye length.

The perturbation fields which we consider are uniform in $z$, have electric field $\vec{E}$ perpendicular to $\hat{z}$, and have time dependence $\exp(-i\omega t)$. The fields obey Maxwell's equations

$$\frac{c^2}{\omega^2}\nabla \times (\nabla \times \vec{E}) = \vec{E} - \frac{4\pi}{i\omega}\vec{J} \tag{3.2}$$

$$\vec{B} = \frac{c}{i\omega}\nabla \times \vec{E} \tag{3.3}$$

Because of uniformity in $z$ and because $E_z = 0$ we have $\vec{B} = B\hat{z}$ and $J$ is perpendicular to $\hat{z}$. For our frequency range ion motions are negligible.

Because the problem is independent of $z$ we need only a two-dimensional distribution function $f(\vec{r},\vec{v}) + \delta f(\vec{r},\vec{v},t)$, where all the vectors are two dimensional. The unperturbed distribution function satisfies the Boltzmann equation

$$\vec{v} \cdot \nabla f - \frac{e}{m}(E_a\hat{x} + \frac{\vec{V}}{c} \times B_o\hat{z}) \cdot \frac{\partial f}{\partial \vec{v}} = (\frac{\partial f}{\partial t})_{coll} \tag{3.4}$$

where $E_a$ is the ambipolar electric field.

The linearized Boltzmann equation for the perturbed distribution function is

$$\frac{\delta f(\vec{r},\vec{v},t)}{\partial t} + \vec{v} \cdot \nabla \delta f - \frac{e}{m}(E_a \hat{x} + \frac{\vec{v}}{c} \times B_o \hat{z}) \frac{\partial \delta f}{\partial \vec{v}}$$

$$= \frac{e}{m} (\vec{E} + \frac{\vec{v}}{c} \times \vec{B}) \frac{\partial f}{\partial \vec{v}} + (\frac{\partial \delta f}{\partial t})_{coll} \qquad (3.5)$$

We will assume $\nu << \omega$ so that the last term is negligible, and we will ignore the perturbed magnetic field by making the quasi-static approximation $\nabla \times \vec{E} = 0$ . This is only valid if $\lambda^2 << c^2/\omega^2$ .

A formal solution for $\delta f$ can be found by integrating along unperturbed trajectories. The left side of (3.5) is the convective derivative $D/Dt$ of $\delta f$ , which is zero when evaluated along an unperturbed trajectory. The drift approximation will be used to provide explicit but approximate trajectories. With the approximations used above we have

$$\frac{D}{Dt} \delta f(\vec{r}(\vec{r}_o,\vec{v}_o,t), \vec{v}(\vec{r}_o,\vec{v}_o,t),t) = \frac{e}{m}[\vec{E}(\vec{r}(\vec{r}_o,\vec{v}_o,t),t))] \frac{\partial f}{\partial \vec{v}} \qquad (3.6)$$

where $\vec{r}_o,\vec{v}_o$ define the unperturbed orbit. Assuming that $\vec{E}$ vanishes at $t = -\infty$, we find

$$\delta f = \frac{e}{m} \int_{-\infty}^{t} \vec{E}(\vec{r}(\vec{r}_o,\vec{v}_o,t'),t') \frac{\partial f}{\partial \vec{v}} dt' \qquad (3.7)$$

To transform from orbit coordinates to arbitrary ones, we multiply by $\delta(\vec{r} - \vec{r}(\vec{r}_o,\vec{v}_o,t))\ \delta(\vec{v} - \vec{v}(\vec{r}_o,\vec{v}_o,t))$ and integrate.

$$\delta f(\vec{r},\vec{v},t) = \frac{e}{m}\int_{-\infty}^{t}\iint d^2r_o d^2v_o\ \delta(\vec{r}-\vec{r}(\vec{r}_o,\vec{v}_o,t))$$

$$\delta(\vec{v}-\vec{v}(\vec{r}_o,\vec{v}_o,t))\ \vec{E}(\vec{r}(\vec{r}_o,\vec{v}_o,t'),t')\ \frac{\partial f}{\partial \vec{v}}\,dt' \qquad (3.8)$$

On the unperturbed trajectory, if $t = 0$ is the initial time, then $r(\vec{r}_o,\vec{v}_o,0) = r_o$ and $\vec{v}(\vec{r}_o,\vec{v}_o,0) = v_o$. We must now express $\vec{r}(\vec{r}_o,\vec{v}_o,t)$ in terms of $\vec{r}(\vec{r}_o,\vec{v}_o,t') \equiv r_o'$ so that we can perform the integral. If we consider $t'$ as the reference time on the path, then

$$\vec{r}(\vec{r}_o,\vec{v}_o,t) = \vec{r}(\vec{r}(r_o,v_o,t'),\ \vec{v}(\vec{r}_o,\vec{v}_o,t'),t-t') \equiv r(r_o',v_o',t-t') \qquad (3.9)$$

$$\vec{v}(\vec{r}_o,\vec{v}_o,t) = \vec{v}(\vec{r}(\vec{r}_o,\vec{v}_o,t'),\ \vec{v}(\vec{r}_o,\vec{v}_o,t'),t-t') \equiv \vec{v}(\vec{r}_o',\vec{v}_o',t-t') \qquad (3.10)$$

Substituting this transformation into (3.8), defining $t - t' = \tau$, and assuming $\vec{E}(\vec{r},t) = \vec{E}(\vec{r})\ e^{-i\omega t}$, we have

$$\delta f(\vec{r},\vec{v},t) = \frac{e}{m}\int_{0}^{\infty} d\tau \iint d^2r_o \iint d^2v_o\,\delta(\vec{r}-\vec{r}(r_o',v_o',\tau))$$

$$\delta(\vec{v}-\vec{v}(\vec{r}_o',\vec{v}_o',\tau))\ \vec{E}(\vec{r}_o')e^{-i\omega(t-\tau)}\ \frac{\partial f}{\partial \vec{v}} \qquad (3.11)$$

Since $\vec{J} = -e\int d^3v\ \delta f$ and we assume $\vec{J}(\vec{r},t) = \vec{J}(\vec{r})\ e^{-i\omega t}$ we have

$$\vec{J}(\vec{r}) = -\frac{e^2}{m}\int_{0}^{\infty} d\tau\ e^{i\omega\tau}\int d^2r_o\int d^2v_o\ \delta(r - r(r_o,v_o,\tau))$$

$$v(r_o,v_o,\tau)\ \vec{E}(\vec{r}_o)\ \frac{\partial f(r_o,v_o)}{\partial \vec{v}_o} \qquad (3.12)$$

Now we will need explicit unperturbed orbits. The equation of motion of a single electron is

$$m \frac{d\vec{v}_o}{dt} = -e[\vec{E}_a + \frac{\vec{v}_o}{c} \times B_o \vec{z}] \tag{3.13}$$

If we let $\vec{v}_o = \vec{w} + \vec{u}$, where the drift velocity is $\vec{u} = \frac{c\vec{E}_a \times \vec{B}_o}{B_o^2}$, we obtain

$$\vec{v}_o(t) = \vec{u} + \vec{w} \cos \omega_c t - \vec{w} \times \vec{z} \sin \omega_c t \tag{3.14}$$

$$\vec{r}_o(t) = \vec{u}t + \frac{1}{\omega_c} \vec{w} \sin \omega_c t + \frac{1}{\omega_c} \vec{w} \times \vec{z}(\cos \omega_c t - 1) \tag{3.15}$$

where $\omega_c = \frac{eB}{mc}$. In the present case $\vec{u} = u\hat{y}$ and $\vec{E} = E_x$ because of the uniformity in $y$ and $z$.

We will expand $E_x f(x_o, \vec{v}_o)$ in a Taylor series about $x$ and integrate by parts on $v_{ox}$ to obtain

$$J_x(x) = \frac{e^2}{m} \int_0^\infty d\tau \, e^{i\omega\tau} \sum_{\ell=0}^{\infty} \frac{1}{\ell!} \int d^2 v_o \Gamma_\ell(x, \vec{v}_o, \tau) \frac{\partial^\ell}{\partial x^\ell}[f(x, \vec{v}_o) E_x(x)] \tag{3.16}$$

The unperturbed trajectories are contained in

$$\Gamma_\ell(x, \vec{v}_o, \tau) \equiv \frac{\partial}{\partial v_{ox}} \int dx_o \, v_x(x_o, v_o, \tau) \, \delta(x - x(x_o, \vec{v}_o, \tau))(x_o - x)^\ell \tag{3.17}$$

The spatial derivatives can be taken outside the integral by using the identity

$$\sum_{\ell=0}^{\infty} \frac{\Gamma_\ell}{\ell!} \frac{\partial^\ell}{\partial x^\ell} (fE_x) = \sum_{\ell=0}^{\infty} \frac{1}{\ell!} \frac{\partial^\ell}{\partial x^\ell} (B_\ell f E_x) \tag{3.18}$$

This identity can be verified by expanding the RHS, reversing the order of summation, and comparing equal derivatives to obtain

$$\Gamma_\ell = \sum_{p=0}^{\infty} \frac{1}{p!} \frac{\partial^p B_{p+\ell}}{\partial x^p} \tag{3.19}$$

If the series is reverted by successively solving for higher derivatives of $B_\ell$ in terms of derivatives of $\Gamma_\ell$, then one finds

$$B_\ell = \sum_{k=0}^{\infty} \frac{(-)^k}{k!} \frac{\partial^k \Gamma_{\ell+k}}{\partial x^k} \tag{3.20}$$

Substituting into (3.16) we have

$$J_x(x) = \frac{e^2}{m} \sum_{\ell=0}^{\infty} \frac{1}{\ell!} \frac{d^\ell}{dx^\ell} \{E_x(x) \int_0^{\infty} d\tau\, e^{i\omega\tau} \int d^2v_o B_e(x,\vec{v}_o,\tau) f(x,\vec{v}_o)\} \tag{3.21}$$

In the present case,

$$\Gamma_\ell = \frac{\partial}{\partial v_{ox}} \{v_x(x_o,\vec{v}_o,\tau)[x_o - x(x_o,\vec{v}_o,\tau)]^\ell\} \tag{3.22}$$

Using the fact $u_x = 0$ and assuming $\partial u/\partial x = 0$ we find that $B_\ell = \Gamma_\ell$. Using the unperturbed trajectories from (3.14) we can write

$$\int d^2v_o B\, f(x,\vec{v}_o) = (2\omega_c)^{-\ell} \frac{\partial}{\partial\phi} A_\ell(x,\phi) \tag{3.23}$$

where $\phi = \omega_c t$ and

$$A_\ell(x,\phi) = \int d^2v_o\, f(x,\vec{v}_o) \sin\phi[-2v_o \sin\phi + 2w_y(1-\cos\phi)]^\ell \tag{3.24}$$

If we introduce the definition

$$\langle v_x^r w_y^s \rangle \equiv \frac{1}{n_o(x)} \int d^2v_o\, f(x,\vec{v}_o)\, v_x^r\, w_y^s \tag{3.25}$$

then we can write

$$A_o(x,\phi) = n_o(x) \sin \phi$$

$$A_1(x,\phi) = n_o(x)[-\langle v_x \rangle (1 - \cos 2\phi) + \langle w_y \rangle (2 \sin \phi - \sin 2\phi)]$$

$$A_2(x,\phi) = n_o(x) \left[ \langle v_x^2 \rangle (3 \sin \phi - \sin 3\phi) + \langle v_x w_x \rangle (-4 + 2 \cos \phi + 4 \cos 2\phi - 2 \cos 3\phi) + \langle w_y^2 \rangle (5 \sin - 4 \sin 2\phi + \sin 3\phi)\right]$$

The integrals over $\tau$ can be expressed in terms of

$$S_n = \frac{1}{i\omega} \int_0^\infty d\tau \, e^{i\omega\tau} \frac{\partial \sin n\omega_c \tau}{\partial(\omega_c \tau)} = \frac{n}{\omega^2 - n^2 \omega_c^2} \tag{3.26}$$

$$C_n = \frac{1}{i\omega} \int_0^\infty d\tau \, e^{i\omega\tau} \frac{\partial(\cos n\omega_c \tau)}{\partial(\omega_o \tau)} = \frac{n\omega_c}{i\omega} S_n \tag{3.27}$$

From (3.2) we find $E_x = \frac{4\pi}{i\omega} J_x$ . Combined with (3.21) this yields

$$E_x(x) = \omega_p^2(x) \, S_1 E_x + \frac{1}{2\omega_c} \frac{d}{dx} \{\omega_p^2(x)[\langle v_x \rangle C_2 + \langle w_y \rangle (2S_1 - S_2)] E_x\}$$

$$+ \frac{1}{8\omega_c^2} \frac{d^2}{dx^2} \{\omega_p^2[\langle v_x^2 \rangle (3S_1 - S_3) + \langle v_x w_y \rangle (2C_1 + 4C_2 - 2C_3)$$

$$+ \langle w_y^2 \rangle (5S_1 - 4S_2 + S_3)] E_x\} + \cdots \tag{3.28}$$

where $\omega_p^2 = \frac{4\pi n(x) e^2}{m}$ .

Now we will show that $\langle v_x \rangle$ can be ignored compared with $\langle w_y \rangle$ . Consider three planes at $x$ and $x \pm r_c$ . Electrons will diffuse by moving their center of gyration approximately one gyroradius per collision. The number of electrons moving to the left per second is on the

order of $\frac{1}{2} n(x+r_c)$ and the number moving to the right across the plane at $x$ is on the order of $\frac{1}{2} n(x-r_c)$ . The average speed $\langle v_x \rangle$ is on the order of $\frac{\nu}{\omega_c} \frac{r_c v}{L}$ , where $L$ is the plasma scale length. $\langle w_y \rangle$ is on the order of the drift velocity $u$ . The ambipolar electric field is approximately [3]

$$E_a = -\left(\frac{D_e - D_i}{\mu_i + \mu_e}\right) \frac{\nabla n}{n} \tag{3.29}$$

For a Lorentzian gas the diffusion and mobility coefficients are approximately [4]

$$\mu_e = \frac{e}{m\nu} \frac{1}{1 + (\frac{\omega_c}{\nu})^2} \quad , \quad D_e = \frac{m}{e} \frac{\langle v^2 \rangle}{3} \mu_e$$

Defining $\alpha = \frac{1 - D_i/D_e}{1 + \mu_i/\mu_e}$ we have

$$|E_a| = \frac{D_e}{\mu_e} \alpha \left|\frac{\nabla n}{n}\right| \sim \alpha \frac{mv^2}{e} \frac{1}{L} \sim \frac{\alpha v^2 B_o}{CL\ \omega_c}$$

Thus $\langle w_y \rangle \sim u \sim \frac{c}{B_o} \frac{\alpha \langle v^2 \rangle B_o}{cL\ \omega_c} \sim \frac{\alpha \langle v^2 \rangle}{L\omega_c}$

Since in our experiments $T_i < T_e$ , $\alpha$ is somewhat smaller than 1. Thus $\langle v_x \rangle$ is smaller than $\langle w_y \rangle$ by a factor $\nu/\omega_c$ and will be ignored. Because $u$ is small compared to $v_{th}$, $\langle w_y^2 \rangle$ is approximately equal to $\langle v_x^2 \rangle$ and $v_x w_y$ is negligible in comparison with $\langle v_x^2 \rangle$ .

With these simplifications and with the definitions

$$\xi(x) = \frac{\omega_p^2(x)}{\omega^2 - \omega_c^2}$$

$$\Lambda(x) = \frac{3\langle v_x^2\rangle}{4\omega_c^2 - \omega^2}\,\xi(x)$$

one can write

$$E(x) = \xi(x)\,E(x) + \frac{d}{dx}\left\{\omega_c \langle w_y\rangle \frac{E(x)\,\Lambda(x)}{\langle v_x^2\rangle}\right\} + \frac{d^2}{dx^2}\left\{\Lambda(x)\,E(x)\right\} \quad (3.30)$$

$\langle w_y\rangle$ represents the balance between the electron pressure gradient, the Lorentz force, and the ambipolar electric field. Multiply (3.4) by $v_x$ and integrate over $d^2v$ to obtain

$$\frac{\partial}{\partial x}\left[n_o(x)\,\langle v_x^2\rangle\right] + \frac{e}{m}\,n_o(x)\left[E_a(x) + \frac{\langle v_y\rangle}{c}\,B_o\right]$$

$$= \left(\frac{\partial}{\partial t}\,n_o(x)\,\langle v_x\rangle\right)_{coll} \quad (3.31)$$

Ignoring the collision term relative to the first term and defining $u = -cE_a(x)/B_o$ we have

$$\langle w_y\rangle \equiv \langle v_y\rangle - u = -\frac{1}{n_o(x)\omega_c}\frac{d}{dx}\left[n_o(x)\,\langle v_x^2\rangle\right]$$

$$= -\frac{1}{\omega_c \omega_p^2(x)}\frac{d}{dx}\left[\omega_p^2(x)\langle v_x^2\rangle\right] \quad (3.32)$$

Substituting this into (3.30) yields

$$E(x) = \xi(x)\,E(x) - \frac{d}{dx}\left\{\frac{d\Lambda}{dx}\,E(x)\right\} + \frac{d^2}{dx^2}\left\{\Lambda E(x)\right\}$$

$$E(x) = \xi(x)\,E(x) + \frac{d}{dx}\left\{\Lambda\,\frac{dE}{dx}\right\} \quad (3.33)$$

This is the equation for the electric field in a one-dimensional plasma slab which was derived by Pearson and which will be used to find a finite temperature correction to the plasma ringing response.

## 3.3 Growth of Thermal Modes for Small Times

We start from Pearson's equation for the electric field in a one-dimensional plasma slab, Eq. (3.33), which has also been derived by Henderson using Baldwin's different method [1]. Pearson's equation did not include an external driving field. When that is included, or by using Henderson's method, one obtains

$$[1 - \xi(x)]\, E(x,t) - \frac{d}{dx}[\Lambda(x)\, \frac{dE(x,t)}{dx}] = E_{ext}(t) \tag{3.34}$$

We wish to consider the response to an impulse, so we will set $p^2 = -\omega^2$ to convert the problem to a Laplace transform with zero initial conditions.

The first term in the equation is the so-called cold plasma term and gives the initial ringing or the transient response to the applied impulses. The cold plasma response will be used to compute a warm plasma correction by a perturbation approach.

After expanding the equation, it is

$$E + \frac{dE}{dx} \frac{3}{4\omega_c^2 + p^2} \frac{1}{p^2 + \omega_{uH}^2} \frac{d}{dx}[\omega_p^2 \langle v_x^2 \rangle]$$

$$+ \frac{3}{4\omega_c^2 + p^2} \frac{1}{p^2 + \omega_{uH}^2} \omega_p^2 \langle v_x^2 \rangle \frac{d^2E}{dx^2} = \frac{p^2 + \omega_c^2}{p^2 + \omega_{uH}^2} E_{ext} \tag{3.35}$$

Now examine the inverse transform, which will be expressed in terms of convolutions.

Several Laplace transforms will be needed.

$$\frac{p^2+\omega_c^2}{p^2+\omega_{uH}^2} = L\{\delta(t) - \frac{\omega_p^2}{\omega_{uH}} \sin \omega_{uH} t\} \tag{3.36}$$

$$\frac{1}{(p^2+4\omega_c^2)(p^2+\omega_{uH}^2)} = \frac{1}{(\omega_p^2 - 3\omega_c^2)} \; L\{\frac{1}{2\omega_c} \sin 2\omega_c t - \frac{1}{\omega_{uH}} \sin \omega_{uH} t\} \tag{3.37}$$

Thus

$$E(x,t) = E_{ext}(t) * [\delta(t) - \frac{\omega_p^2}{\omega_{uH}} \sin \omega_{uH} t]$$

$$- \frac{d}{dx}[\omega_p^2 \langle v_x^2 \rangle] \frac{3}{\omega_p^2 - 3\omega_c^2} \frac{dE(x,t)}{dx} * [\frac{1}{2\omega_c} \sin 2\omega_c t - \frac{1}{\omega_{uH}} \sin \omega_{uH} t]$$

$$- \frac{3\omega_p^2 \langle v_x^2 \rangle}{\omega_p^2 - 3\omega_c^2} \frac{d^2E}{dx^2} * [\frac{1}{2\omega_c} \sin 2\omega_c t - \frac{1}{\omega_{uH}} \sin \omega_{uH} t] \tag{3.38}$$

For simplicity, assume $E_{ext}(t) = E_p t_p \, \delta(t)$ and let $\langle v_x^2 \rangle = 0$ to obtain the cold plasma response $E_o$. The response is considered to be the difference of the cold plasma response $E_o$ and the warm plasma correction $E_1$, which is initially much smaller.

Then the plasma response field (ignoring $\delta(t)$) is

$$E_o = - \frac{\omega_p^2}{\omega_{uH}} E_p t_p \sin \omega_{uH} t \tag{3.39}$$

Now evaluate the correction due to the finite temperature of the plasma. We will always seek the <u>dominant terms</u> for simplicity. The phase $\omega_{uH} t$ will rapidly become large, so the only one of the thermal terms which we will keep will be the one of largest order in

$\omega_{uH}t$ . Thus in differentiating $E_o$ to obtain the driving term for $E_1$ we only consider derivatives of the trig factor.

$$\frac{dE_o}{dx} \simeq - \frac{\omega_p^2}{\omega_{uH}} E_p t_p t \frac{d\omega_{uH}}{dx} \cos \omega_{uH}t \tag{3.40}$$

$$\frac{d^2E_o}{dx^2} \simeq + \frac{\omega_p^2}{\omega_{uH}} E_p t_p (t \frac{d\omega_{uH}}{dx})^2 \sin \omega_{uH}t \tag{3.41}$$

and the second derivative dominates the first.

Now consider the convolution

$$t^2 \sin \omega_{uH}t * [\frac{1}{2\omega_c} \sin 2\omega_c t - \frac{1}{\omega_{uH}} \sin \omega_{uH}t]$$

$$= \int_0^t t'^2 \sin \omega_{uH}t' [\frac{1}{2\omega_c} \sin 2\omega_c(t-t') - \frac{1}{\omega_{uH}} \sin \omega_{uH}(t-t')]dt' \tag{3.42}$$

Only the second term needs to be considered, for only it is in resonance with the driving term. The dominant term from the convolution is

$$- \frac{1}{\omega_{uH}^4} \frac{(\omega_{uH}t)^3}{6} (-\cos \omega_{uH}t)$$

thus

$$E_1(x,t) = \frac{[\omega_p^2 \frac{d\omega_{uH}}{dx}]^2 E_p t_p \langle v_x^2 \rangle t^3 \cos(\omega_{uH}t)}{2(\omega_p^2 - 3\omega_c^2)\omega_{uH}^2}$$

Because $\omega_{uH} = (\omega_p^2 + \omega_c^2)^{1/2}$ and $B_o$ is uniform, we have

$$\frac{d\omega_{uH}}{dx} = \frac{d\omega_p}{dx} \frac{\omega_p}{\omega_{uH}}$$

Thus the final expression for the dominant thermal mode correction is

$$E_1(x,t) = \frac{[\omega_p^3 \frac{d\omega_p}{dx}]^2 E_p t_p \langle v_x^2 \rangle t^3}{2(\omega_p^2 - 3\omega_c^2)(\omega_{uH})^4} \cos \omega_{uH} t \qquad (3.43)$$

When $\omega_c = 0$ this reduces to half of Henderson's result. Theoretical problems arose when we tried to extend the method to large perturbations. One problem is that the equation changes to an $x$ dependent one and no longer describes a local effect which can be simply summed throughout the plasma volume. Instead of theoretically extending this equation to more complicated regimes, a crude model was developed which was convenient for exhibiting echoes and which demonstrates the qualitative features of the phenomenon.

## 3.4 Damping of the Ringing Response by the Growth of Thermal Modes

We start with the equation for the short term growth of thermal modes from the previous section. This equation is valid for times so short that the ringing response has not changed appreciably.

In the model for thermal mode damping it is assumed that thermal modes are short wavelength plasma waves which propagate away from the upper hybrid resonance region with very low group velocity and are therefore quickly dissipated close to their source by even a small collision frequency. Only the time variation of the magnitude of the electric field will be considered. We will assume

$$E = E_o - E_1 \equiv E_o f(t) = E_o \quad \text{at} \quad t = 0 \qquad (3.44)$$

We will choose

$$f(t) = \exp[-\beta \langle v_x^2 \rangle t^3]$$

and we will match the small time behavior of $E_1$

$$E_1 = E_o[1 - f(t)] \tilde{=} E_o \beta \langle v_x^2 \rangle t^3$$

if we choose

$$\beta \equiv \frac{\omega_p^4 \left(\frac{d\omega_p}{dx}\right)^2}{2(3\omega_c^2 - \omega_p^2)\omega_{uH}^3} \tag{3.45}$$

This decay factor has not been derived from first principles, but it approximates the small time perturbation result which was derived with the assumption of constant ringing response. In addition it is a reasonable model for the decay of the ringing response and is very convenient for calculating echo strength. The decay factor will be used to describe the decay of the velocity of one electron when it is excited by an impulse, since the velocity of a charged layer of plasma is proportional to the electric field created by the displacement of that layer.

## 3.5 Echo Amplitude for a Frequency Periodic Temperature

The velocity of an electron following an impulsive excitation at upper hybrid resonance will be taken as

$$v = v_p \cos \omega_{uH} t \tag{3.46}$$

In the echo model we will multiply this single particle response by the decay factor due to thermal mode generation to obtain

$$v = v_p \exp[-\beta t^3 \langle v_x^2 \rangle] \cos \omega_{uH} t \tag{3.47}$$

The frequency periodic effect which is needed to produce echoes will be introduced through $\langle v_x^2 \rangle$ . The first two pulses will gradually decay from ringing response into random thermal energy, and it is assumed in the model that only the randomized fraction of the energy from the first two pulses will contribute to thermal mode growth. This will be expressed in a "degree of thermalization" parameter $\alpha$, which ranges from zero immediately following the second pulse to one at long times after it. Simultaneous with the thermalization process, the plasma cools off by the parallel free-streaming of the perpendicularly heated electrons and by their replacement with cool electrons, as discussed in Section 3.7. With $R$ representing the fraction of hot electrons remaining within the waveguide region, we set

$$\langle v_x^2 \rangle = R\,\alpha\, v_o^2 (1 + \cos \Omega\tau)^2 + (1 - R)\, v_{x\,th}^2 \tag{3.48}$$

where $v_o$ is the speed acquired by a single electron after either of the initial pulses acting alone, $\Omega$ is the upper hybrid frequency, $v_{th}$ is the thermal speed of the unperturbed plasma, and $\tau$ is the spacing of the first two pulses. After the first two impulses, an electron's speed is $v_o(1 + \cos \Omega\tau)$.

This gives for the ringing response to the third pulse

$$v = v_p \exp[-\beta t^3 R\,\alpha\, v_o^2 (1 + \cos \Omega\tau)^2] \exp[-\beta t^3 (1-R) v_{x\,th}^2] \cos \Omega t \tag{3.49}$$

This can be written as the product of three factors using the definition

$$z \equiv \frac{1}{2} \alpha \beta \, Rt^3 \, v_o^2$$

$$v = v_p \exp[-\beta t^3 (1-R) v_{x\,th}] \exp[-3z] \exp[-4z \cos \Omega\tau - z \cos 2\Omega\tau] \cos \Omega t \tag{3.50}$$

Now use the identity [5]

$$\exp(x \cos \theta) = I_o(x) + 2 \sum_1^\infty I_k(x) \cos(k\theta) \tag{3.51}$$

to yield

$$V = V_p \cos \Omega t \exp(-\beta t^3 (1-R) v_{x\,th}^2) \exp(-3z) \left[I_o(-4z) + 2 \sum_1^\infty I_k(-4z) \cos(k\Omega\tau)\right] \left[I_o(-z) + 2 \sum_1^\infty I_L(-z) \cos(2L\Omega\tau)\right]$$

We wish to find the terms in the series that will combine with the $\cos \Omega t$ factor to nullify phase mixing at $t = \tau$ following the third impulse at $t = 0$. Thus we must find the terms from the product of the two series which are proportional to $\cos \Omega\tau$. This requires that $k = 2L \pm 1$.

Using the fact $I_n(-x) = (-)^n I_n(x)$ if $n$ is an integer, we find that the final expression for the pulse induced speed after the third pulse, including only the first echo, is

$$v = v_p \cos \Omega t \exp(-\beta t^3 (1-R) v_{x\,th}^2) \exp(-3z) \Big[I_o(z) I_o(4z) + 2 \cos \Omega\tau \Big\{-I_o(z) I_1(4z) + \sum_{L=1}^\infty (-)^{L+1} I_L(z) [I_{2L-1}(4z) + I_{2L+1}(4z)]\Big\}\Big] \tag{3.52}$$

The qualitative behavior of the first three pulse echoes will now be developed by evaluating the total current induced by the 1D plasma slab in an external circuit, following the method of [6].

If the spacing of the electrode plates is 2a, then the current per electron which flows in the external circuit is

$$I(t) = \frac{qv(t)}{2a} \tag{3.53}$$

since the charge induced on each plate is a linear function of position. This result can be obtained by considering the displacement of layers of charge in a slab. We will temporarily ignore the factor $\exp[-\beta t^3(1-R)v_{x\,th}^2]$.

For the ensemble of electrons we have

$$I(t) = \frac{q}{2a}\int_{-a}^{a} dx\; n(x)\; v(x,t) \cdot (\text{plate area}) \tag{3.54}$$

In this echo model the current after the third impulse is

$$\begin{aligned} I(t) = \frac{qA}{2a}\int_{-a}^{a} dx\; n(x)\; v_p e^{-3z} \cos \Omega t\{ & I_o(z)\; I_o(4z) \\ & + 2\cos \Omega\tau[-\, I_o(z)\; I_1(4z) \\ & + \sum_{L=1}^{\infty} (-)^{L+1}\, I_L(z)(I_{2L-1}(4z) + I_{2L+1}(4z))]\} \end{aligned} \tag{3.55}$$

where higher Fourier components have been dropped.

The transient response is at $t = 0$ and is

$$I_{trans} = \frac{qA}{2a}\int_{-a}^{a} dx\; n(x)\; v_p \tag{3.56}$$

The first echo is at $t = \tau$ when there is a term with no rapidly changing phase factor.

$$I_E(\tau) = \frac{qA}{2a} \int_{-a}^{a} dx\, n(x)\, v_p e^{-3z} \{-I_o(z)\, I_1(4z) + \sum_{L=1}^{\infty} (-)^{L+1} I_L(z)\, [I_{2L-1}(4z) + I_{2L+1}(4z)]\} \qquad (3.57)$$

where $z$ is now evaluated at $\tau$

$$z = \frac{1}{2} \beta(x)\, \tau^3\, d(T)\, v_o^2$$

$\alpha$ = "degree of thermalization"

$v_o$ = pulse induced speed from 1P and 2P

$T$ = spacing of 2nd and 3rd pulses

$$\beta(x) = \frac{\omega_p^4(x) (\frac{d\omega_p}{dx})^2}{2(3\omega_c^2 - \omega_p^2)\omega_{uH}^3}$$

## 3.6 Degree of Thermalization after the First Two Pulses

The degree of thermalization will be obtained by analogy with the above work on temperature dependent decay. Late in the afterglow before any microwave pulses have been applied, the plasma is near room temperature. Returning to equation (3.34), we see that if $\langle v_x^2 \rangle = 0$ the plasma responds as a cold plasma. We make a distinction between random thermal motion represented by $\langle v_x^2 \rangle$ and the coherent (locally in phase) motion of the electrons following an exciting pulse. In a cold plasma the responses to impulses just add vectorially; the plasma must thermalize in order to show temperature

effects. The first two pulses will lose energy by thermal mode generation, since the model predicts that the thermal mode damping process will be much faster than electron-ion or electron-neutral energy transfer.

Thus for the degree of thermalization parameter in this model we will use

$$\alpha = 1 - \exp[-2\beta T^3 \langle v_{x\,th}^2 \rangle] \tag{3.58}$$

where $v_{th}^2 \equiv \frac{3kT_e}{m}$, $T_e$ is the temperature of the electron gas in the afterglow, and $T$ is the time between the second and third pulses. The changing decay rate due to the ongoing process of thermalization will be ignored. This form for $\alpha$ was chosen because if the speed in the coherent motion varies as $\exp[-\beta t^3 \langle v_x^2 \rangle]$ then the energy in the coherent motion will vary as the square of the speed or as $\exp[-2\beta t^3 \langle v_{x\,th}^2 \rangle] = \exp[-\frac{2}{3}\beta t^3 \langle v_{th}^2 \rangle]$.

## 3.7 Loss of Hot Electrons by Free Streaming

So far we have developed a model for three-pulse echoes which results from a temperature dependent response and a frequency periodic temperature caused by the first two pulses. Echoes could be produced as long as the hot layers persisted in the plasma. We must explain the experimental result that the echo strength first increases and then diminishes as the third pulse is moved further from the first two pulses. The large mass difference makes the energy transfer in electron-ion or electron neutral collisions too slow to explain the observations.

One way to weaken 3PE in the present model is to replace hot electrons with cold electrons from outside the waveguide region. The loss of hot electrons must be balanced by an influx of cold electrons to maintain neutrality. This exchange of electrons occurs by free-streaming down the discharge tube parallel to the magnetic field instead of a diffusion process, since the mean free path is much too long and there are no consistent pressure effects in the experimental data.

Because the extraordinary mode only affects the perpendicular motion of the electrons, the electrons are assumed to retain their room temperature Maxwellian velocity distribution for motion parallel to the magnetic field. This would permit the hot layers to dissipate at approximately the correct rate. For example, at $300^{o}$K the rms value of $V_z$ is $(\kappa T/m)^{1/2} = .674 \times 10^{7}$ cm $\sec^{-1}$. Thus the time needed to cross a 7 cm wide waveguide would be 1.04 microseconds. Now we will follow Bruce's work on the damping of the transient response due to parallel free streaming [7].

The distribution of particles for $t > 0$, $R(z,t)$ may be found by a convolution of the initial distribution $R_o(z)$ with the propagation function $R_g(z,t)$ for particles initially located at $z = 0$. We have

$$R(z,t) = \int_{-\infty}^{\infty} R_o(\zeta)\, R_g(z-\zeta,t)\, d\zeta = R_o(z) * R_g(z,t) \qquad (3.59)$$

In this expression the quantity $R_o(\zeta)d\zeta$ is the fraction of particles initially between $\zeta$ and $\zeta + d\zeta$. Of these particles, the fraction $R_g(z-\zeta,t)$ arrive at point $z$ at time $t$. A summation is then taken

over all initial positions $\zeta$ .

First consider only one value of $v_z$ and a uniform spatial distribution of particles from -L/2 to +L/2 .

$$\left.\begin{aligned} R_o(z) &= \frac{1}{L} \qquad \text{if} \qquad -\frac{L}{2} \le z \le \frac{L}{2} \\ &= 0 \qquad \text{elsewhere} \end{aligned}\right\} = \frac{1}{L}\,\pi\left(\frac{z}{L}\right) \tag{3.60}$$

$$R_g(z,t) = \delta(vt-z) \quad \text{so that} \quad \int_{-\infty}^{\infty} R_g(z,t)\,dz = 1$$

Then

$$R(z,t) = \left[\frac{1}{L}\,\pi\left(\frac{z}{L}\right)\right] * \left[\delta(vt-z)\right] \tag{3.61}$$

where we have introduced the function

$$\pi(x) = 1 \quad , \qquad |x| \le \frac{1}{2}$$

$$= 0 \quad , \qquad |x| > \frac{1}{2}$$

Now performing the convolution, we have

$$R(z,t) = \frac{1}{L} \int_{-L/2}^{L/2} d\zeta\ \pi(\zeta/L)\ \delta(vt - z - \zeta) \tag{3.62}$$

$$R(z,t) = \frac{1}{L}\ \pi\left(\frac{z-vt}{L}\right) \tag{3.63}$$

The fraction of particles initially inside the waveguide which have not yet left is

$$R(t) = \frac{1}{L} \int_{-L/2}^{L/2} \pi\left(\frac{z-vt}{L}\right) dz \tag{3.64}$$

$$R(t) = \frac{1}{L}\,(L - vt)\ H(L - vt) \qquad \text{if} \qquad v > 0 \tag{3.65}$$

where $H(Y) = 1$ if $Y \geq 0$

$= 0$ if $Y < 0$

This result is for only one electron speed. Now consider a Maxwell-Boltzmann distribution of parallel velocities, where the distribution function is

$$\left(\frac{m}{2\pi KT}\right)^{1/2} e^{-mvz^2/2KT}$$

and the other velocity components are independently normalized. We will average the above results over an MB distribition in which $3KT = m_e v_{th}^2$ before the microwave pulses are applied. The fraction remaining is

$$R_m(t) = 2 \int_0^\infty dV \frac{1}{L} (L - vt)\, H(L - vt) \left(\frac{3}{2\pi v_{th}^2}\right)^{1/2} e^{-\frac{3v_z^2}{2v_{th}^2}} \tag{3.66}$$

If we let $u = \sqrt{3/2}\ v_z/v_{th}$ then we have

$$R_m(t) = \frac{2}{L}\sqrt{\frac{1}{\pi}} \int_0^\infty du\, e^{-u^2}\, H\left(L - \sqrt{\frac{2}{3}}\, v_{th} ut\right)\left(L - \sqrt{\frac{2}{3}}\, v_{th}\, ut\right) \tag{3.67}$$

Now defining $u_1 = \sqrt{3/2}\ \frac{L}{tv_{th}}$ we have

$$R_m(t) = \mathrm{erf}(u_1) - \frac{1}{\sqrt{\pi} u_1}\left(1 - e^{-u_1^2}\right) \tag{3.68}$$

As $t \to 0$, $u_1 \to \infty$ and $R_m(t) \to 1$. As $t \to \infty$, $u_1 \to 0$ and since $\mathrm{erf}(0) = 0$ and $\lim \frac{1}{u_1}(1 - e^{-u_1^2}) = 0$, $R_m(t) \to 0$. Thus the limiting values are correct.

Figure 3.1 is a graph of $R_m(t)$ describing the decrease in the fraction of hot electrons due to parallel free streaming. This migration causes the effective perpendicular temperature of the electrons at

a given radial position in the discharge tube to change as described by equation (3.48).

## 3.8 Computed Echo Strength

The final expressions for the strength of the first 3PE and the transient response are

Transient

$$I_{trans} = \frac{qA}{2a} \int dx\, n(x)\, v_p \tag{3.69}$$

First echo:

$$I_E = \frac{qA}{2a} \int dx\, n(x)\, v_p \exp(-\beta\tau^3(1 - R_m)v_{th}^2/3)\, e^{-3z}$$

$$\times \left\{ \sum_{n=1}^{\infty} (-)^{n+1} I_n(z)[I_{2n-1}(4z) + I_{2n+1}(4z)] - I_o(z)I_1(4z) \right\} \tag{3.70}$$

where

$$z = \frac{1}{2}\beta(x)\, \tau^3 R_m \alpha(T)\, V_o^2$$

$$\alpha = 1 - \exp[-\frac{2}{3}\beta(x)\, T^3 \langle v_{th}^2 \rangle]$$

$$\beta(x) = \frac{\omega_p^4 (\frac{d\omega_p}{dx})^2}{2\omega_{uH}^3(3\omega_c^2 - \omega_p^2)}$$

$$v_{th}^2 = \frac{3KT_e}{m}$$

$$R_m(t) = \mathrm{erf}(u_1) - \frac{1}{u_1\sqrt{\pi}}(1 - e^{-u_1^2})$$

$$u_1 = \sqrt{3/2}\ \frac{L}{T\, v_{th}}$$

$T$ is the spacing of the second and third impulse, $\tau$ is the spacing of the first and second, and $V_o$ is the electron speed increment

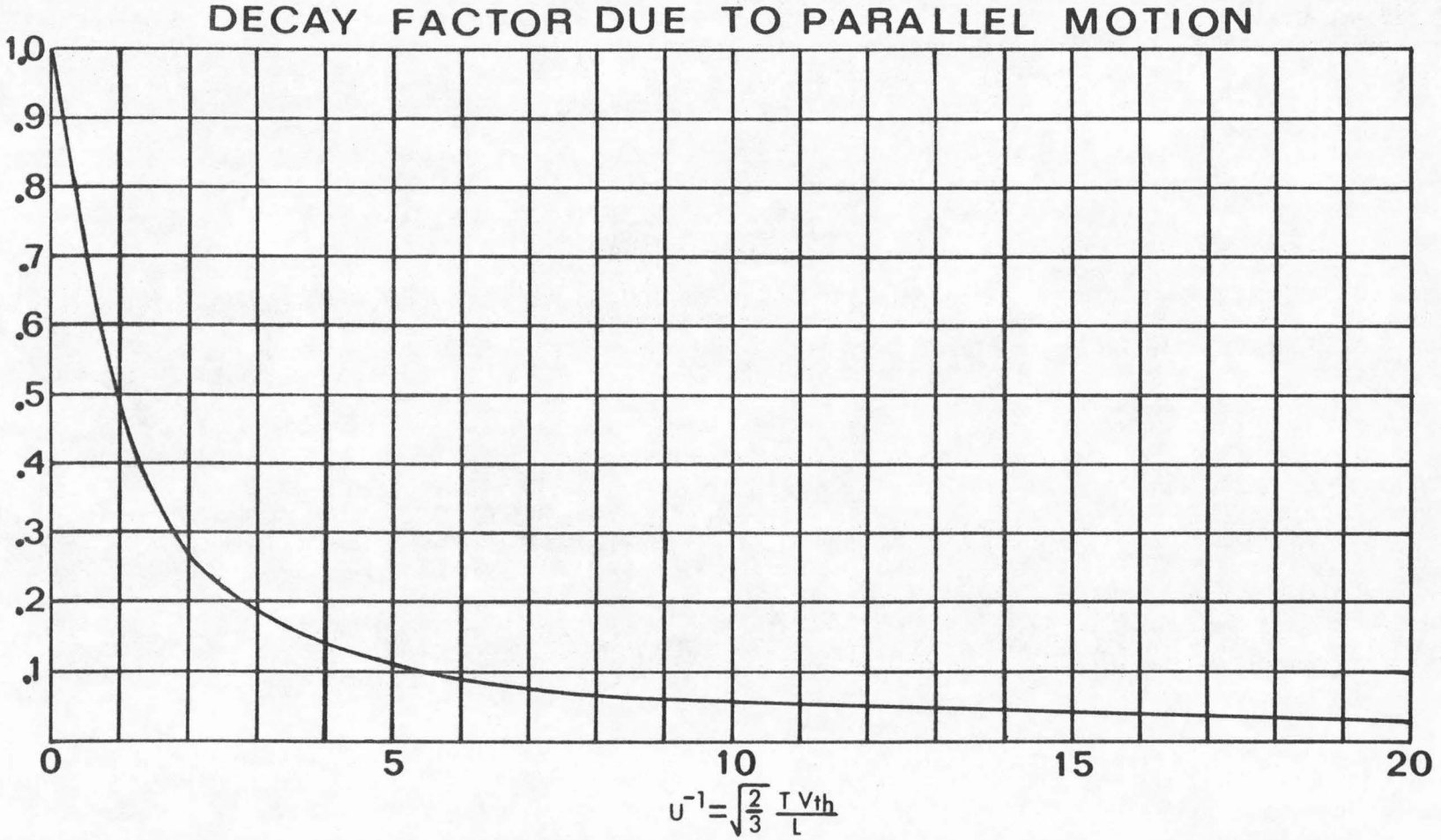
DECAY FACTOR DUE TO PARALLEL MOTION
1.0
.9
.8
.7
.6
.5
.4
.3
.2
.1
0
5
10
15
20
$U^{-1}=\sqrt{\frac{2}{3}}\frac{T\,Vth}{L}$

Fig. 3.1

which would be caused by either of the first pulses alone. Because the electron density gradient was shown to be an important parameter, for example in Fig.2.7 a truncated Gaussian electron distribution was used: $n(x) = n_{max} \exp(-\Gamma(x/a)^2)$.

This is a simple model for computations, although it has several obvious flaws. It is a one-dimensional instead of cylindrical model, it ignores the cosinusoidal variation of the electric field across the waveguide, and the finite spectral width of the exciting pulses has not been included. However, these complications seem unnecessary when the basic mechanism for echoes and their qualitative behavior are not well understood. The present model also makes the simplifying assumption that "thermalization" is independent of the free-streaming cooling process, and this tends to make the predicted optimum third pulse spacing too small, especially at low densities.

Of more consequence are the arbitrary assumptions which were made in modeling the effect of thermal mode growth on the ringing response and on the behavior of the plasma after the first two pulses. The pulsed response decay factor produces an answer consistent with the small time perturbation, which is the only case for which the theory has been done, and the decay factor is a simple and convenient model for the loss of ringing response energy to thermal modes and for the computation of echoes. The concept of thermalization is more dubious, and it is an attempt to explain how the frequency-periodic heating of the plasma by the first two pulses results at a later time in a frequency periodic response to the third pulse.

After mentioning these serious objections to this echo model we will enumerate its desirable features.

(1) The echo does not directly depend upon electron neutral collisions, and this is a necessary feature of the model which was dictated by experiment.

(2) The electron density gradient appears prominently in the theory and acts to make the effect stronger at higher gradients which is experimentally observed.

(3) The time required after the second pulse to create the 3PE decreases as the density increases, which is the most significant feature of the present experiments.

(4) By considering the decay of the magnitude of impulsive excitation, the echo obtained is proportional to the third pulse amplitude as required.

Now we must examine the time scale and magnitude of the model. First estimate $\beta$ , let $\omega_p^2/\omega_c^2 = .1$ , $\omega_{uH} \tilde{=} \omega_c \tilde{=} 1.5 \times 10^{10}$ , $d/dx \tilde{=} 1/a = \frac{1}{1\ cm}$ , and let $\tau = 10^{-7}$ sec.

With these approximations

$$\beta \equiv \frac{\omega_p^4 \left(\frac{d\omega_p}{dx}\right)^2}{2\omega_{uH}^3 \left(3\omega_c^2 - \omega_p^2\right)} = 2.6 \times 10^6$$

If the electrons acquire 1 eV after an impulse, then

$$V_o = 6 \times 10^7 \text{cm sec}^{-1}$$

If the plasma is initially at room temperature, $300^oK$, then

$$\sqrt{\frac{KT}{m}} = .674 \times 10^7 \text{cm sec}^{-1}$$

and

$$v_{th} = 1.167 \times 10^{7} \text{cm sec}^{-1}$$

Let $T = 10^{6}$ seconds. Then

$$\alpha \equiv 1 - \exp[-2\beta T^{3} \langle v_{th}^{2} \rangle] \tilde{=} 1 - e^{-710} \tilde{=} 1$$

$$u_1 \equiv \frac{\overline{3}}{2} \frac{L}{TV_{th}} \tilde{=} .737 \quad , \quad u_1^{-1} \tilde{=} 1.36$$

from Figure 3.1 this gives $R_m \tilde{=} .38$

$$z \equiv \frac{1}{2} \beta \tau^{3} R_m \alpha V_o^{2} \tilde{=} 1.78$$

From a plot of the integrand of equation (3.70) vs. $z$ it can be shown that the above value of $z$ corresponds to a sizable echo. Explicit graphs of the echo strength will be shown later.

## Computational Methods

In order to compute the integral it was necessary to evaluate it in three ranges of the parameter $z$. For small $z$ the Bessel functions were expanded in power series.

Define a function $F(z)$ by

$$F(z) = \exp(-3z) \{-I_o(z) I_1(4z) + \sum_{n=1} (-)^{n+1} I_n(z)[I_{2n-1}(4z) + I_{2n+1}(4z)]\} \qquad (3.71)$$

Using

$$I_n(x) = (\tfrac{1}{2}x)^n \sum_{k=0}^{\infty} \frac{(\frac{1}{4}x^2)^k}{k!(n+k)!}$$

for small $z$, we have

$$F(z) \overset{\sim}{=} -2z + 7z^2 - \frac{33}{2}z^3 + (29 + \frac{19}{24})z^4 + \cdots \tag{3.72}$$

For intermediate $z$, the series of Bessel functions was evaluated. Note that the forward recurrence relations cannot be used because round-off errors grow rapidly.

For large $z$, $F(z)$ changes very slowly and the summation becomes too tedious. Thus we use half the first Fourier component of $F(z)$ by an asymptotic expansion.

$$F(z) = \frac{1}{2\pi}\int_0^{2\pi} \cos\theta\, e^{-2z(1+\cos\theta)^2}\, d\theta \tag{3.73}$$

When $z$ is large, only $\theta$ near $\pi$ will contribute. Expand $1 + \cos\theta$ near $\theta = \pi$.

$$1 + \cos\theta \overset{\sim}{=} \frac{1}{2}\theta^2 - \frac{1}{4}\theta^4 + \frac{1}{6!}\theta^6 \cdots$$

The asymptotic series consists of terms like

$$A(\tfrac{2}{z})^{1/4}[1 + B(\tfrac{2}{z})^{1/2} + C(\tfrac{2}{z}) + D(\tfrac{2}{z})^{3/2} + \cdots]$$

We will keep terms up to and including $(\frac{2}{z})^{\frac{3}{2}+\frac{1}{4}}$.

The range of integration over $d\theta$ will be extended to $\pm\infty$, and we will use the result

$$\int_0 X^n \, e^{-(rx)^m} dx = \frac{1}{m r^{n+1}} \Gamma\left(\frac{n+1}{m}\right) \quad \text{[Ref. 8, 860.19]}$$

All powers in the exponent will be expanded in series except $\exp(-z\phi^4/2)$.

After some computation, one obtains

$$F(z) \overset{\sim}{=} -\frac{1}{4\pi}\left(\frac{2}{z}\right)^{1/4} \left\{\Gamma\left(\frac{1}{4}\right) - \frac{3}{8}\,\Gamma\left(\frac{3}{4}\right)\left(\frac{2}{z}\right)^{1/2} - \frac{5}{512}\,\Gamma\left(\frac{1}{4}\right)\left(\frac{2}{z}\right) - C\,\Gamma\left(\frac{3}{4}\right)\left(\frac{2}{z}\right)^{3/2} + \cdots\right\} \tag{3.74}$$

where $C = .008252$ and $\frac{5}{512} \overset{\sim}{=} .0097656$ .

The following three figures show the results of the echo model described above. The curves plot the amplitude of the echo in dB below the transient response vs. the time interval between the second and third applied impulses. The electron distribution is assumed to have a truncated Gaussian profile so that the density gradient can be easily varied by changing the parameter $\Gamma$ , and the column radius or slab half-width is assumed to be 1.33 cm. The other parameters are shown on the graphs.

In Fig. 3.2 the maximum electron density is varied as the other parameters are held fixed. As the density decreases, the maximum amplitude and the rise and fall rates of the echo become smaller. This behavior agrees qualitatively with that of Figs. 2.10 and 2.11, and the optimum third pulse spacings agree rather well. However, the maximum amplitude of the echoes disagrees drastically. In Fig. 2.11 the echo strength at $T = 1$ μsec varies from 10 to 14 dB below

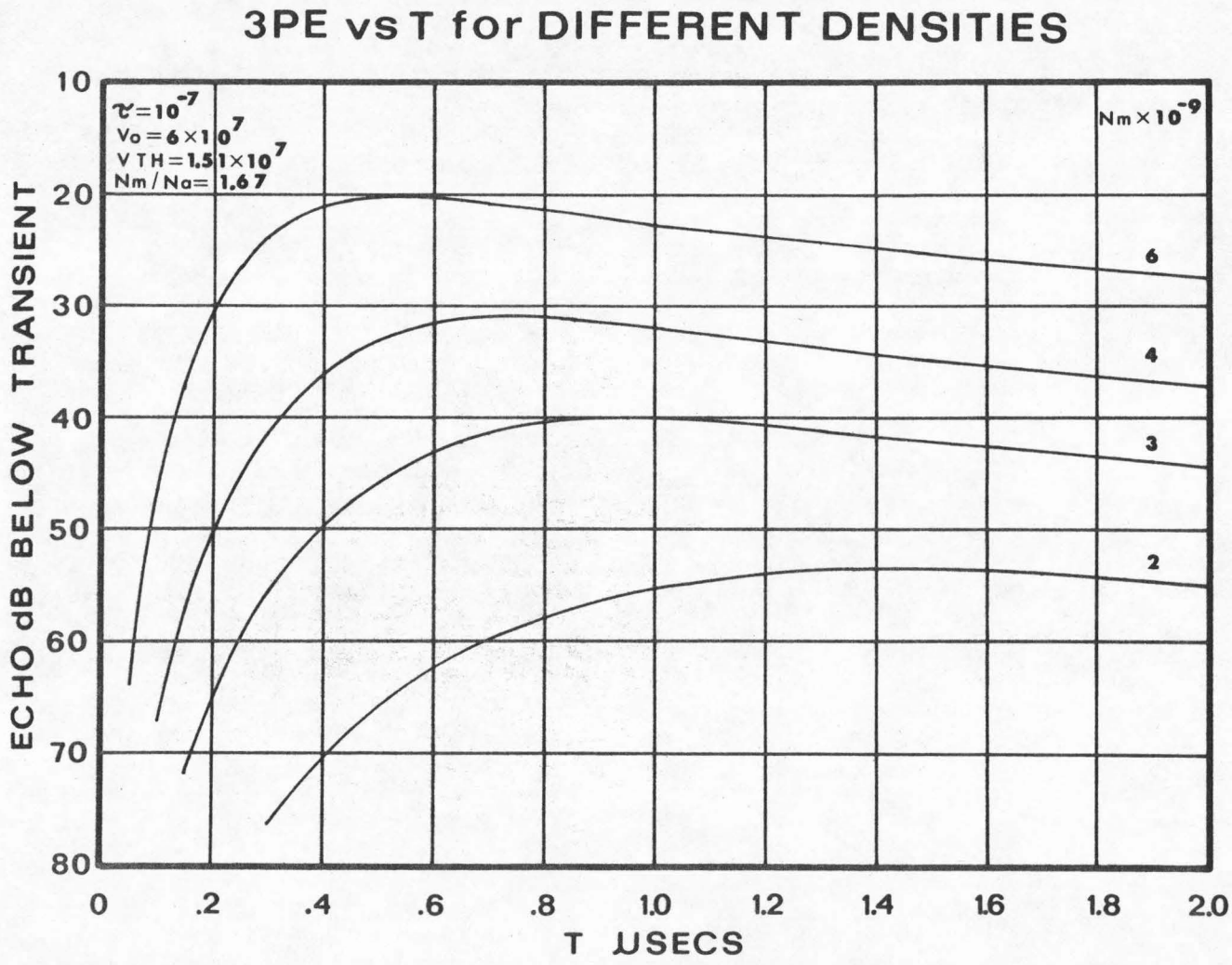
3PE vs T for DIFFERENT DENSITIES
τ=10^-7
Vo=6×10^7
VTH=1.51×10^7
Nm/Na= 1.67
Nm×10^-9
6
4
3
2
ECHO dB BELOW TRANSIENT
10
20
30
40
50
60
70
80
0
.2
.4
.6
.8
1.0
1.2
1.4
1.6
1.8
2.0
T μSECS

Fig. 3.2

the transient response, whereas the computed curve of Fig. 3.2 shows a rapid decrease of the maximum echo strength as the density decreases. Furthermore, the decrease with density of the rate of fall-off is not as pronounced in Fig. 3.2 as in Fig. 2.11.

These discrepancies can be remedied by varying the other parameters in the model. Recall that the plasma column profile appeared to become more peaked in the radial direction as the plasma decayed in the afterglow, as shown in Fig. 2.7. We speculate that this is caused by the shorter parallel diffusion length further from the axis of the two magnet coils. Figure 3.3 shows an attempt to coordinate decreasing density and temperature with an increasing ratio of $n_{max}$ to $n_{avg}$. The variation in peak echo amplitude is now in much better agreement with experiment, and the fall-off rate becomes much more gradual as the temperature decreases.

Figure 3.4 shows the predicted variation with the first two pulse powers as parameters. The calculations show a strong dependence of echo strength on $V_o$ which does not agree with experiment. Also, as $V_o$ becomes large enough, the echo can "saturate" and vary only slightly over a range of $T$. This behavior is not seen experimentally, and it may be removable by the effects of collisions which have been ignored in this study. If the effect of collisions were to remove heated electrons at a faster rate than thermal free streaming, and if the echo parameters were such as to cause "saturation" of the thermal mode process, then we speculate that the results of Fig. 2.9 would result, in which the echo is only slightly changed by a 10 dB change in pulse power.

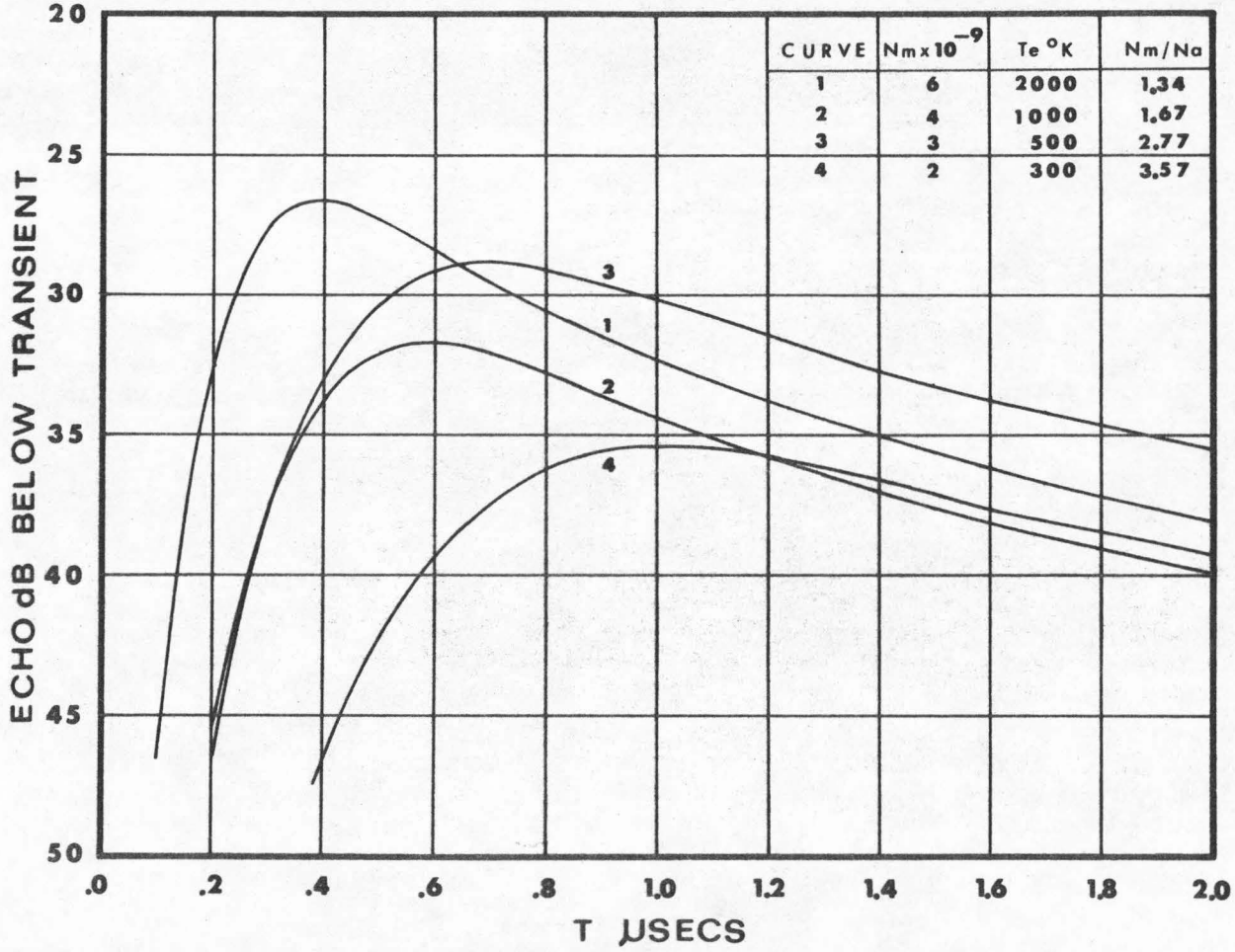
3PE for SIMULATED AFTERGLOW
CURVE | Nm x 10⁻⁹ | Te °K | Nm/Na
1 | 6 | 2000 | 1.34
2 | 4 | 1000 | 1.67
3 | 3 | 500 | 2.77
4 | 2 | 300 | 3.57
ECHO dB BELOW TRANSIENT
20
25
30
35
40
45
50
.0
.2
.4
.6
.8
1.0
1.2
1.4
1.6
1.8
2.0
T μSECS
1
2
3
4

Fig. 3.3

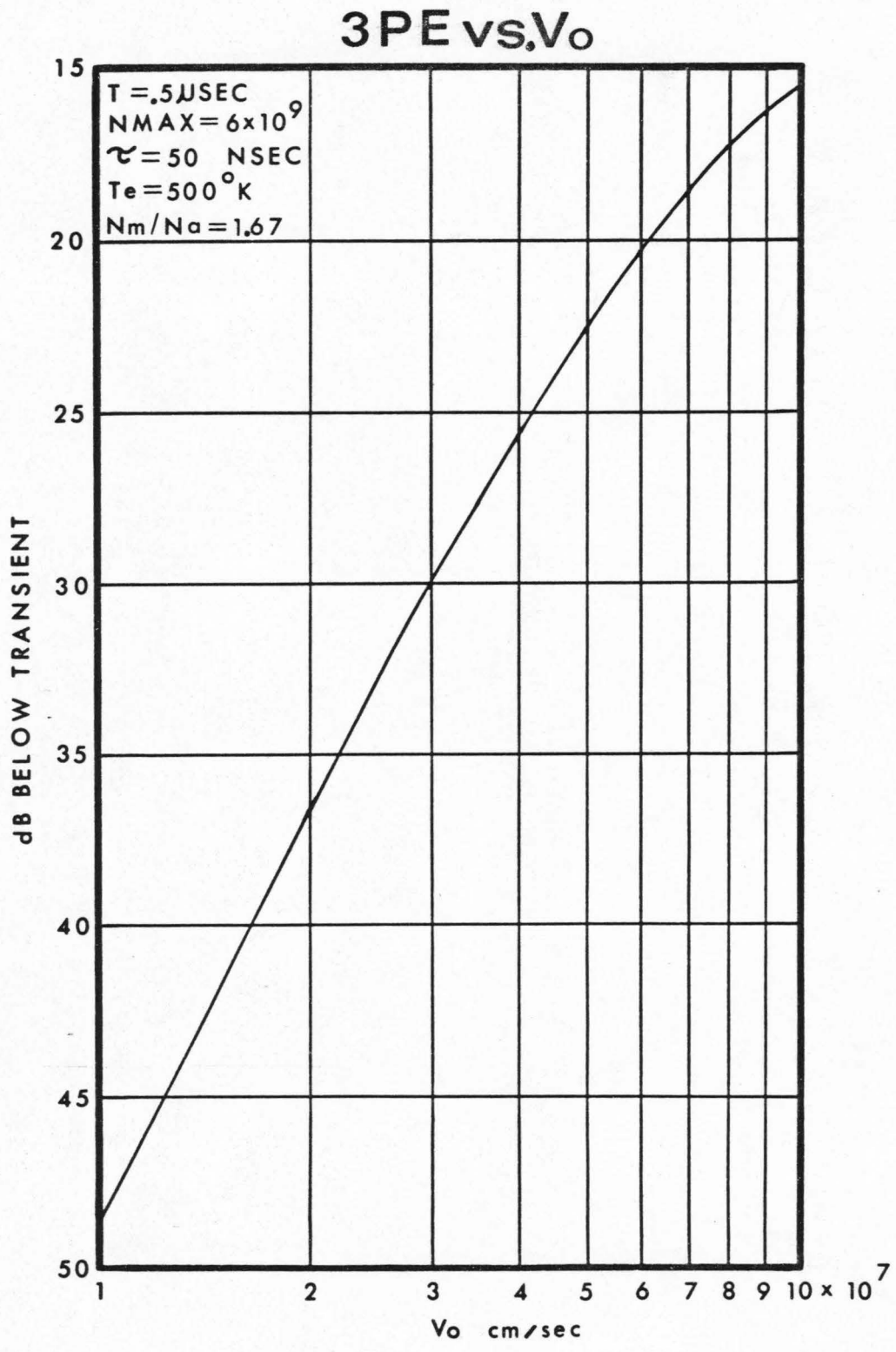
3PE vs. Vo
T = .5 μSEC
NMAX = 6x10^9
τ = 50 NSEC
Te = 500 °K
Nm/Na = 1.67
dB BELOW TRANSIENT
15
20
25
30
35
40
45
50
1
2
3
4
5
6
7
8
9
10 x 10^7
Vo cm/sec

Fig. 3.4

At this point it should be mentioned that this model contains no free parameters which can be manipulated to change the gross characteristics of the results. The numbers used in the computations are quite close to those of the experiments, and it is encouraging that the magnitudes of the echo and of $T_{max}$ in particular are close to the experimental values. Although $V_o$ was not experimentally measured, Bruce could calibrate his input power against $V_o$ by measuring the initial collisional decay rate of the transient response at very low densities. With his very similar equipment he could obtain $V_o$'s up to $10^8$ cm $sec^{-1}$.

References for Chapter III

1. D. M. Henderson, PhD thesis, Yale University (1970)

2. G. A. Pearson, Phys. Fluids 9, 2454 (1966)

3. D. J. Rose and M. Clark Jr., Plasmas and Controlled Fusion, M.I.T. Press, Cambridge, 1961, p. 77.

4. Ref. 3, p. 145

5. Handbook of Mathematical Functions, M. Abramowitz and I. Stegun, editors, U. S. Govt. Printing Office, 1966, eq. 9.6.34.

6. R. S. Harp, R. L. Bruce, and F. W. Crawford, J. Appl. Phys. 38, 3385 (1967)

7. R. L. Bruce, PhD thesis, Stanford University, 1969, p. 29; R. L. Bruce, J. Plasma Phys. 5, 385 (1971)

8. H. B. Dwight, Tables of Integrals and Other Mathematical Data, MacMillan, 1961

# IV. INSTABILITY OF A DELTA FUNCTION DISTRIBUTION IN VELOCITY SPACE

## 4.1 Instability Theory

During the course of this thesis, the modulated absorption effects were discovered before the thermal mode damping was conceived. The modulated absorption was originally interpreted as confirmation of the perturbed density model, although instabilities were eventually abandoned as an attempt to explain echoes. To explain the creation of density perturbations we considered the possibility of plasma instabilities which would result from the first two pulses and would cause turbulent diffusion from the hot layers.

Tataronis [1] has computed unstable behavior in plasmas due to a ring distribution of perpendicular velocities. In that case the plasma is far out of equilibrium, and for sufficiently high densities there are plasma waves propagating perpendicularly to the static magnetic field with complex $\omega$ and/or $K$. Tataronis found a lower density threshold for instability when oblique propagation was allowed, although that case is more complicated.

In discussing cyclotron echoes it is usually assumed that the applied fields are impulsive and that the electrons with a given resonant frequency are all excited with the same original phase and speed (see Gould diagrams, Fig. 1.1). This leads to the $\delta$ function electron velocity space distribution function, which is even further from equilibrium than the ring distribution and thus is expected to have a lower density threshold for instability. We will follow the same method used by Tataronis except for the slight additional

complexity caused by the lack of cylindrical symmetry in velocity space.

The plasma is described by the collisionless Boltzmann or Vlasov equation

$$\frac{\partial f}{\partial t} + \vec{V} \cdot \vec{\nabla}_r f - \frac{e}{m}(\vec{E} + \vec{V} \times \vec{B}) \cdot \vec{\nabla}_v F = 0 \tag{4.1}$$

We will use the electrostatic approximation for the perturbation fields

$$\vec{E}_1(\vec{r},t) = - \vec{\nabla}\phi_1(\vec{r},t) \quad \text{and} \quad \vec{\nabla} \times \vec{E}_1 = 0 \tag{4.2}$$

Also, the source of the perturbation field is

$$\nabla \cdot E_1 = \rho/\varepsilon_o \tag{4.3}$$

where

$$\rho(\vec{r},t) = -en_e \int d\vec{V}\, f_e(\vec{r},\vec{v},t) \tag{4.4}$$

The normalization is

$$\int d\vec{V}\, f_e = 1 \tag{4.5}$$

In linearizing the problem we will have zero and first order distribution functions, a zero order magnetic field, and a first order electric field. We will assume an infinite homogeneous plasma, so there will be no zero order spatial gradients and hence no zero order ambipolar electric field. This was not assumed in the theory of Chapter III. The linearized equations for the zero and first order distribution functions are

$$\frac{\partial f_o}{\partial t} - \frac{e}{m}(\vec{V}\times\vec{B}_o)\cdot\vec{\nabla}_v f_o = 0 \tag{4.6}$$

$$\frac{\partial f_1}{\partial t} + \vec{V}\cdot\vec{\nabla}_r f_1 - \frac{e}{m}(\vec{V}\cdot\vec{B}_o)\cdot\vec{\nabla}_v f_1 = \frac{e}{m}\vec{E}_1\cdot\vec{\nabla}_v f_o \tag{4.7}$$

Here the velocity is actually the unperturbed or zero order velocity. The left hand side can be recognized as the total or convective derivative of the first order distribution function along the zero order trajectory.

$$\frac{D}{Dt} f_1 = \frac{e}{m}\vec{E}_1\cdot\vec{\nabla}_v f_o \tag{4.8}$$

This is to be integrated from $t = 0$ when the sources are turned on until the time $t$ when the particle's position and velocity coincide with the Eulerian coordinates $\vec{r}$ and $\vec{v}$. We are considering an initial value problem and pursuing a method of formally integrating the equation for $f_1$. The initial conditions are zero.

$$f_1 = \frac{e}{m}\int_0^t E_1(t')\cdot\vec{\nabla}_{v'} f_o(r',v',t')dt' \tag{4.9}$$

This formal solution for $f_1$ will be used to find the electrostatic perturbation $E_1$

$$\vec{\nabla}\cdot\vec{E}_1 = \rho/\varepsilon_o = -\frac{ne}{\varepsilon_o}\int d\vec{V}\, f_1 + \frac{\rho_{source}}{\varepsilon_o} \tag{4.10}$$

For instabilities no sources are needed, so we have

$$\vec{\nabla} \cdot E_1 = -\omega_p^2 \int dV_o' \int_0^t \vec{E}_1(t',r_o') \frac{f_o(r_o',v_o',t')}{\partial \vec{V}_o'} dt' \qquad (4.11)$$

where we have used $\omega_p^2 = ne^2/\varepsilon_o m$ .

After following Tataronis' method as shown in the Appendix, one obtains for the dispersion function for electrostatic waves propagating perpendicular to $B_o$ in a spatially uniform plasma with a delta function distribution function

$$\kappa = 0 = 1 + \frac{\omega_p^2}{\omega_c^2} \frac{1}{\sin \pi\Omega} \int_0^\pi \sin x \sin(\Omega x + \mu \sin x) dx \qquad (4.12)$$

where $\Omega = \omega/\omega_c$ and $\mu = \dfrac{K V_o}{\omega_c}$ and we have used the distribution function

$$f_o(V_{\parallel}, \psi, V_{\perp}) = \delta(V_{\parallel}) \, \delta(\psi - \omega_c t) \, \delta(V_{\perp} - V_o) \qquad (4.13)$$

which is "created" at the position $(0,0,V_o)$ at $t = 0$ by the applied impulse.

Equation (4.12) reduces to the correct cold plasma limit as $\mu \to 0$ , as shown in the Appendix.

Now we will show the results of numerically solving eq. (4.12) for $\Omega$ and $\mu$ .

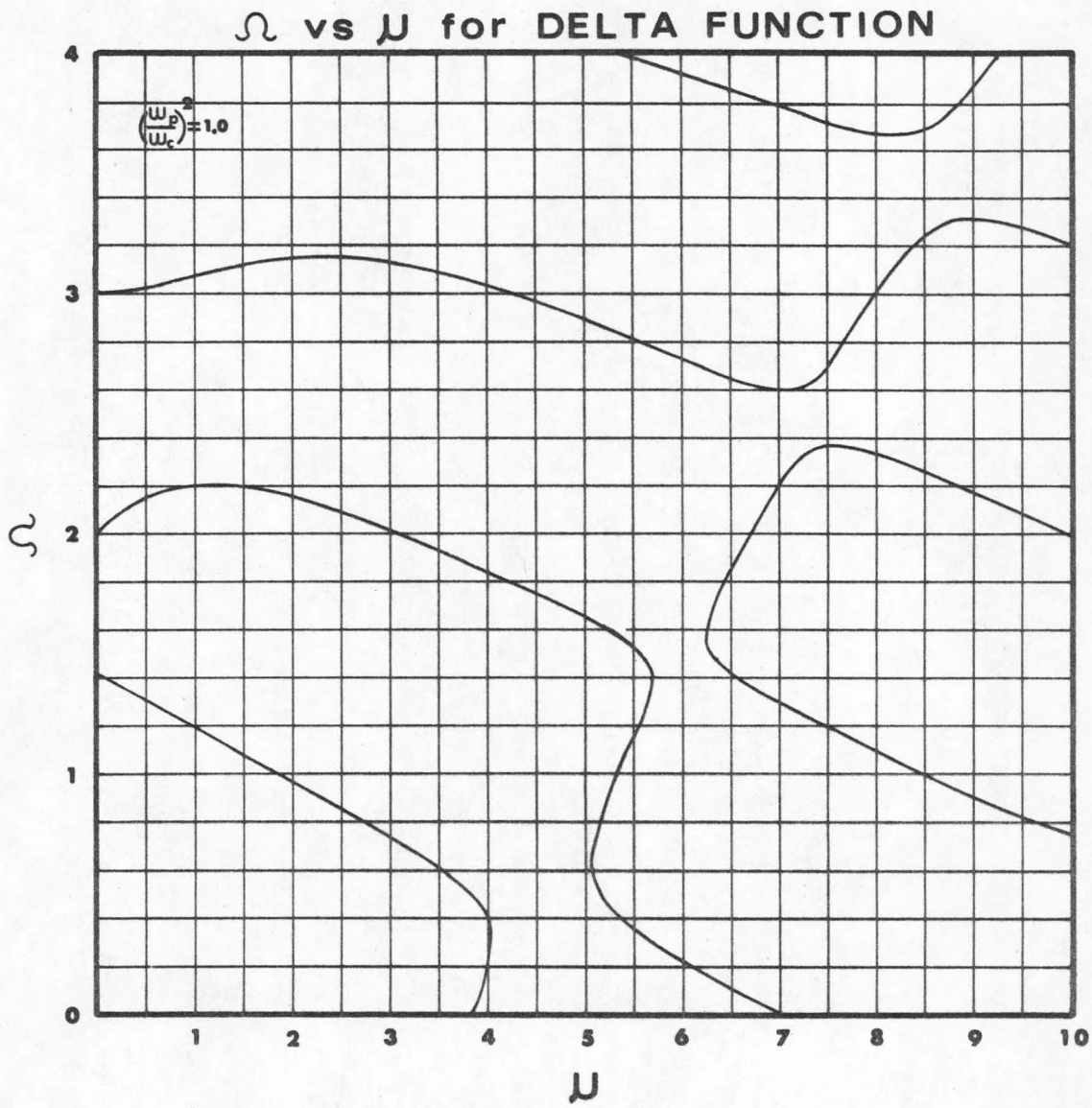
Ω vs μ for DELTA FUNCTION
$\left(\frac{\omega_p}{\omega_c}\right)^2 = 1.0$
Ω
μ
0
1
2
3
4
5
6
7
8
9
10

Fig. 4.1

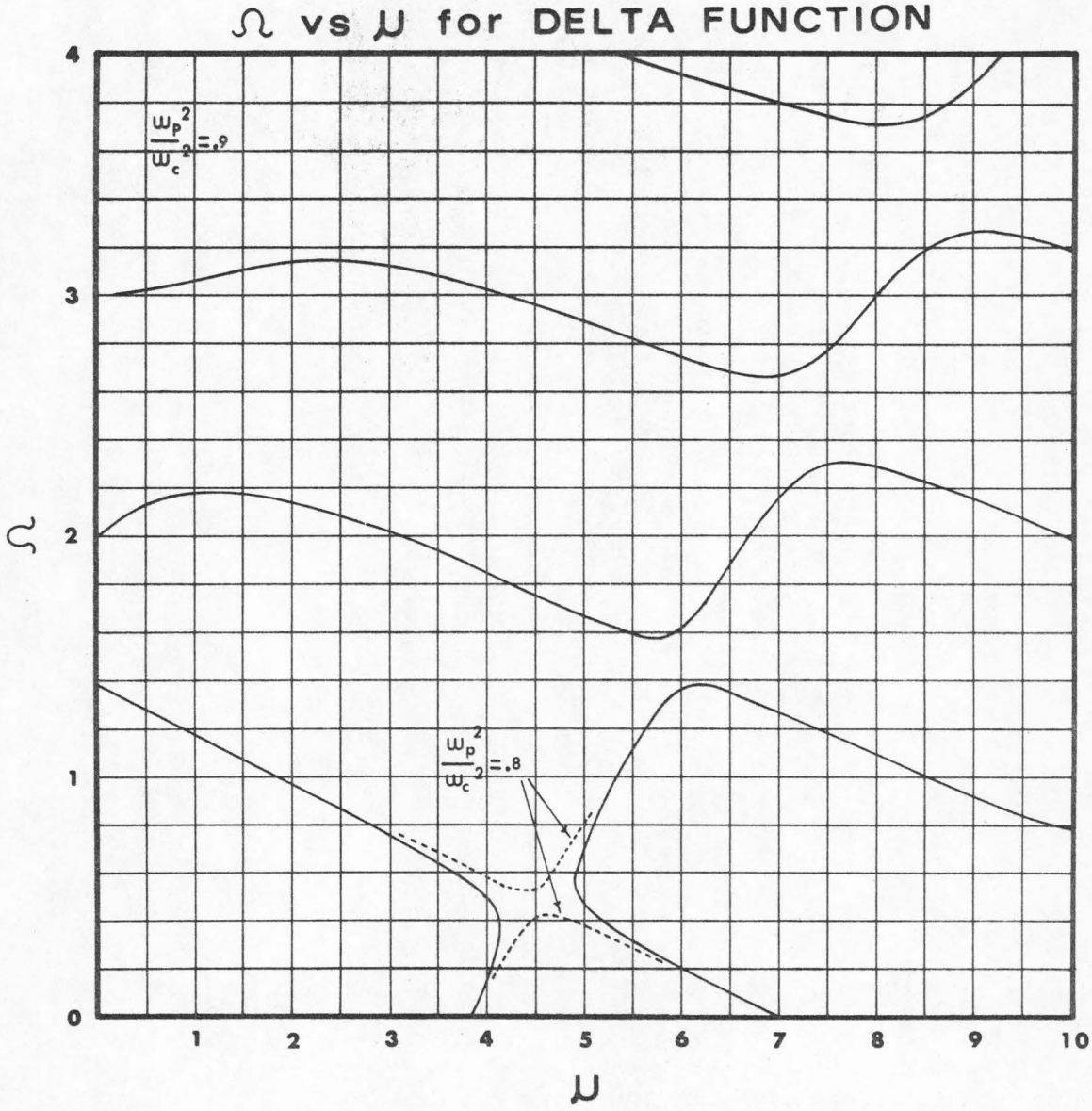
Ω vs μ for DELTA FUNCTION
$\frac{\omega_p^2}{\omega_c^2}$=.9
$\frac{\omega_p^2}{\omega_c^2}$=.8
Ω
μ
0
1
2
3
4
5
6
7
8
9
10

Fig. 4.2

## 4.2 Dispersion Curves and Implications for Echoes

When equation (4.12) is solved numerically to find the zeroes of $K$, and when the plasma density is large enough, gaps appear in the dispersion curves which are due to coupling of the different modes and which indicate instability [1,2]. However, the critical density is approximately $\omega_p^2/\omega_c^2 = .811$ which is much higher than the three pulse echo experiment densities. Thus this approach could not explain 3PE through enhanced diffusion as had been hoped, and the analysis of these instabilities was not pursued.

In Figs. 4.1 and 4.2 we see the dispersion curves resulting from the zeroes of $K$ for several values of $\omega_p^2/\omega_c^2$. The points at which the solution crosses $\Omega = n$ agree well with the values obtained by approximating $K$.

There were also experimental grounds for abandoning this approach. Instabilities should manifest themselves as noise emission at frequencies other than the usual range from the cyclotron to upper hybrid frequency range and near the harmonics, but no such unusual noise frequencies could be seen with a Tektronix 1L30 spectrum analyzer when the plasma was heated with the 10 watt pulsed traveling wave tube which was used in the echo experiments. Thus we concluded that this type of instability was not related to three pulse echoes.

## 4.3 References for Chapter IV

1. J. A. Tataronis, PhD Thesis, Stanford University, 1967. Also SUIPR Report #205.

2. P. A. Sturrock, Phys. Rev. 112, 1488 (1958).

# V. SLOW WAVES AFTER ONE MICROWAVE PULSE

## 5.1 Dependences upon Magnetic Field and Pulse Power

In echo experiments the observed signals can be cluttered with spurious reflections, and the usual way of deciding if a given peak is indeed an echo is to turn off one of the exciting pulses. The signal in question will then disappear if it is due to an echo, and after only one exciting pulse there is usually only a transient reflected pulse. However, using the echo set-up very close to the end of the RF breakdown, it is possible to observe an additional pulse following the first transient. This pulse moves in time with respect to the first pulse as the magnetic field is varied slightly. The effect seemed to occur for frequencies just under the maximum upper hybrid frequency, and there was no noticeable difference in the time separations of the incident and response pulse when the effect was observed in reflection and in transmission. When the extra pulse was isolated by a PIN diode modulator and spectrum analyzed, its spectrum was similar to that of the incident pulse. The response pulse was shown to be proportional to the input pulse power by an experiment in which the transmitter and receiver attenuations were varied together in such a way that the total attenuation was constant. The extra pulse amplitude varied by less than 10% on a square law scale, thus showing that the extra pulses are linear with respect to the input pulse. The amplitude of these pulses was about 40 dB below the incident pulse. The extra pulses were thought to be slow wave pulses, SWP.

In Fig. 5.1 we see the SWP moving away from the incident pulse as the magnetic field is increased slightly. The maximum electron

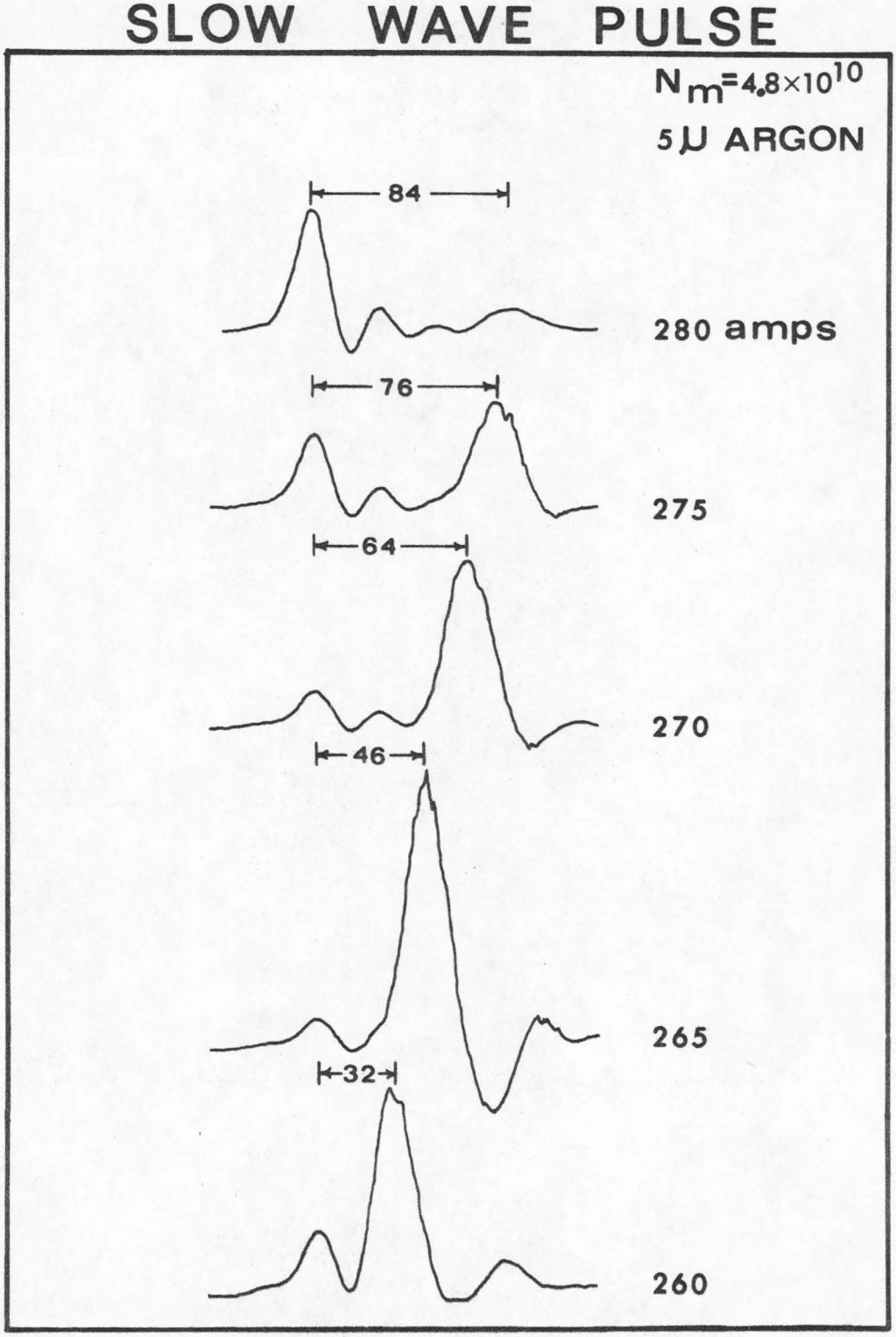
SLOW WAVE PULSE
$N_m = 4.8 \times 10^{10}$
5 μ ARGON
84
280 amps
76
275
64
270
46
265
32
260

Fig. 5.1

density was measured to be $4.8 \times 10^{10}$ by the cessation of absorption method described on page 23 at a coil current of 260 amps. The gas pressure was 5μ argon, the signal frequency was 3 GHz, and the experiment was performed 15 μsec in the afterglow, when the plasma was probably still quite warm. A circulator was used for convenience in measuring the density, and an HP 462A pulse amplifier allowed the crystal detector to be used at a lower power level where it was closer to having a square-law response. The detected pulses were sampled by a PAR 160 boxcar integrator with a 10 nsec time window, and the time separation of the input pulse and the SWP is shown on the figure in nanoseconds.

These extra pulses were not a beat phenomenon between the incident signal and the maximum upper hybrid frequency. If the period of such a beat phenomenon is denoted by $\tau$, then

$$\frac{1}{\tau} = \frac{1}{2\pi} \{\sqrt{\omega_c^2 + \omega_{po}^2} - \omega\} \tag{5.1}$$

since the signal frequency must be less than or equal to the maximum upper hybrid frequency if there is to be a resonant interaction with the plasma. As the magnetic field is increased the frequency difference would also increase and the time spacing would decrease, which is the opposite of the observed behavior.

## 5.2 Model for Temporal Separation of Incident and Slow Wave Pulses

Because the extra pulses were linear with respect to the input pulse amplitude, and because of their time behavior when the magnetic field was varied, it was decided to model the phenomenon as the

conversion of electromagnetic energy into electrostatic slow waves inside the plasma [1]. The waves are assumed to be launched at an upper hybrid layer, then travel diametrically through the plasma column to the opposite upper hybrid layer where they are converted back to EM waves and detected [2-5].

The waves are assumed to be electrostatic plasma waves obeying the dispersion relation [6,7].

$$\kappa = 0 = 1 - \frac{\omega_p^2}{\omega_c^2} \sum_{-\infty}^{\infty} \frac{e^{-\lambda} I_n(\lambda)}{\lambda} \frac{n\omega_c}{\omega - n\omega_c} \tag{5.2}$$

where $\lambda = \left(\frac{\kappa V_t}{\omega_c}\right)^2$ and $V_t \equiv \sqrt{\frac{\kappa T_e}{m_e}}$

The dispersion relation has been solved numerically to find the so-called cyclotron harmonic waves and the results have been experimentally verified [1,8]. We will use an approximate dispersion relation obtained by expanding $\kappa$ to second order in $\lambda$ so that an analytic form for the group velocity of the slow waves can be used in computing propagation delays across the column. The electron density will be assumed to have a parabolic variation with radius.

Using the fact

$$I_n(\lambda) = \left(\frac{\lambda}{2}\right)^n \sum_{\kappa=0}^{\infty} \frac{\left(\frac{\lambda^2}{4}\right)^\kappa}{\kappa!(\kappa+n)!}$$

we find

$$I_1(\lambda) \simeq \frac{\lambda}{2} + \frac{\lambda^3}{16}$$

$$I_2(\lambda) \simeq \frac{\lambda^2}{8}$$

$$I_3(\lambda) \simeq \frac{\lambda^3}{48}$$

With the notation $\frac{\omega_p^2}{\omega_c^2} = X^2$ and $\frac{\omega}{\omega_c} = \Omega$, the dispersion relation is approximately

$$0 \simeq 1 - X^2\left(\frac{1-\lambda+\frac{\lambda^2}{2}}{\lambda}\right)\left\{\left(\frac{\lambda}{2}+\frac{\lambda^3}{16}\right)\left(\frac{\omega_c}{\omega-\omega_c}-\frac{\omega_c}{\omega+\omega_c}\right)\right.$$
$$\left.+\frac{\lambda^2}{8}\left(\frac{2\omega_c}{\omega-2\omega_c}-\frac{2\omega_c}{\omega+2\omega_c}\right)+\frac{\lambda^3}{48}\left(\frac{3\omega_c}{\omega-3\omega_c}-\frac{3\omega_c}{\omega+3\omega_c}\right)\right\} \tag{5.3}$$

which to second order in $\lambda$ is

$$0 \simeq 1 - \frac{X^2}{\Omega^2-1} + \frac{3\lambda X^2}{(4-\Omega^2)(\Omega^2-1)} - \frac{15\lambda^2 X^2}{(\Omega^2-1)(4-\Omega^2)(9-\Omega^2)} \tag{5.4}$$

Now let $A = X^2$, $Z = \Omega^2$

$$(Z-1)(4-Z)(9-Z) - A(4-Z)(9-Z) + 3\lambda A(9-Z) - 15\lambda^2 A = 0 \tag{5.5}$$

The group velocity is defined by

$$V_G \equiv \frac{d\omega}{d\kappa} \tag{5.6}$$

and since

$$\frac{d\Omega^2}{d\lambda} = \frac{d\Omega^2}{d\kappa}\frac{1}{d\lambda/d\kappa} = 2\Omega\frac{d\Omega}{d\kappa}\frac{1}{2\kappa\frac{V_\perp^2}{\omega_c^2}} = \frac{\omega}{\kappa}\frac{1}{V^2}V_G = \frac{\Omega}{V_\perp\sqrt{\lambda}}V_G$$

We can find $V_G$ without solving explicitly for $\omega$. Expanding the approximate dispersion relation and differentiating with respect to $\lambda$, we find that the final expression for the group velocity is

$$V_G = \frac{V_t \sqrt{\lambda}}{\Omega} \frac{3 \frac{\omega_p^2}{\omega_c^2} [\Omega^2 + 10\lambda - 9]}{3(4 - \Omega^2)^2 - 2\Omega^2(2 + \frac{\omega_p^2}{\omega_c^2}) + 1 + \frac{\omega_p^2}{\omega_c^2}(13 - 3\lambda)} \tag{5.7}$$

and $\lambda$ is related to $\Omega$ by

$$\lambda = \frac{1}{2}\left(\frac{9 - \Omega^2}{5} - \sqrt{\left(\frac{9-\Omega^2}{5}\right)^2 - \frac{4(4 - \Omega^2)(9 - \Omega^2)}{5}\left(1 - \frac{\omega_o^2(\Omega^2-1)}{\omega_p^2}\right)}\right) \tag{5.8}$$

Figure 5.2 shows the dispersion curve and ratio of $V_G/V_t$ predicted by the approximate theory. The numerical results mentioned above show that the group velocity should go to zero at $\Omega = 1$, but the approximate expression is satisfactory for the experimental conditions in which the working frequency is always close to the local upper hybrid frequency.

The density profile has a radius $a$ which is approximately 1.33 cm. We will use the normalized radius $x = r/a$. The normalized radius at which the upper hybrid layer occurs will be called $L$. For the case of a parabolic profile we have

$$\omega_p^2(x) = \omega_{po}^2(1 - x^2) \tag{5.9}$$

$$L = \left\{1 - \frac{\omega^2 - \omega_c^2}{\omega_{po}^2}\right\}^{1/2} \tag{5.10}$$

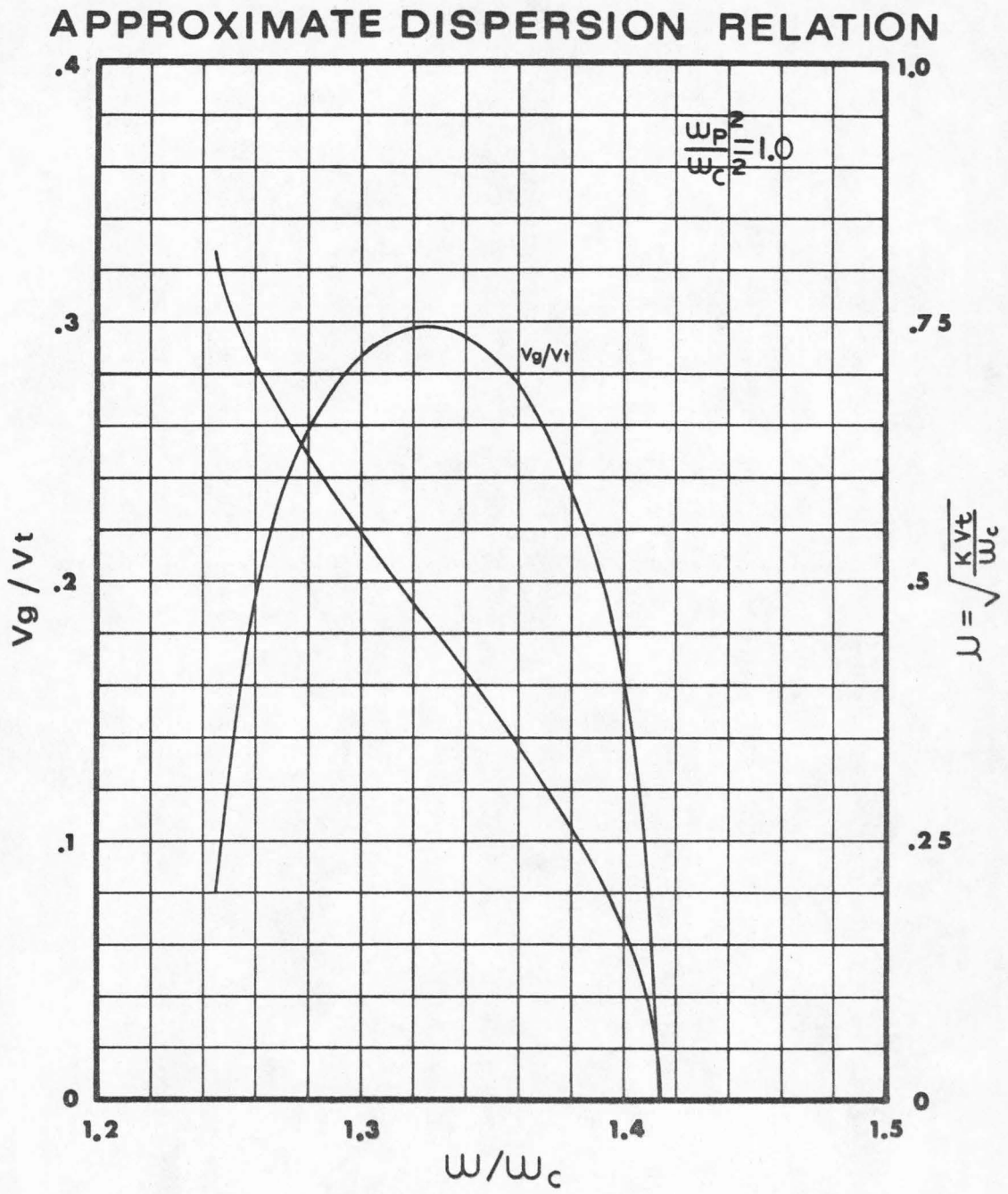
APPROXIMATE DISPERSION RELATION
$\frac{\omega_p^2}{\omega_c^2} = 1.0$
$V_g/V_t$
$V_g / V_t$
$\mu = \sqrt{\frac{K V_t}{\omega_c}}$
$\omega/\omega_c$
.4
.3
.2
.1
0
1.0
.75
.5
.25
0
1.2
1.3
1.4
1.5

Fig. 5.2

Although the time of flight should be computed from the integral of $dx/V_G$ , which would converge in this case, it was more convenient for the purpose of modeling the experiment to use

$$T = \frac{2a\ L}{\langle V_G \rangle} \quad \text{where} \quad \langle V_G \rangle = \frac{1}{L} \int_0^L V_G(x)\ dx \tag{5.11}$$

As the magnetic field is increased, the radius of the hybrid layer increases, the slow wave pulses must travel further, and the temporal separation between the incident pulse and the SWP increases. This is shown in Fig. 5.3 and indicates that the experimental observations can indeed be explained in terms of slow waves being created and then reconverted to EM waves. Unfortunately in this model the distance traveled and the average group velocity approach zero at nearly the same rate when the magnetic field is raised to the value at which the hybrid layer is exactly at the center of the column, so the interval does not go to zero at a coil current of 250 amps.

By examining Fig. 5.3 we see that another drawback of the model is the unreasonably high electron temperature which must be assumed in order to make the predicted and observed pulse spacings comparable.

These discrepancies point to a fundamental flaw in the model, and they may be related to Gruber's claim [ 9 ] that the conversion process occurs in the volume of plasma inside the hybrid layer and not just at that layer. If the conversion process does occur in the interior volume of plasma, then it is possible that the distance travelled by the plasma waves could approach zero more rapidly than the average group velocity as the hybrid layer approaches the center of the column.

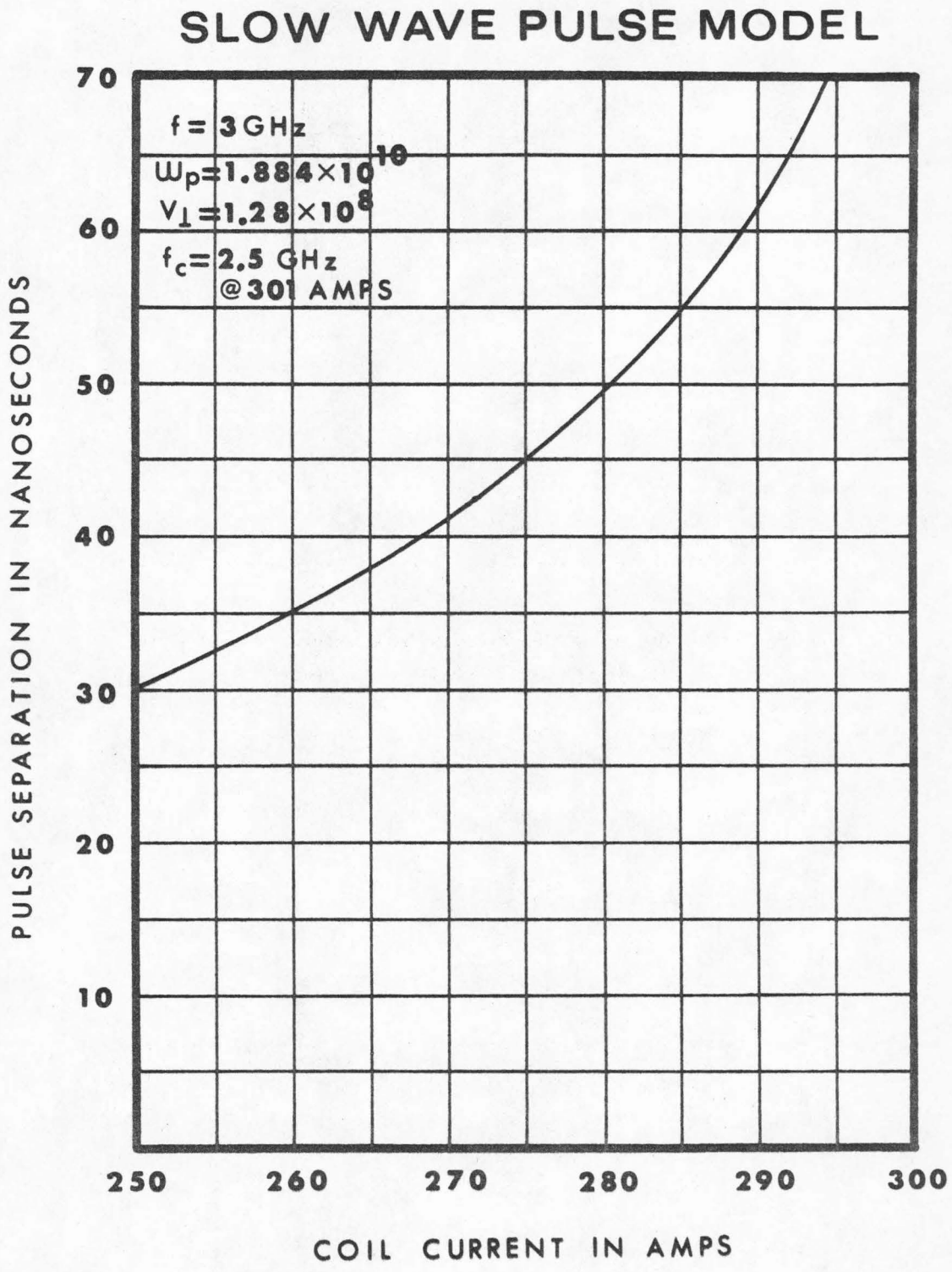
SLOW WAVE PULSE MODEL
f = 3 GHz
$W_p = 1.884 \times 10^{10}$
$V_\perp = 1.28 \times 10^{8}$
$f_c$ = 2.5 GHz
@301 AMPS
70
60
50
40
30
20
10
250
260
270
280
290
300
PULSE SEPARATION IN NANOSECONDS
COIL CURRENT IN AMPS

Fig. 5.3

A more likely source of error is the fact that the electron profile is probably not the parabolic distribution which was assumed. A more peaked distribution would reduce the time of flight, but at the experimentally early times in the afterglow ($\leq$ 50 μsec) the plasma profile is expected to be fairly uniform. Finally, eq. 5.2 is for an infinite plasma and this will cause errors in the region of small $\mu$ near the hybrid layer which is approached as the time of flight decreases to its minimum.

We see that the present model of slow wave pulses is inadequate in the electron temperatures which must be assumed and in the limiting behavior of the predicted pulse intervals as the static magnetic field is increased to the value for which the pulse center frequency equals the maximum upper hybrid frequency. Nevertheless, because the predicted behavior is in sufficient qualitative agreement with experiment and because the observed second pulse is linearly related to the input pulse power, we conclude that conversion of EM waves into plasma waves does occur in the present experimental arrangement.

## 5.3 Relation to Echo Work

In Chapter 3 a model for three-pulse echoes was developed which postulated the conversion of the applied microwave pulses into short wavelength plasma waves in a way which depended upon the plasma temperature. Although the model agreed in important ways with experimental results, it was not known whether such a temperature dependent conversion actually occurred under the experimental conditions present. The slow wave pulses described in the present chapter demonstrate that the mode conversion process does indeed occur. The observed pulses were

on the order of 40 db below the applied pulse. This amplitude is the result of two successive conversion processes plus the loss from propagating across the column, thus the conversion efficiency at the first UH layer must be appreciable.

Of course, the conditions in the 3PE experiments are different, and there are factors which imply that mode conversion in that case is larger and factors implying that conversion is smaller than in the SWP experiments. According to Stenzel [10] the plasma temperature at the end of an RF breakdown pulse is about 1 eV at a density of about $10^{11} cm^{-3}$. Thus the local temperature in a 3PE experiment can be as high as in the SWP experiment, but the density is one to two orders of magnitude less. This would tend to reduce the conversion efficiency, according to the model of Chapter 3. However, in the high density SWP experiments the microwave energy which actually reaches the UH layer may be significantly reduced due to the existence of an evanescent layer in which microwave propagation in the extraordinary mode is cut off.[11]. This layer would be much less influential in a lower density plasma, and this consideration would tend to increase the significance of mode conversion in 3PE work.

## 5.4 Estimate of Conversion Amplitude

H. H. Kuehl [3] has computed the fraction of incident power that is converted from an electromagnetic wave into a plasma wave when the plasma is inhomogeneous only in the direction of propagation. When the interaction region is small compared to a free space wavelength, which is also the case in the present echo experiments, Kuehl obtained the power conversion coefficient

$$T_p = \frac{4\pi\eta}{[q(\infty) + 1]^2} \tag{5.12}$$

where $$\eta = \frac{\omega_c^2}{\omega^2 \beta} \tag{5.13}$$

$$\beta = \frac{\left.\frac{d\omega_p^2}{dX}\right|_{X=UH\ layer}}{\omega^2 - \omega_c^2} \quad , \qquad X = \frac{\omega}{c} x \tag{5.14}$$

In his model, he assumed that the density rises smoothly from zero up to a constant value far away from the upper hybrid region. Here we will use the maximum plasma frequency to evaluate $q(\infty)$ from

$$q^2 = -\frac{[\omega_p^2 - \omega(\omega+\omega_c)][\omega_p^2 - \omega(\omega-\omega_c)]}{\omega^2 (\omega_p^2 + \omega_c^2 - \omega^2)} \tag{5.15}$$

In my 3 PE experiment, $\omega = 2\pi \times 2.5 \times 10^9$ , the bandwidth is about 100 MHz $\cong \frac{1}{4\pi} \frac{\omega_{po}^2}{\omega_c}$ , suppose $\omega$ is halfway between $\omega_c$ and $\omega_{UH\ max}$ , and let $\frac{d}{dX} = \frac{c}{\omega} \frac{d}{dx} = \frac{c}{\omega a}$ , where $a = 1.33$ cm . then we have

$$q^2 \cong 3 \quad , \quad q(\infty) \cong 1.73$$

$$\frac{\omega}{c} = \frac{2.5 \times 2\pi \times 10^9}{3 \times 10^{10}} = .524$$

$$\omega_{po}^2 \cong 1.97 \times 10^{19}$$

$$\beta = \frac{\frac{1}{.524} \quad \frac{1.97 \times 10^{19}}{1.33}}{2\pi \quad \beta\omega \quad \omega_c} \cong 2.87$$

$$\eta \cong \left(\frac{\omega_c}{\omega}\right)^2 \frac{1}{\beta} = \frac{1}{2.87} \left(\frac{1}{1+\frac{1}{2}\frac{2\pi\beta\omega}{2\pi f_c}}\right)^2$$

$$\eta \cong \frac{.96}{2.87} = .334$$

From Kuehl's graphs, when $\eta = .334$ and $q = 1.73$, $T_p \cong .15$, or a conversion loss of about 8 db.

Now estimate the conversion efficiency under the conditions of the slow wave experiment

$$N_{max} = 4.8 \times 10^{10}$$

$$\omega = 2\pi \times 3 \times 10^9 = 1.885 \times 10^{10}$$

$$\omega_c = 2\pi \times \frac{260}{301} \times 2.5 \times 10^9 = 1.356 \times 10^{10}$$

$$\omega_{po}^2 = (5.64)^2 \times 10^8 \times \eta_{max} \cong 1.527 \times 10^{20}$$

Suppose the critical cyclotron frequency is at 250 amps. Then we have

$$\omega_p^2 + \omega_c^2 - \omega^2 = \omega_c^2 - \omega_{co}^2 = \left(\left(\frac{26}{25}\right)^2 - 1\right) \omega_{co}^2$$

$$q^2 = 4.97$$

$$q \cong 2.23$$

$$\eta = \frac{\omega_c^2 (\omega^2 - \omega_c^2)}{\omega^2 \frac{c}{\omega a} \omega_{po}^2} = .486$$

For these parameters, $T_p \cong .1$, which is roughly a 10 db conversion loss. This is not inconsistent with the observed slow wave pulse amplitudes being 40 db below the incident pulse power, since in the SWP experiment there are two mode conversions and additional losses in propagating through the plasma region between the two hybrid locations.

Thus Kuehl's model implies a significant steady state conversion from EM waves to plasma waves for the conditions of my slow wave pulse, three pulse echo, and absorption experiments. His calculations make more plausible my explanation of the slow wave pulse experiment and my hypothesis of mode conversion after impulsive excitation, since in that case the ringing response is like a continuous driving source for plasma waves.

## 5.5 References for Chapter V


1. F. Leuterer, "Experiments with Bernstein Waves", Institute for Plasma Physics, Garching, Germany, report No. IPP 3/102 (1969).
2. T. H. Stix, Phys. Rev. Letters 15, 878 (1965).
3. H. H. Kuehl, Phys. Rev. 154, 124, (1967).
4. Ting-Wei Tong, Phys. Fluids 13, 121, (1970).
5. H. H. Kuehl, B. B. O'Brien, and G. E. Steward, Phys. Fluids 13, 1595 (1970).
6. I. B. Bernstein, Phys. Rev. 109, 10, (1958).
7. T. H. Stix, "The Theory of Plasma Waves", McGraw-Hill book company New York, (1962).
8. R. S. Harp, "The Dispersion Characteristics of Longitudinal Plasma Oscillations Near Cyclotron Harmonics", Proceedings of the 7th Int. Conference on Phenomena in Ionized Gases, Vol.II, Belgrade, (1966), p.254.
9. S. Gruber, Phys. Fluids 11, 858, (1968).
10. R. L. Stenzel and R. W. Gould, Review of Sci. Instr. 40, 1461, (1969).
11. M. A. Heald and C. B. Wharton, Plasma Diagnostics With Microwaves, John Wiley & Sons, Inc. New York (1965), p.127.

## VI Summary and Conclusions

This thesis has investigated three pulse cyclotron echoes (3 PE) in rare gas afterglow plasmas. The static magnetic field was parallel to the discharge tube, which passed perpendicularly through the short sides of a S-band waveguide. The experiment used the extraordinary mode of propagation in plasmas, and the static magnetic field was adjusted so that the center frequency of the applied pulses fell in the upper hybrid range of frequencies. That is, $\omega^2 = \omega_p^2(r) + \omega_c^2$ for some radius $r$, where $\omega_c$ is the electron cyclotron frequency and $\omega_p$ is the electron plasma frequency.

In Chapter I and II the experimental properties of echoes were shown to be incompatible with the existing models. The echo amplitude is a linear function of the third applied pulse amplitude, and this is in qualitative disagreement with the so-called collisional model, which invokes more rapid de-phasing of the higher energy electrons as the necessary non-linear mechanism. It was noted that the non-linear collective oscillation model which Blum and Bauer used to describe two pulse echoes is too weak an effect to account for the observed echo strengths.

Experiments on 3 PE in Chapter II showed that the electron density is the most significant parameter, especially with regard to the growth and decay of the echo following the first two pulses. The time interval between the second and third pulses must be the most important in creating the conditions for a linear echo after the third pulse. That is, the non-linearity operates between the second and third pulses. The electron density was shown to have a qualitative as well as

quantitative effect on the echo, and this is not explained by echo models which depend upon electron-neutral collisional effects. 2 PE and 3 PE were seen to be similar in the lengthening of optimum pulse spacings as the electron density decreased. Periodic modulation of both the emission and absorption of the plasma was observed following the first two pulses for probably the first time, and the excited layers were shown not to interact. These additional methods of investigating echo processes will be helpful in formulating a satisfactory theory.

A model containing the experimentally important parameters was developed. Because the actual experimental conditions are very difficult to handle theoretically, the model was based upon the much simpler case of the generation of plasma waves following an impulsive excitation for times so small that the original transient response has lost negligible energy to the plasma waves. The model produced an easily evaluated echo strength which is in better agreement with experiment than previous theories, especially in the dependence of the echo strength on the third pulse position for different densities.

Because of the impulsive nature of the applied microwave signals, unstable electron velocity space distributions could be created. This was briefly examined and discarded as a possible influence in echo experiments.

The possibility of converting microwave pulses into electrostatic plasma waves is experimentally verified for the particular geometry and plasma conditions of the echo experiments by the detection and qualitative theoretical explanation of slow wave pulses created inside the plasma column by the applied microwave pulses. This supports the mode conversion

echo model.

Any extension of the work in this thesis should first concentrate on improving the theory. The complexity would be very great if collisions were included to damp the plasma waves and if the differential equation for the electric field is solved numerically to find the field at all points in space and time, especially if the actual waveguide geometry with its holes in the side walls is considered.

Instead of attempting to deal with finite geometry effects and with boundary value problems, it would be better to explore as far as possible a local model, that is, consider the plasma response as a summation of responses by independent regions in the plasma. The two frequency heating experiments tend to support this approach. A specific theoretical problem to consider is the power radiated in the form of plasma waves from a freely oscillating dipole layer located at the upper hybrid position in a semi-infinite plasma with only $x$ dependent properties as a function of dipole energy density, electron density, and density gradient.

Some method of experimentally detecting plasma waves created after the third pulse would be very desirable, although the low density and temperature of the afterglow plasmas would certainly suffer major perturbations in the form of sheaths by even the finest metallic probe.

The present model could be extended to include 2 PE, but that would require the solution of a non-linear equation to find the damping of the first two pulses by thermal mode generation. For 3 PE, a non-linear approach was avoided by the choice of the model. That is, the heating effects of the first two pulses were not considered in calculat-

ing the subsequent energy transfer from the first two pulses' transient responses into the frequency periodic hot layers in the plasma. It was possible, and in fact dictated by experiment, to consider the linear interaction of the third input pulse with the frequency periodic plasma conditions set up by the first two pulses. The exact manner in which the frequency periodic temperature was created was relatively unimportant. That is, given such a temperature distribution from some cause, there would be a linear 3 PE after the third pulse. On the other hand, describing 2 PE would require much more care in the exact interaction of the first two pulses.

In conclusion, density dependent collective effects have been shown to be important in three pulse and two pulse cyclotron echoes. Although it is not an exact theory, the mode conversion model agrees well with experiment in several important ways. This new mechanism for echo processes deserves further study.

## APPENDIX

### DISPERSION RELATION FOR A DELTA FUNCTION DISTRIBUTION

In this Appendix we will continue the derivation of the dielectric function for a delta function distribution which was begun in Chapter 4. After eq. (4.11) we must specify the zero order state of the plasma.

In coordinate space the distribution function is uniform, and the electrons are assumed to be neutralized by a positive background of fixed ions. The form of $f_o$ in velocity space is determined by (4.6).

It will be convenient to use cylindrical velocity space coordinates as in the diagram, Fig. A.1.

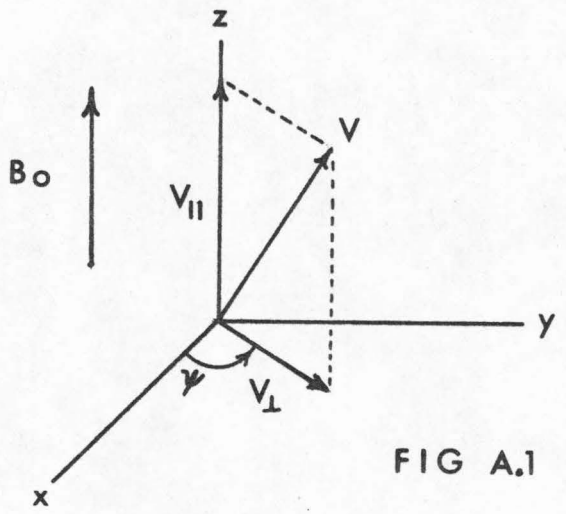


FIG A.1

With these coordinates we have

$$-\frac{e}{m}(\vec{V}\times\vec{B}_o)\cdot\vec{\nabla}_v f_o = -\frac{eB_o}{m}\left(V_y\frac{\partial f_o}{\partial V_x} - V_x\frac{\partial f_o}{\partial V_x}\right) \qquad (A.1)$$

Defining $\omega_c = eB/m$ and using the relations

$$\frac{\partial V}{\partial V_x} = \cos\psi \qquad \frac{\partial V}{\partial V_y} = \sin\psi$$

$$\frac{\partial \psi}{\partial V_x} = -\frac{\sin\psi}{V} \qquad \frac{\partial \psi}{\partial V_y} = \frac{\cos\psi}{V} \tag{A.2}$$

we obtain

$$-\frac{e}{m}(\vec{V}\times\vec{B}_o)\cdot\vec{\nabla}_v f_o = \omega_c \frac{\partial f}{\partial \psi}$$

which, when inserted into equation (4.6), gives us

$$\frac{\partial f_o}{\partial t} + \omega_c \frac{\partial f}{\partial \psi} = 0 \tag{A.3}$$

Thus we see that the unperturbed distribution function must be of the form (characteristics)

$$f_o = f_o(V_\perp,\ \psi-\omega_c t, V_{||}) \tag{A.4}$$

Now the unperturbed orbits must be specified by solving

$$\frac{d\vec{r}_o(t')}{dt'} = \vec{V}_o(t')$$

$$\frac{d\vec{V}_o(t')}{dt'} = -\frac{e}{m}\vec{V}_o(t')\times\vec{B}_o = -\omega_c\vec{V}_o(t')\times\hat{z} \tag{A.5}$$

The solution can be expressed in matrix notation as

$$\vec{r}_o(t-t') = \vec{r} - \frac{1}{\omega_c} \overleftrightarrow{T}(t-t') \cdot \vec{V} = \vec{r}'_o$$

$$\vec{V}_o(t-t') = \overleftrightarrow{R}(t-t') \cdot \vec{V} = \vec{V}'_o \qquad \text{(A.6)}$$

where $r$ and $v$ are the values at $t'=t$ and

$$T_{ij} = \begin{bmatrix} \sin\phi & (1-\cos\phi) & 0 \\ -(1-\cos\phi) & \sin\phi & 0 \\ 0 & 0 & \phi \end{bmatrix} \qquad \text{(A.7)}$$

$$R_{ij} = \begin{bmatrix} \cos\phi & \sin\phi & 0 \\ -\sin\phi & \cos\phi & 0 \\ 0 & 0 & 1 \end{bmatrix} \qquad \text{(A.8)}$$

and $\phi = \omega_c(t-t')$. $r'_o$ and $v'_o$ specify the unperturbed orbits.

Now in this spatially uniform problem we can Fourier transform in space and Laplace transform in time to solve for $E_1$ with real $K$.

$$\vec{E}_1(\vec{K},\omega) = \int dr \int_0^\infty dt\, E_1(r,t) \exp[-i(\omega t - \vec{K}\cdot\vec{r})] \qquad \text{(A.9)}$$

$$\vec{E}_1(\vec{r},t) = \int \frac{d\vec{K}}{(2\pi)^3} \int_C \frac{d\omega}{2\pi} \vec{E}_1(\vec{K},\omega) \exp[i(\omega t - \vec{K}\cdot\vec{r})] \qquad \text{(A.10)}$$

The contour $C$ is a straight line parallel to the real axis and in the lower half complex $\omega$ plane, below all singularities of the integrand. This assures zero response before the sources are turned on at $t = 0$.

Now Fourier transform the equation for $E_1$, eq. (4.11), introduce the unperturbed orbits, and use the spatial uniformity of $f_o$.

$$-i\vec{K}\cdot\vec{E}_1(\vec{K},t)+\omega_p^2\int d\vec{r}_o\, e^{i\vec{K}\cdot\vec{r}}\int dV_o'\int_0^t \vec{E}_1(t',r_o')\cdot\nabla_{v_o'}f_o\,dt' = 0 \tag{A.11}$$

$$-i\vec{K}\cdot\vec{E}_1(\vec{K},t)+\omega_p^2\int d\vec{r}\, e^{i\vec{K}\cdot\vec{r}}\int dV_o'\int_0^t dt'\,\vec{E}_1(\vec{r}-\frac{1}{\omega_c}\overleftrightarrow{T}(t-t')\cdot\vec{V},t') \times \frac{\partial f_o}{\partial V_o'} = 0 \tag{A.12}$$

Now let $\vec{q}=\vec{r}-\frac{1}{\omega_c}\overleftrightarrow{T}(t-t')\cdot\vec{V}$ and note that the second term in $\vec{q}$ is spatially invariant. By using equation (A.9) this becomes

$$-i\vec{K}\cdot\vec{E}_1(\vec{K},t)+\omega_p^2\int dV_o'\int_0^t dt'\,\vec{E}_1(\vec{K},t')\cdot\frac{\partial f}{\partial\vec{V}_o'} \times \exp(\frac{i}{\omega_c}\vec{K}\cdot\overleftrightarrow{T}(t-t')\cdot\vec{V}) = 0 \tag{A.13}$$

Because the derivative is evaluated on the unperturbed path given by equation (A.6), the integrand is a product of a function of $(t-t')$ and $\vec{E}_1(K,t')$. Then we will find the Laplace transform of equation (A.13) by using the convolution theorem

$$\int_0^\infty dt\, e^{-i\omega t}\int_0^t dt' f_1(t')\, f_2(t-t') = f_1(\omega)f_2(\omega) \tag{A.14}$$

We will use the electrostatic approximation in which

$$\vec{E}_1(\vec{K},t') = i\vec{K}\,\phi(\vec{K},t') \tag{A.15}$$

By choosing the coordinate system as shown in Fig. A.2 we will need only two components of $\vec{K}$. In fact, only the special case of

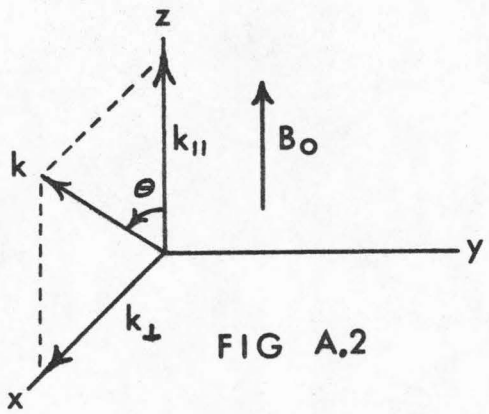


FIG A.2

$K_{\parallel} = 0$ will be considered.

By combining equations (A.13), (A.14), and (A.15) we have

$$\left\{1 + \frac{\omega_p^2}{K^2} \int_0 dt \int dV_o(t)\; i\vec{K} \cdot \frac{\partial f}{\partial \vec{V}_o(t)} \exp[-i\omega t + \frac{i}{\omega_c} \vec{K} \cdot \overleftrightarrow{T}(t) \cdot \vec{V}]\right\} \phi(\vec{K},t) = 0 \qquad (A.16)$$

For self-excited oscillations the bracket, which is the equivalent dielectric function for electrostatic oscillations, must vanish. By using the coordinate system of Fig. A.2 we have

$$\vec{K} \cdot \overleftrightarrow{T}(t) \cdot \vec{V} = 2K\, V \sin \frac{\omega_c t}{2} \cos(\psi - \frac{\omega_c t}{2}) \qquad (A.17)$$

and

$$\vec{K} \cdot \frac{\partial f_o}{\partial \vec{V}_o(t)} = K \frac{\partial f_o}{\partial V_{ox}(t)} = K \left[\frac{\partial f_o}{\partial V} \frac{\partial V}{\partial V_{ox}} + \frac{\partial f_o}{\partial \psi} \frac{\partial \psi}{\partial V_{ox}}\right] \qquad (A.18)$$

By using the transformation equations

$$V_{ox}(t) = \cos\phi V_x + \sin\phi V_y$$

$$V_{oy}(t) = -\sin\phi V_x + \cos\phi V_y$$

$$\phi = \omega_c t \tag{A.19}$$

and their inverses, we can show

$$\frac{\partial V}{\partial V_{ox}} = \cos(\psi - \phi)$$

$$\frac{\partial \psi}{\partial V_{ox}} = -\frac{1}{V}\sin(\psi - \phi) \tag{A.20}$$

and the expression for the derivative is

$$K\ \frac{\partial f_o}{\partial V_{ox}(t)} = K\ \frac{\partial f_o}{\partial V}\cos(\psi - \phi) - \frac{K}{V}\frac{\partial f_o}{\partial \psi}\sin(\psi - \phi) \tag{A.21}$$

If we now define

$$G(\psi,t) = \exp[-i\omega t + \frac{2iK\ V}{\omega_c}\sin\frac{\omega_c t}{2}\cos(\psi - \frac{\omega_c t}{2})] \tag{A.22}$$

We can define the quantity in brackets in equation (A.16) as

$$\kappa = 1 + \frac{\omega_p^2}{k^2}(I_1 + I_2) \tag{A.23}$$

where

$$I_1 = \int_{-\infty}^{\infty} dv_{\parallel} \int_0^{\infty} V\ dV \int_0^{2\pi} d\psi \int_0^{\infty} i\{K\ \frac{\partial}{\partial V}\ [\frac{\delta(V - V_o)}{V}]$$

$$\delta(\psi - \omega_c t)\ \delta(V_{\parallel})\ \cos(\psi - \omega_c t)\ G(\psi,t)\} \tag{A.24}$$

$$I_2 = \int_{-\infty}^{\infty} dV_{\parallel} \int_0^{\infty} V\, dV \int_0^{2\pi} d\psi \int_0^{} dti \left\{ -\frac{K}{V} \delta(V - V_o) \right.$$

$$\left. \frac{\partial}{\partial \psi} [\delta(\psi - \omega_c t)]\, \delta(V_{\parallel})\, \sin(\psi - \omega_c t)\, G(\psi, t) \right\} \qquad (A.25)$$

where we have introduced the delta function distribution in velocity space which is "created" at the position $(0,0,V_o)$ at $t = 0$ by the applied impulse

$$f_o(V_{\parallel}, \psi, V_{\perp}) = \delta(V_{\parallel})\, \delta(\psi - \omega_c t)\, \delta(V - V_o) \qquad (A.26)$$

Integrate over $\psi$, $v_{\parallel}$ and set $2 \sin \frac{\omega_c t}{2} \cos \frac{\omega_c t}{2} = \sin \omega_c t$

$$I_1 = \int_0^{\infty} V\, dV \int_0^{\infty} dti\, K \frac{\partial}{\partial V} \left( \frac{\delta(V - V_o)}{V} \right) e^{-i\omega t} + \exp\left[ \frac{iK\, V}{\omega_c} \sin \omega_c t \right] \qquad (A.27)$$

Integrate $\int dV$ by parts. Let $\omega_c t = \tau$, $\Omega = \omega/\omega_c$, $\frac{K\, V_o}{\omega_c} = \mu$. Then we have

$$I_1 = -\int_0^{\infty} dt\, \frac{iK}{V_o} \exp[-i\omega t + i\mu \sin \omega_c t][1 + i\, \mu \sin \tau] \qquad (A.28)$$

We will convert the infinite integral over the periodic function into an integral over one period.

$$\int_0^{\infty} dt = \sum_{n=0}^{\infty} \int_{2\pi n}^{2\pi(n+1)} \frac{d\tau}{\omega_c} \qquad (A.29)$$

$$I_1 = \frac{iK}{V_o} \sum_0^\infty \int_{2\pi n}^{2\pi(n+1)} \frac{d\tau}{\omega_c} e^{-i\Omega\tau} e^{i\mu \sin\tau} [1 + i\mu \sin\tau]$$

$$= -\frac{iK}{V_o\omega_c} \sum_0^\infty e^{-2\pi i n\Omega} \int_0^{2\pi} d\tau\, e^{-i\omega\tau}\, e^{i\mu \sin\tau} [1 + i\mu \sin\tau] \quad (A.30)$$

where $\Omega$ has small negative imaginary part.

Note that

$$\sum_{n=0}^{\infty} e^{-2\pi n\Omega i} = \frac{e^{\pi\Omega i}}{2i \sin \pi\Omega} \quad (A.31)$$

$$I_1 = \frac{-iK}{\omega_c V_o} \frac{e^{\pi i\Omega}}{2i \sin \pi\Omega} \int_0^{2\pi} [1 + i\mu \sin\tau] e^{-i\Omega\tau} e^{i\mu \sin\tau}\, d\tau \quad (A.32)$$

Divide this integral into two subintegrals

$$A_1 = \int_0^{2\pi} e^{\pi i\Omega}\, e^{-\Omega\tau i}\, e^{i\mu \sin\tau} \quad (A.33)$$

$$A_2 = \int_0^{2\pi} e^{\pi i\Omega}\, e^{-\Omega\tau i}\, e^{i\mu \sin\tau}\, [i\mu \sin\tau] \quad (A.34)$$

Now let $\tau \to \tau + \pi$

$$A_1 = \int_{-\pi}^{\pi} e^{\pi i\Omega}\, e^{-i\Omega\tau}\, e^{-i\pi\Omega}\, e^{i\mu \sin(\tau+\pi)}$$

$$= \int_0^{\pi} e^{-i\Omega\tau}\, e^{-i\mu \sin\tau}\, d\tau + \int_{-\pi}^{0} e^{-i\Omega\tau}\, e^{-i\mu \sin\tau}\, d\tau \quad (A.35)$$

Reverse the range on the second integral and let $\tau \to -\tau$

$$A_1 = 2 \int_0^{\pi} \cos[\mu \sin\tau + \Omega\tau]\, d\tau \quad (A.36)$$

Similarly,

$$A_2 = 2\mu \int_0^{\pi} \sin\tau \sin(\Omega\tau + \mu \sin\tau)d\tau \tag{A.37}$$

Thus

$$I_1 = \frac{-K}{\omega_c V_o \sin \pi\Omega} \int_0^{\pi} \{\cos(\mu \sin\tau + \Omega\tau) - \mu \sin\tau \sin(\mu \sin\tau + \Omega\tau)\}\, d\tau \tag{A.38}$$

We have set $K_\perp = K$. Returning to $I_2$, equation (A.25), and performing manipulations analogous to those for $I_1$, we find

$$I_2 = \frac{K}{\omega_c V_o} \frac{1}{\sin \pi\Omega} \int_0^{\pi} \cos(\tau\Omega + \mu \sin\tau)d\tau \tag{A.39}$$

Using $KV_o/\omega_c = \mu$, the final answer for $\kappa$ is

$$\kappa = 1 + (I_1 + I_2) \frac{\omega_p^2}{K^2}$$

$$= 1 + \frac{\omega_p^2}{K^2} \left[ + \frac{K}{\omega_c V_o} \frac{1}{\sin \pi\Omega} \int_0^{\pi} d\tau \{\cos(\tau\Omega + \mu \sin\tau) \right.$$

$$\left. - \cos(\mu \sin\tau + \Omega\tau) + \mu \sin\tau \sin(\tau\Omega + \sin\tau)\} \right. \tag{A.40}$$

$$\kappa = 1 + \frac{\omega_p^2}{\omega_c^2} \frac{1}{\sin \pi\Omega} \int_0^{\pi} \sin\tau \sin(\Omega\tau + \mu \sin\tau)d\tau \tag{A.41}$$

Now the dielectric constant can be easily evaluated for any $\Omega$ and $\mu$ by numerical integration. Test the answer in the cold plasma limit by letting $\mu \to 0$ and keeping zero order terms in $\mu$.

Expand the integral for small $\mu$ .

We find that

$$\lim_{\mu \to 0} \kappa = 1 + \frac{\omega_p^2}{\omega_c^2(1 - \frac{\omega^2}{\omega_c^2})} = 1 - \frac{\omega_p^2}{\omega^2 - \omega_c^2} \tag{A.42}$$

which is the usual cold plasma result.

Now as an aid to computation we will locate the points where the dispersion curves for real $K$ and $\omega$ cross harmonics of the cyclotron frequency. Expand $\kappa$ assuming $\Omega - n$ is small.

Examining just the integral we have

$$\int_0^{\pi} \sin x \sin(\Omega x + \mu \sin x) = \int_0^{\pi} \sin x[\sin \Omega x \cos(\mu \sin x) + \cos x \sin(\mu \sin x)] \tag{A.43}$$

where we have changed $\tau$ to $x$. By using well known identities [1] this becomes

$$\kappa = \int^{\pi} \sin x[\sin \Omega x \{J_o(\mu) + 2 \sum_{m=1}^{\infty} J_{2m}(\mu) \cos(2mx)\} + \cos \Omega x \{2 \sum_{m=0}^{\infty} J_{2m+1}(\mu) \sin(2m+1)x\}dx \tag{A.44}$$

After some manipulation we find that the series expansion for $\kappa$ is

$$\kappa = 1 + \frac{\omega_p^2}{\omega_c^2}\{J_o(\mu) \frac{1}{1 - \Omega^2} + \sum_1^{\infty} J_{2m}(\mu) \frac{2m-1}{\Omega^2 - (2m-1)^2} - \frac{2m+1}{\Omega^2 - (2m+1)^2}] + \sum_0^{\infty} \Omega J_{2m+1}(\mu)[\frac{1}{(2m+2)^2\Omega^2} - \frac{1}{4m^2 - \Omega^2}]\} \tag{A.45}$$

Now look for solutions near multiples of $\omega_c$ .

Near $\Omega = 0$:

$$\kappa \tilde{=} 1 + \frac{\omega_p^2}{\omega_c^2} J_1(\mu) \frac{1}{\Omega} \tag{A.46}$$

$\kappa = 0$ when $J_1(\mu) = -\frac{\omega_c^2}{\omega_p^2}$ ; $J_1 < 0$ for $3.8 < \mu < 7.1$ so the zero frequency solutions are near $\mu = 3.8$ and 7.1.

Near $\Omega = 1$:

$$\kappa \tilde{=} 1 + \frac{\omega_p^2}{\omega_c^2} \left\{ \frac{J_o(\mu)}{1 - \Omega^2} + \frac{J_2(\mu)}{\Omega^2 - 1} \right\} \tag{A.47}$$

This implies

$$J_o(\mu) - J_2(\mu) = -\frac{\omega_c^2}{\omega_p^2} (1 - \Omega^2) \tag{A.48}$$

Thus the solutions pass through $\Omega = 1$ near $\mu = 1.84$ and 5.33 .

The numerical solutions of eq. (A.41) are shown in Figs. 4.1 and 4.2.

Reference for Appendix

1. M. Abramowitz and I. A. Stegun, Eds., Handbook of Mathematical Functions, U. S. Government Printing Office, 1966; Equations 9.1.42 and 9.1.43.